SEDIMENT TRANSPORT IN NORTON SOUND, ALASKA

by

David A. Cacchione
David E. Drake

United States Department of Interior
Geological Survey
Open File Report 79-1555

TABLE OF CONTENTS

Sediment transport in Norton Sound, Alaska

by

David A. Cacchione and David E. Drake

INTRODUCTION

An investigation of sediment dynamics in Norton Sound and other sections of the northern Bering Sea was conducted to define the principal pathways and mechanisms of bottom and suspended materials transport. A major topic of this research is the complicated interrelationships of sediment movement and hydrodynamic stresses that occur in the marine environment. Temporal contrasts like those caused by seasonal cycles and quiescent versus storm conditions are of particular interest. This research is pertinent to two major impact areas of petroleum development in the marine environment: (1) transport of materials including pollutants; and (2) hazardous sea floor conditions caused by wave and current erosion.

The northern Bering Sea is characterized by several unique and extreme environmental conditions: (1) sea ice covers the sea surface over 50% of the year, (2) late summer and fall storms that travel along the polar front often bring severe weather to the area, and (3) the Yukon River effluent, second largest among North American rivers, enters the ocean at the southwestern side of Norton Sound.

Nelson (1977, 1978) and McManus et al. (1977) have developed a comprehensive picture of the geological and geophysical setting for this region. Their work provides the background information that is a prerequisite for the more topically-focused research in this project. For example, Nelson and Creager (1977) and others have shown that the large amount of sediment introduced to Norton Sound

by the Yukon River has not yielded sediment accumulations commensurate with the rate of supply. The causes and modes of transport for this apparent exit of materials from the sound are topics included in this investigation.

The ability to predict accurately the movements of pollutants in the sea is strongly dependent on our knowledge of local transport processes. Specific geographic regions, like Norton Sound, will have unique aspects to the mechanisms which control the paths and amounts of material that is moved. This study attempts to identify and elaborate upon the most important transport-producing mechanisms in this region, and to relate these mechanisms to entrainment and movement of near-bottom materials. The eventual understanding which this study has as its goal will hopefully permit an accurate description of bottom transport of sediments, pollutants, nutrients, and other particulate matter in Norton Sound.

BACKGROUND INFORMATION

Norton Sound is a shallow arm of the Northern Bering Sea, located on the western margin of Alaska, south of the Seward Peninsula (Fig. 1). It is approximately rectangular in shape, 250 km long in an E-W direction, and 130 km long in an N-S direction. Water depth is everywhere less than 35 meters, average depth is 18 meters. Nome, Alaska, population 2400, is situated along the northwest coast.

The suspended sediment in Norton Sound is derived principally from the Yukon River, which discharges about 70 to 100 million tons of material per year into the southwestern corner of this area. Despite this enormous sediment source, Nelson and Creager (1977) and McManus et al. (1977) show that in recent times (<5000 years B.P.) modern Yukon fine sands and silts have been accumulating on the Yukon subdelta in southern Norton Sound at a surprisingly low rate. This thin accumulation of sediments has been attributed to the erosive action of

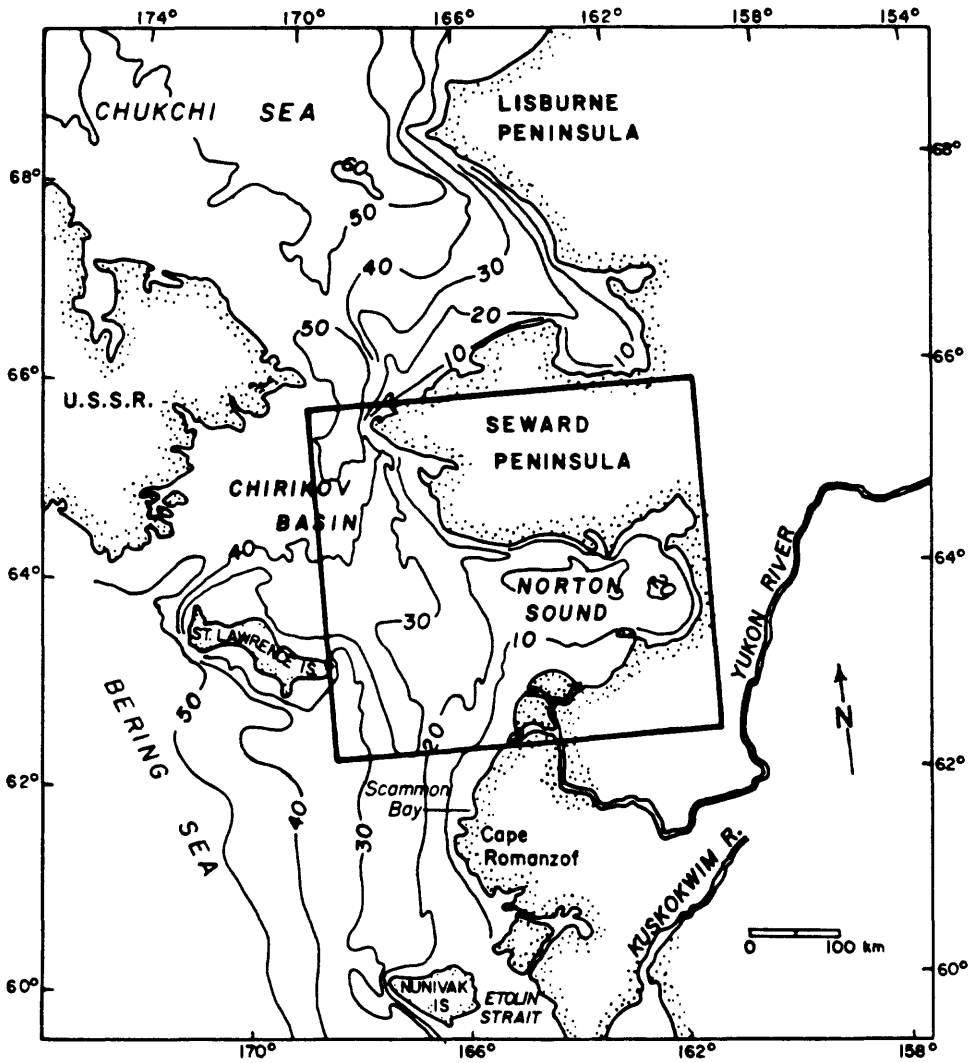

Figure 1. Generalized bathymetry (in meters) of the northern Bering Sea and southern Chukchi Sea. The outlined area is the site of the present study and is shown in more detail in figure 2.

storms that occur in the early fall prior to the formation of ice cover (Nelson and Creager, 1977). The fine-grained fraction of Yukon-derived materials is presumably transported through the Northern Bering Sea with the Alaskan Coastal water and deposited in the southern Chukchi Sea (Nelson and Creager, 1977; McManus et al., 1974).

Modern Yukon very fine sands and silts do not form a continuous blanket in Norton Sound (Fig. 2). Despite the proximity of this large sediment supply, the modern muds tend to deposit along the southern border of the sound leaving substantial areas in the northcentral area with little or no recent cover (<20 cm). The explanation for the slow rates of accumulation in the northern half of the Sound was not known prior to our work. We now believe this situation is the result of strong tidal and storm currents along with an advective transport pattern that diverts the bulk of the Yukon silt to other areas.

Investigations of the large-scale current patterns in the northern Bering and Chukchi Seas have been summarized by Coachman et al. (1975). When viewed in a regional sense, the mean circulation is relatively simple. Bering Sea shelf water flows toward the Arctic Ocean and the magnitude of this transport is modulated primarily by atmospheric pressure changes. Owing to topography, the current speed increases toward the north; the effect of flow constriction is particularly apparent north of 64°30' N latitude. Bottom sediments in the approaches to Bering Strait are predominantly sands which have been molded into a progression of bedform types that are characteristic of progressively stronger bottom currents. There is little chance for permanent deposition of fine-grained sediments in this area (north of 64°30') and suspended material moves rapidly through Bering Strait and into the Chukchi Sea (Drake et al., in press).

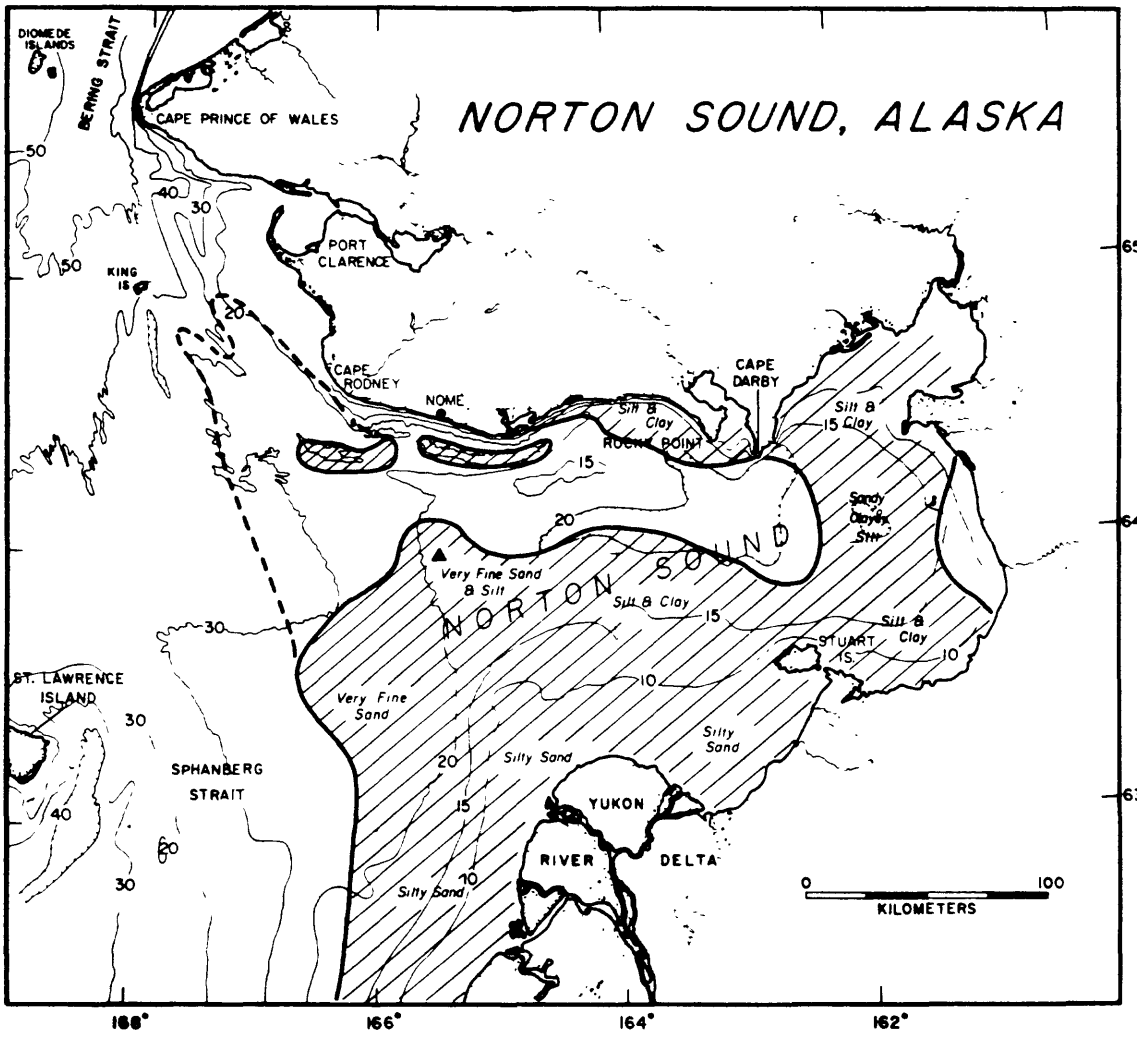

Figure 2. Distribution of modern (<9500 B.P.) sediment in Norton Sound is depicted by cross-hatched area (after McManus and others, 1977). Textural and mineralogical data show that this sediment is derived primarily from the Yukon River. The dashed line depicts the northern extent of trace amounts of coarse silt in bottom sediments. GEOPROBE location in 1976 and 1977 is shown by triangle 60 km south of Nome.

Whereas the gross aspects of the regional flow field are reasonably well known, the physical oceanography of Norton Sound has only recently been examined. As is typical of most investigations of "unknown" areas the initial gains in knowledge tend to come easily but the detail needed to achieve a quantitative understanding comes only after several years of intensive research.

Studies in 1976 by Muench, Charnell and Coachman (1977) and Cacchione and Drake (1977) were the first adequate investigations of the physical oceanography of Norton Sound. Among many results the following should be noted:

1. Muench et al. (1977) suggested that the circulation in the outer part of Norton Sound is characterized by a cyclonic gyre.

2. Exchange of water between the outer sound and the eastern "cul-de-sac" is limited. In fact, the bottom water in the cul-de-sac late in the summer of 1976 was probably remnant from the previous winter (Muench et al., 1977).

3. Geoprobe data for September-October 1976 showed that tidal currents were surprisingly strong in 18 m of water (60 km south of Nome). Sediment transport calculations suggested that the tidal currents plus the mean flow should produce bed shear stresses close to the those needed to initiate sand motion (Cacchione and Drake, 1977).

4. The regional sampling by Cacchione and Drake revealed a pronounced tongue of turbid water originating near the Yukon Delta and extending across the mouth of Norton Sound toward the Nome coast.

Geologic studies by Nelson (1978) have revealed the presence of a number of circular depressions on the Yukon delta front. The origin of these features is presently unknown but it is possible that they are related to intense currents during storms. The delta front is an area of rapid sand and silt deposition in the summer, and these materials should be readily eroded during the late summer storms.

Field methods

We employed two complimentary methods of data collection in our Norton Sound work. The first method involved regional sampling of hydrographic parameters (temperature and salinity) and suspended particulate matter in order to examine the spatial variation in sediment transport. Sampling cruises were conducted on the U.S. Geological Survey ship SEA SOUNDER in September-October 1976 and July 1977 and winter season sampling was accomplished in February-March 1978 using a NOAA helicopter. The second method focused on the temporal variation in bottom currents and sediment transport at a site near the northern edge of the modern Yukon prodelta (Fig. 2). An instrumented, bottom tripod system (GEOPROBE) was deployed at that site for 21 days in September-October 1976 and for 80 days in 1977 (July 8-September 26). The GEOPROBE system is designed to measure bottom currents and pressure, temperature and light transmission and scattering for periods of about 3 months (Fig. 3). The tripod is also equipped with a 35 mm camera system which obtains pictures of the bottom at fixed time intervals and also at times when the current exceeds preselected speeds. GEOPROBE operation and data analysis is discussed in more detail by Cacchione and Drake (1979) and in subsequent sections of the present report.

RESULTS

Distribution of suspended sediment - summer season

The distribution and composition of suspended matter in Norton Sound is dominated by Yukon River sediment during the summer (Figs. 4-7). Concentrations of total suspended matter (TSM) increase throughout the water column toward the major western distributaries of the delta, and the south half of the sound is rimmed with low-salinity turbid water that spreads north and east from the delta.

Although our two surveys were a year apart and the sampling was done at

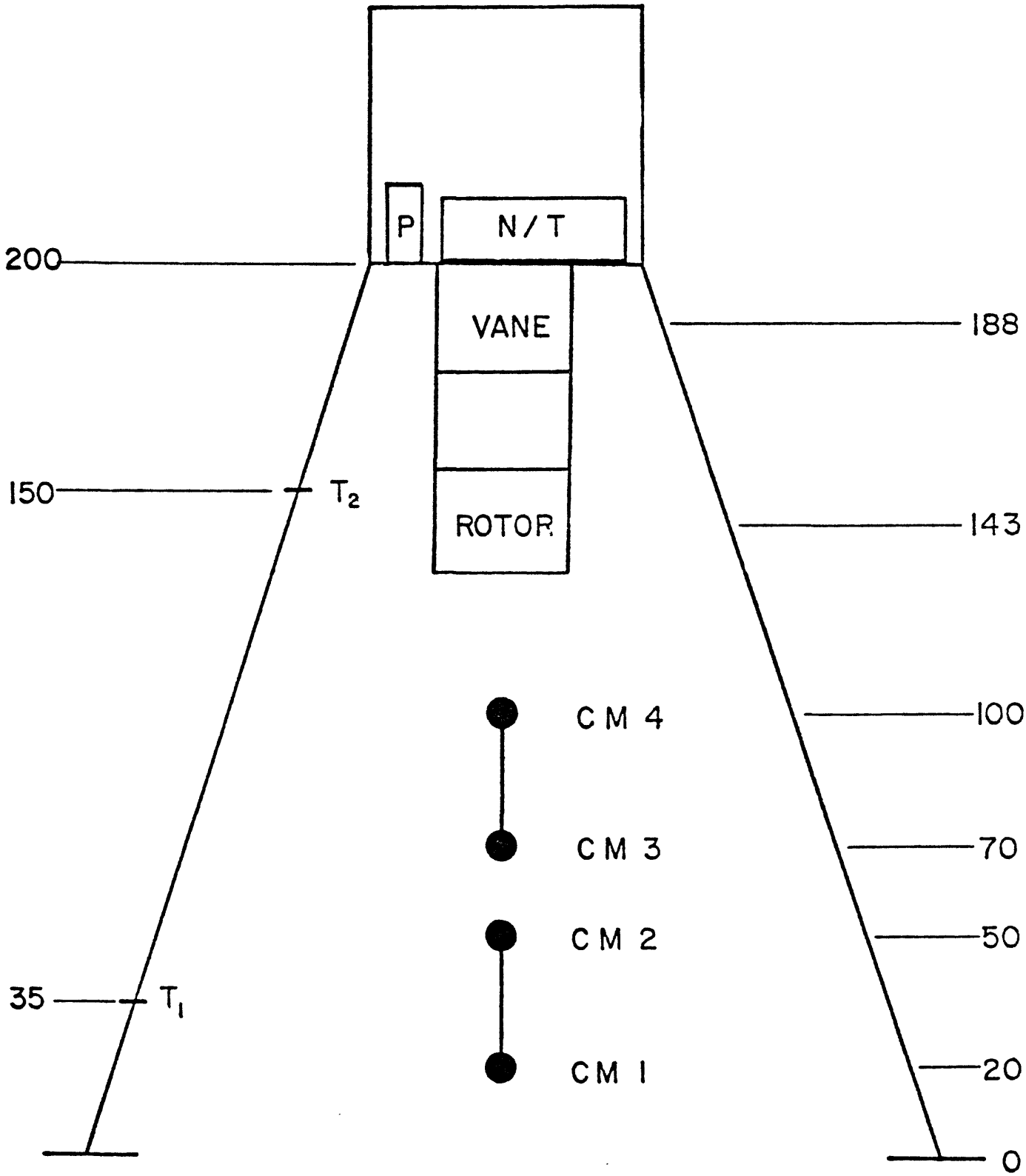

Figure 3. Schematic of GEOPROBE tripod showing locations of the basic sensors in centimeters above the footpads. CM1 - CM4 are the electromagnetic current meters; T_2 and T_2, P, N/T, and vane/rotor are the temperature, pressure, nephelometer/transmissometer, and Savonius rotor current meter, respectively.

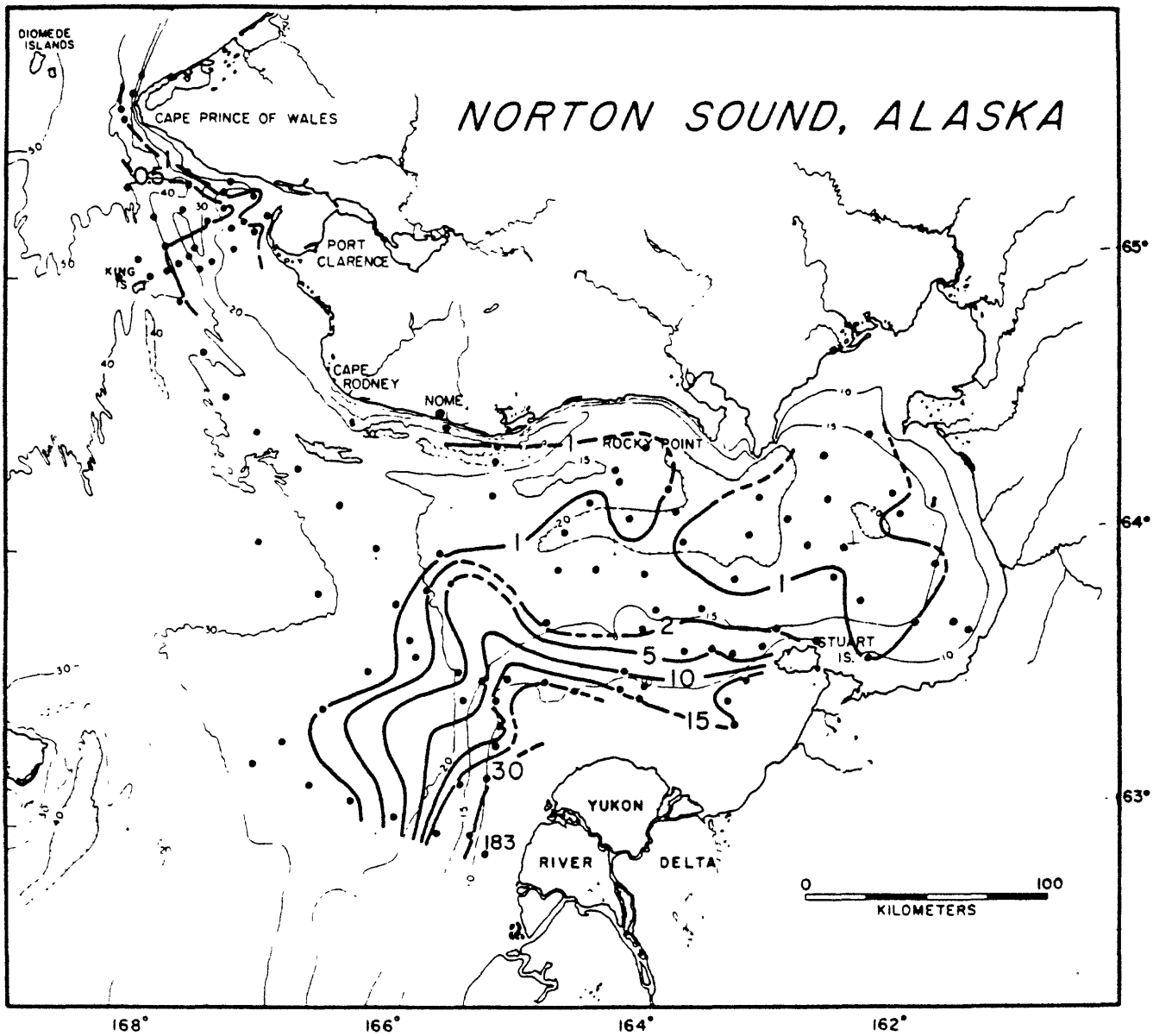

Figure 4. Total suspended-matter concentrations (in mg/L) one meter below sea surface during September-October 1976. The distribution of suspended matter is strongly influenced by discharge from the two major distributaries on the western side of the delta.

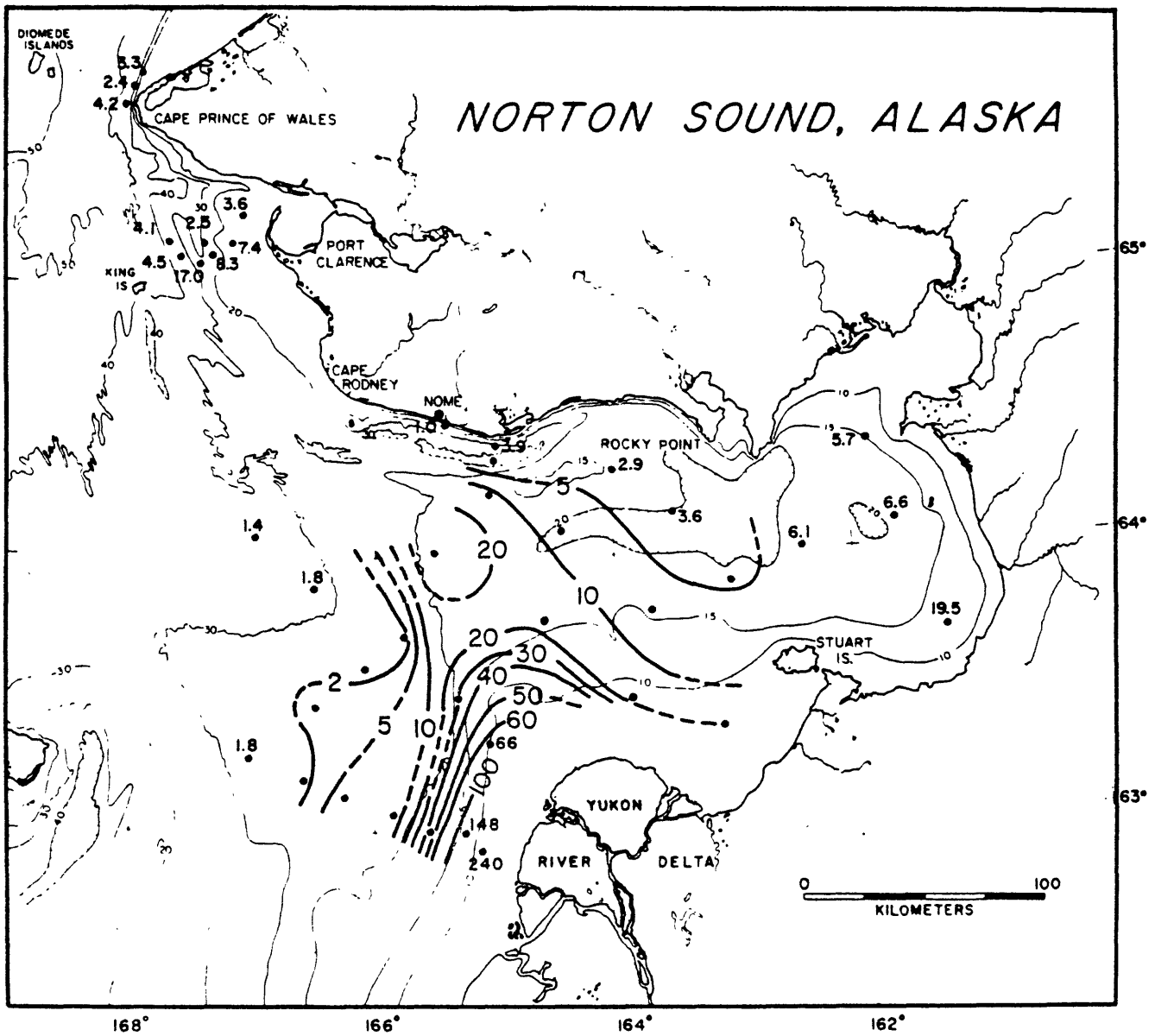

Figure 5. Total suspended-matter concentrations (in mg/L) one meter above sea floor during September-October 1976.

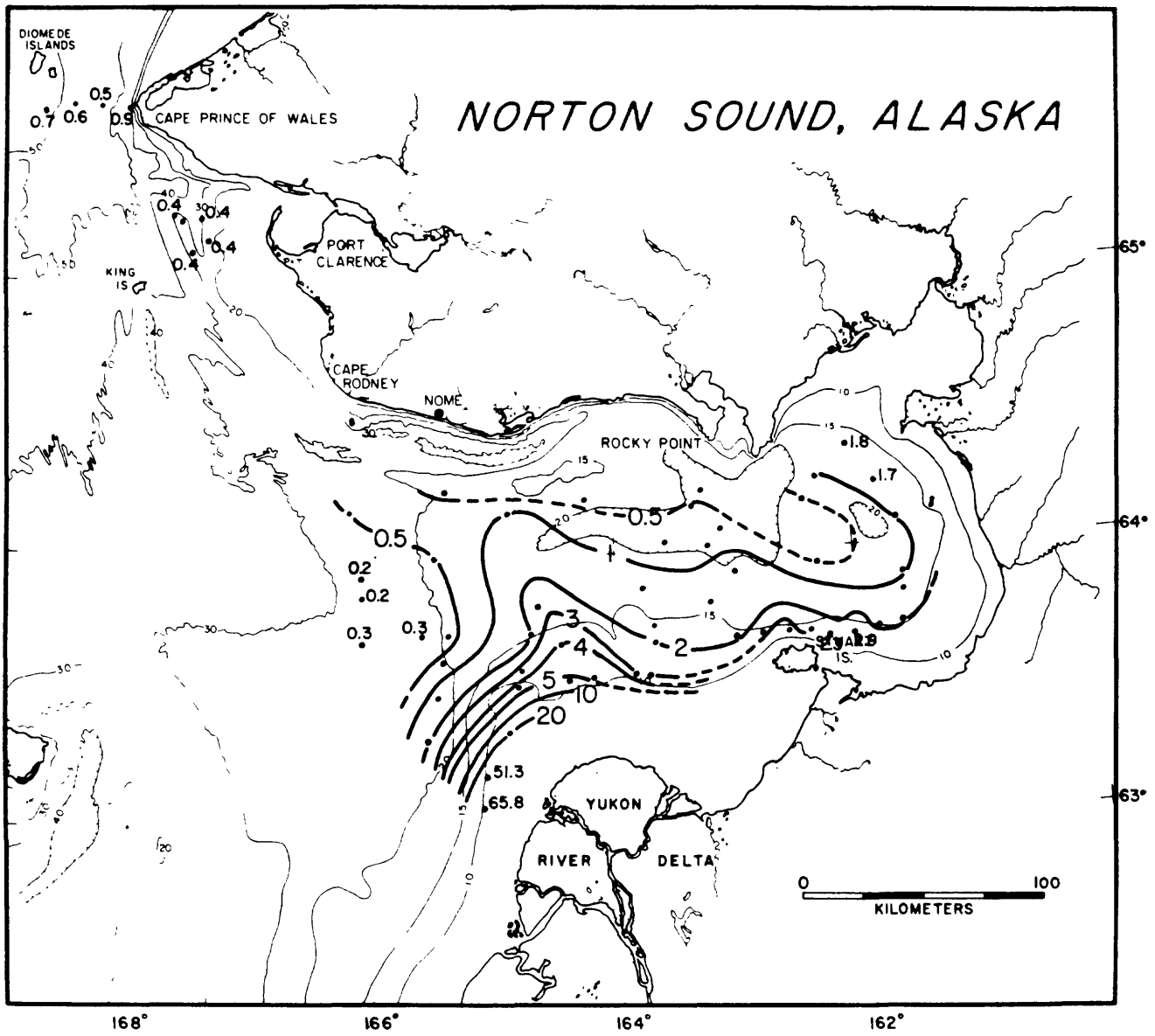

Figure 6. Total suspended-matter concentrations (in mg/L) one meter below sea surface during July 1977.

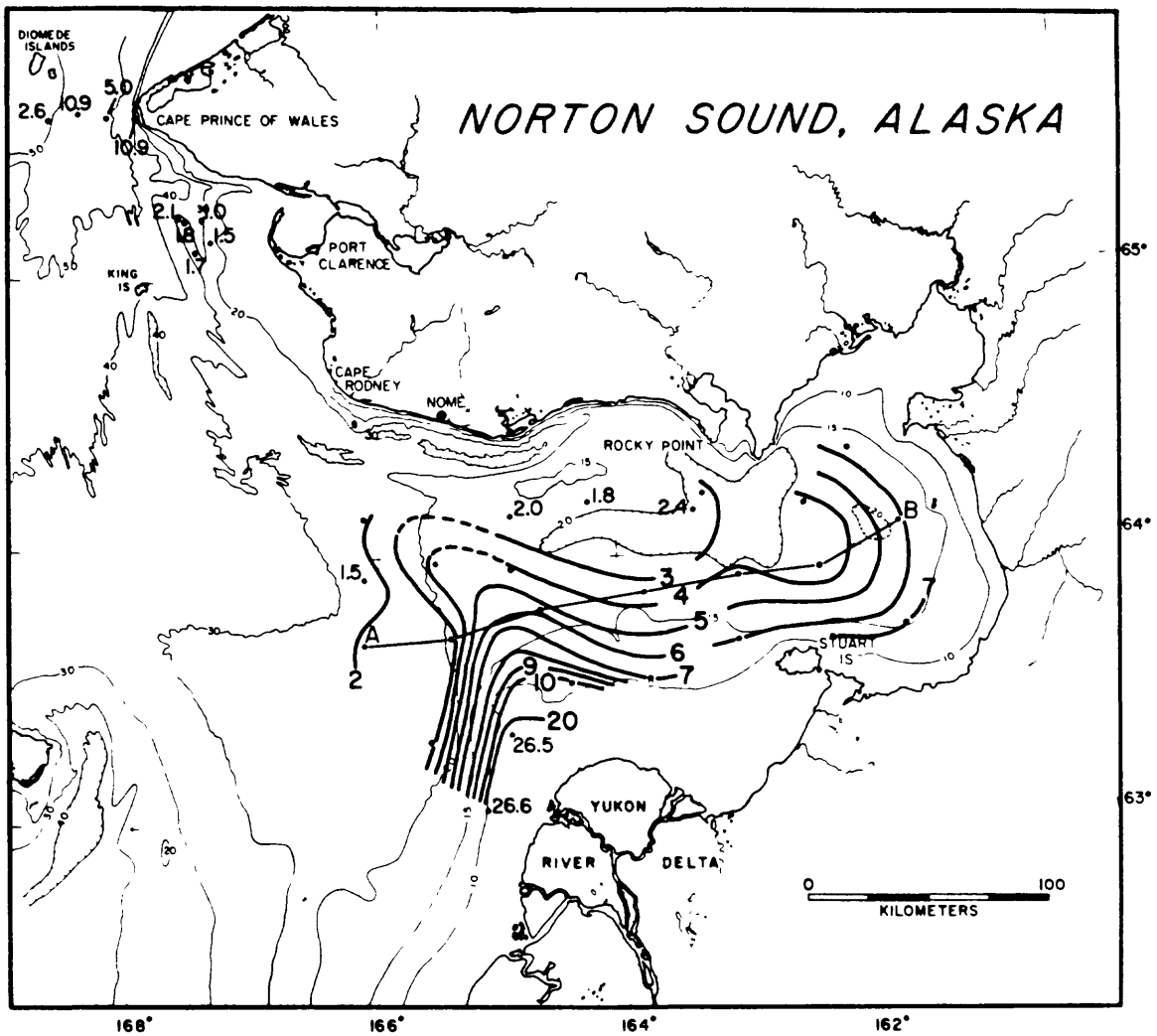

Figure 7. Total suspended-matter concentrations (in mg/L) one meter above sea floor during July 1977.

different times in the summer (September 1976 and July 1977), the two data sets of TSM distributions are strikingly similar. The distribution in the outer part of the sound is dominated by a well-defined turbidity plume extending north and northwest from the Yukon Delta. High concentrations of inorganic silt and clay are present throughout the water column along the path of this plume, and temperature and salinity values show that the plume is a mixture of Alaskan Coastal Water and Yukon River water (Figs. 8 and 9). This plume appears to be a permanent feature marking the path of the coastal current as it traverses the mouth of Norton Sound; an interpretation supported by our inspection of satellite images for the period 1973-77 (Fig. 10). The distribution of TSM, particularly during July 1977, suggests a flux of suspended matter into the eastern sound (Fig. 6). The surface and near-bottom distributions of TSM immediately north of Stuart Island indicate that most of this suspended matter is transported in a surface layer separated from the remnant bottom water by strong density gradients. The bulk of this sediment is most likely delivered to Norton Sound by the northeastern distributary of the Yukon River, the smallest of the three delta distributaries (Fig. 2).

By late summer, the distributions of temperature, salinity, and TSM demonstrate a separation of Norton Sound into outer and inner regions (Figs. 8 and 9). The outer region, west of Stuart Island and Rocky Point, actively communicates with the Alaskan Coastal Water and Bering Sea shelf waters. In contrast, the horizontal uniformity of temperature, salinity, and TSM values in both the upper and lower water layers within the eastern cul-de-sac reflects a minimal exchange with the western sound.

Because of the broad shoals surrounding the Yukon Delta, we were unable to sample the near-shore (<30 km from shore) waters directly. Fortunately, this data gap can be closed, at least qualitatively, by Landsat images and NOAA

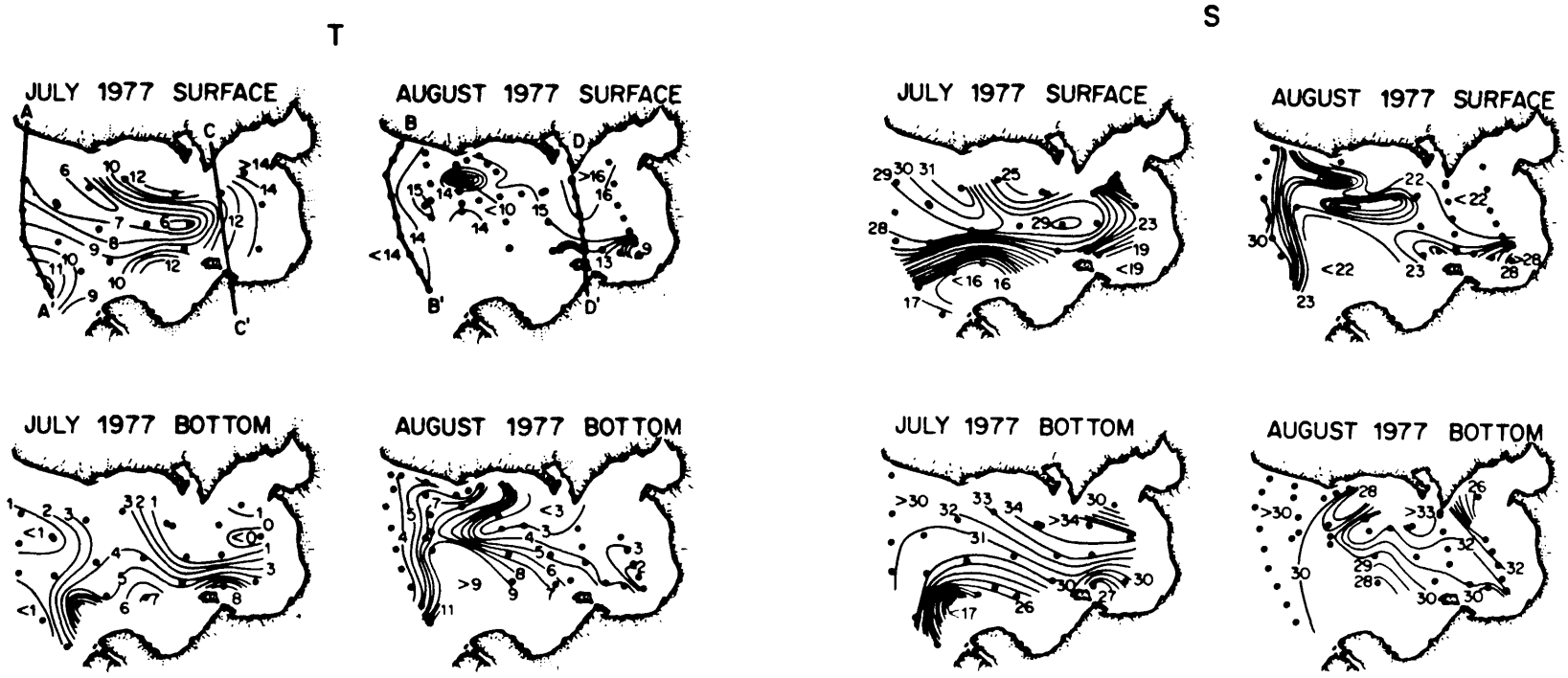

Figure 8. Temperature (°C) and salinity (°/$_{oo}$) distributions during July and August 1977 (after Drake and others, in press). Cold and saline water produced during the winter tends to remain in the depressions in Norton Sound throughout the summer. This water is overlain by warm, low salinity water in the eastern half of the sound.

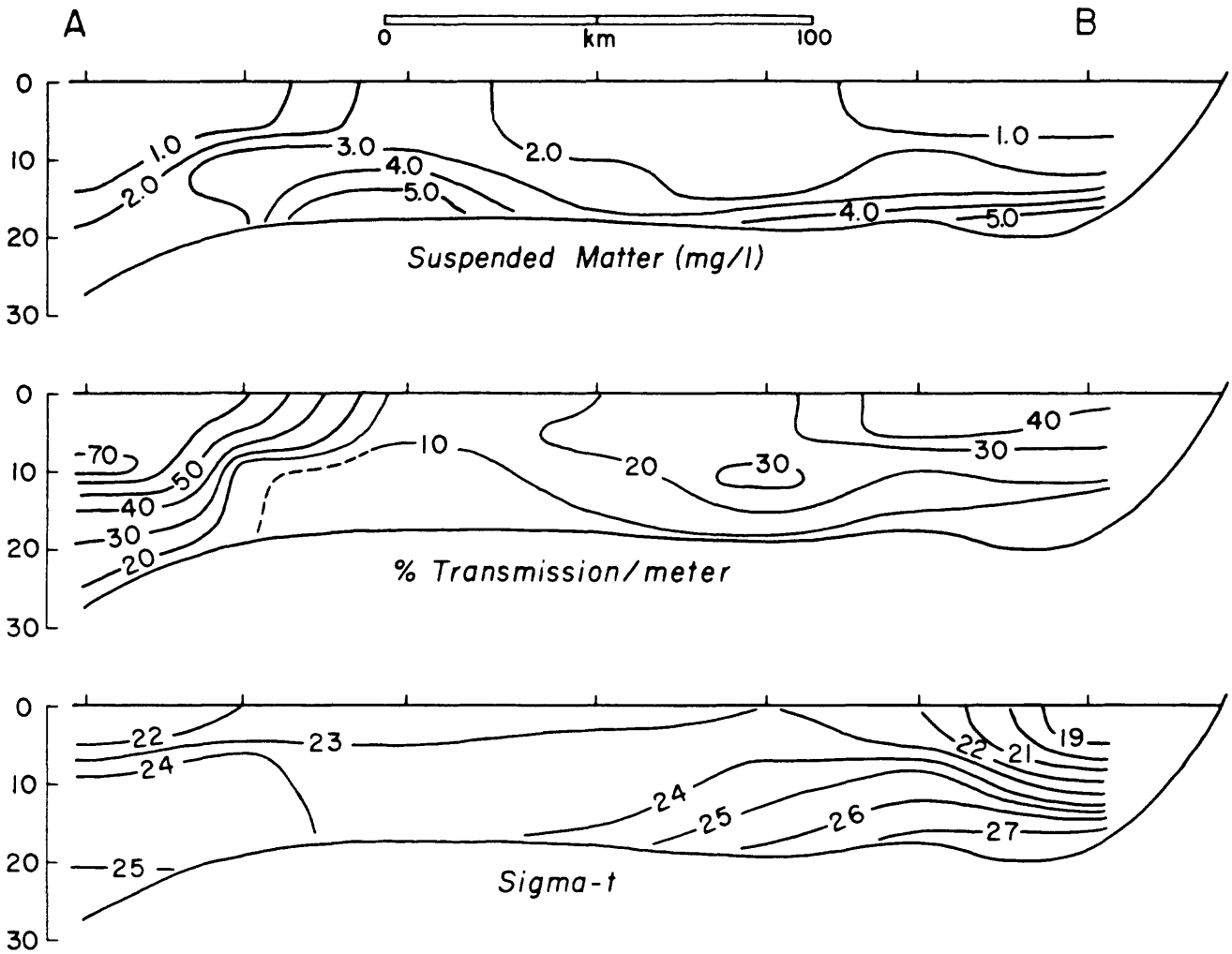

Figure 9. Vertical distribution of total suspended matter (mg/L), light beam transmission (%) and water density [sigma-t = 1000 (density)] along section A-B shown in figure 7. Note high suspended matter concentrations and relatively low density water over Yukon prodelta. The remnant winter water in the eastern part of the sound is clearly shown.

satellite photography. Sharma et al. (1974) examined Landsat images obtained in July, August, and September of 1973, and we have studied images and photographs for subsequent summers through 1977. These data show that the TSM distributions observed by us in 1976 and 1977, which were also observed in 1973 by Sharma et al., are representative of the dispersal pattern of Yukon-derived suspended sediment in Norton Sound throughout the ice-free season (Fig. 10). The delta coast is typically rimmed by turbid surface water to approximately 30-40 km offshore, with peak concentrations of suspended matter near the three distributaries.

The most surprising aspect of the TSM distributions revealed by these images is that near-shore flow is sometimes directed to the south along the west shore of the delta. Most satellite images show that turbid water from the major southwestern distributary extends about 10-40 km south. However, a sequence of exceptionally clear images for June 1976 reveals Yukon-derived suspended matter as far south as Scammon Bay (Fig. 11). Modern sediment from the Yukon River is accumulating in lagoons and bays between the present delta and Cape Romanzof (Dupré, 1978). Therefore, we believe that a substantial amount of silt and clay from the western distributaries of the Yukon Delta is transported to the south by near-shore currents during the summer. Unfortunately, we have no current meter data with which to support these qualitative conclusions.

Seaward of the southerly coastal current in June 1976, the transport of shelf water was decidedly to the north, in agreement with the current measurements of Muench et al. (1978). Satellite images show that suspended matter diffuses seaward and eventually returns to the mouth of Norton Sound (Fig. 11). The northward advection continues across the outer part of the sound, through Chirikov Basin and Bering Strait, and into the Chukchi Sea (Coachman et al., 1975).

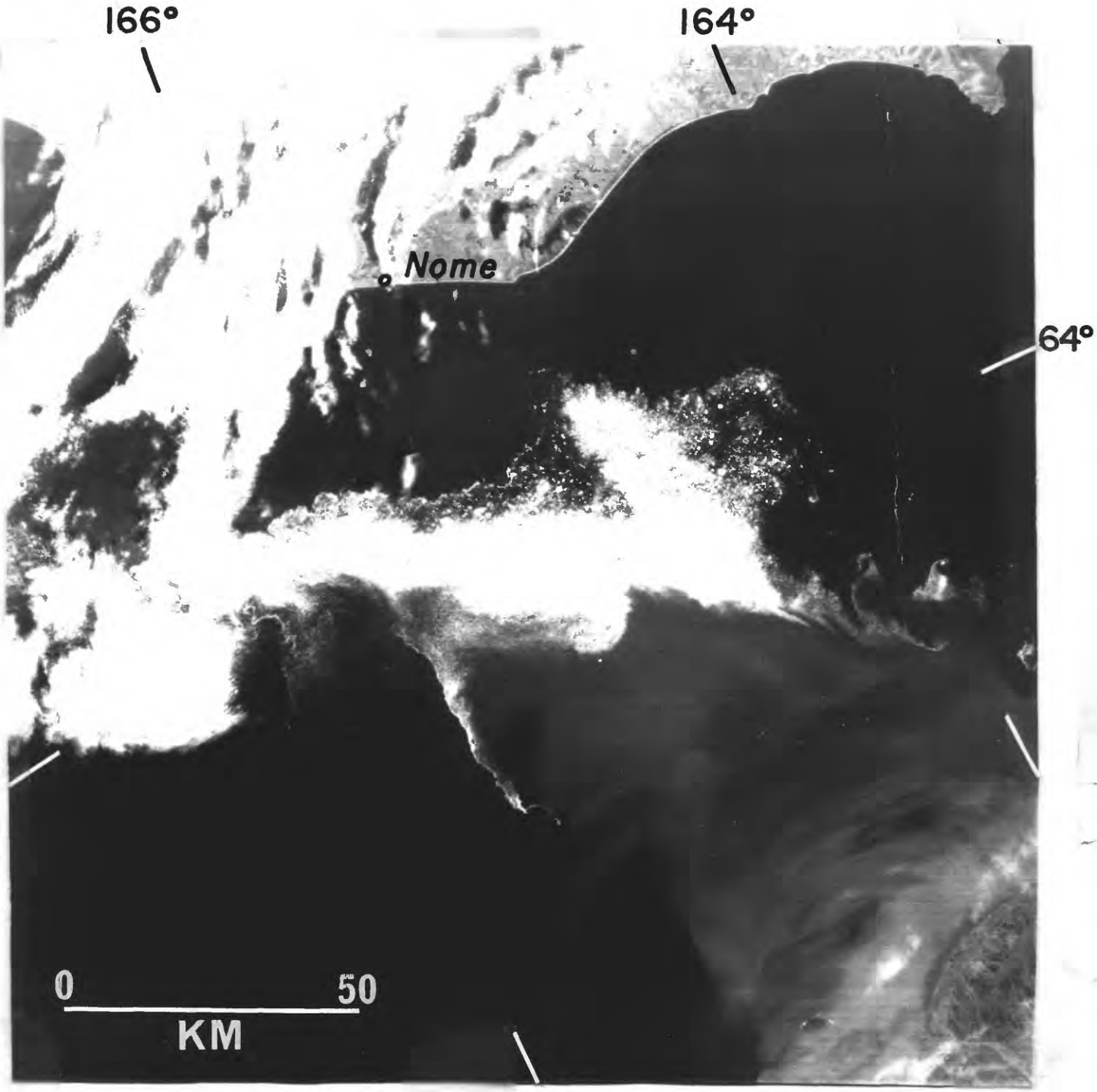

Figure 10. Landsat image (multispectral scanner band 4) of western Norton Sound on 30 June 1976. The Yukon delta is at lower right corner. Close inspection of the image shows that relatively high suspended sediment concentrations (light grey tones) extend beyond the ice to the Nome coastline.

14-165

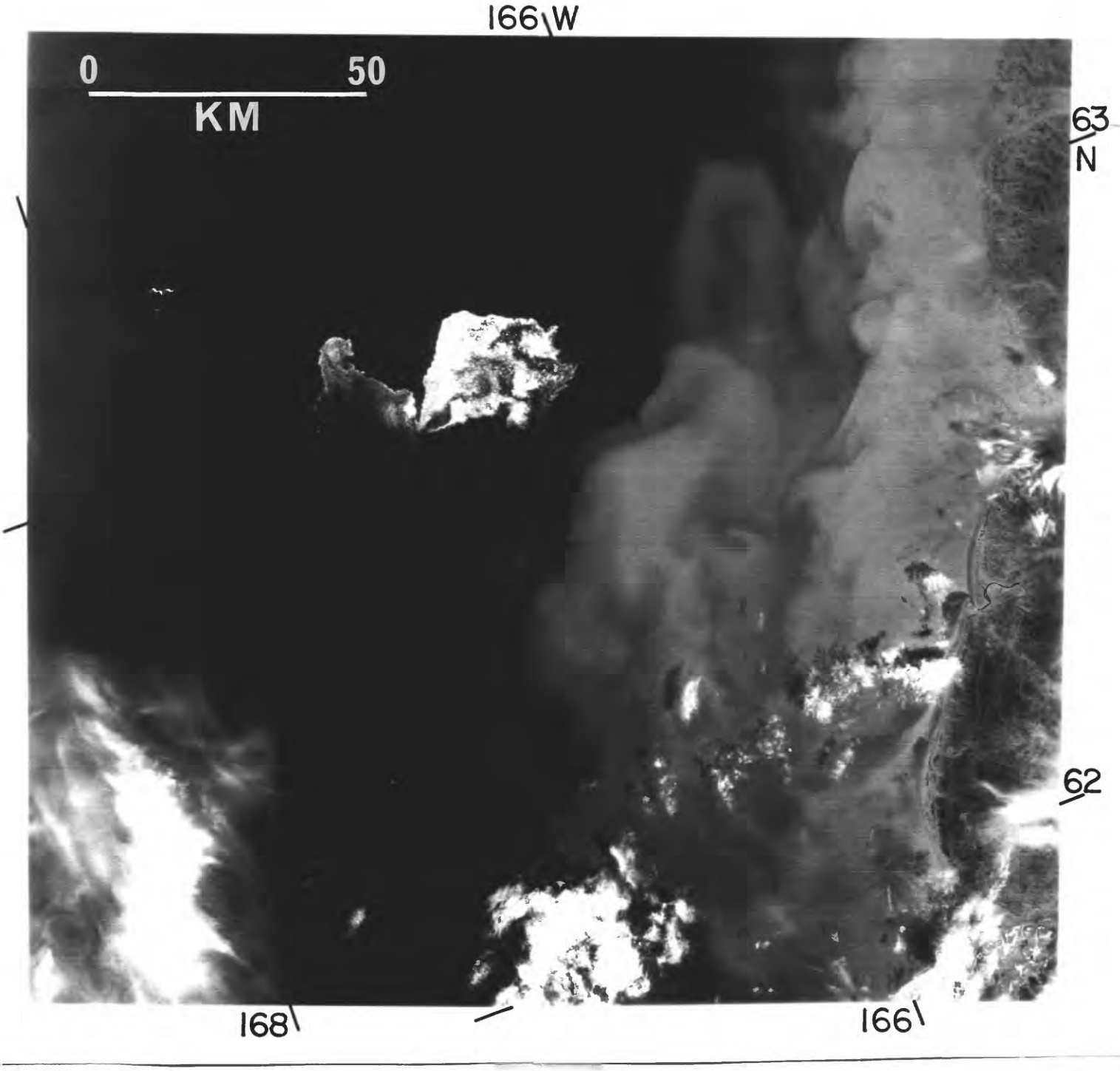

Figure 11. Landsat image (MSS 5) of eastern part of Shpanberg Strait on 30 June 1976. The Yukon delta is at upper right corner of this image.

Distribution of suspended sediment - winter season

The winter sampling operations were carried out from a helicopter capable of carrying about 700 kg of gear and scientists. Nome, Alaska was our base of operations and typically 5 to 7 ice stations were completed each day. Owing to the payload restriction and the necessity that all sampling gear fit through a 20-cm-diameter ice-hole, sample collection was limited to 1.7-liter Niskin bottles and a 10-cm pathlength LED (light emitting diode) transmissometer. The University of Washington researchers used a specially configured Plessey conductivity-temperature-depth sensor.

Upon locating a suitable landing site for the helicopter (reasonably flat ice at least 30 cm thick), a hole was drilled through the ice and water samples were obtained from near-surface, near-bottom and intermediate levels in the water column. The samples were immediately transferred to rinsed one-liter plastic bottles. Light transmission profiles were obtained at 5 stations but recurring power cable and sensor icing problems forced curtailment of this operation at most of our stations.

At the end of each day on the ice the water samples were returned to Nome and filtered through pre-weighed Nuclepore polycarbonate filters (47 mm diameter, 0.4 μm pore size). The filters were carefully rinsed with pre-filtered distilled water and stored in plastic petri dishes.

Further analysis of the particulate matter was carried out in Menlo Park, California. The sample filters plus blanks were dried for 24 hours at 50°C and reweighed to an accuracy of 10 μg . A selected series of filters was cut in half with one portion being used for ash residue analysis and one portion being archived. The filter halves were combusted for 6 hours at 550°C in tared platinum foil crucibles in order to obtain an estimate of the organic matter concentrations. All samples were analyzed for texture and general composition using standard light microscopy.

The distribution of total suspended matter (TSM) one meter below the pack ice and one meter above the seafloor in winter 1978 were essentially identical. Figure 12 presents the TSM distribution near the seafloor. Concentrations of TSM ranged from a high of 8.4 mg/L near the delta to 1.3 mg/L at stations in the central part of Sphanberg Strait and west of Cape Rodney (Fig. 2). The vertical uniformity in TSM was further substantiated by light transmission measurements obtained at stations south of Nome (Fig. 13). Beam attenuation coefficients (alpha) typically varied less than 5% from just below the ice to the seafloor. Comparison of near-surface and near-bottom TSM concentrations for all of the winter stations reveals a mean increase of only 9% near the seafloor. For example, at three shallow stations north of the Yukon delta, the average "surface" TSM was 7.4 mg/L and the near-bottom average was 7.5 mg/L. This trend was also present at the deeper stations west and northwest of Norton Sound.

The composition and texture of the suspended matter were largely independent of position in the water column, although a slight coarsening of the inorganic material was detected near the bottom at most stations on the prodelta and there was somewhat more combustible material in the surface samples (Table 1). Regardless of depth, suspended matter over the Yukon prodelta was predominantly inorganic fine and medium silt with subordinate amounts of clay. However, very fine quartz sand was present in significant amounts (5-10%) near the bottom at two stations north of the delta. These two stations represent our closest approach to the shallow (<10 m) bank which rims the delta. Attempts to obtain samples closer to the delta was unsuccessful because of dangerous ice conditions (severe ice ridging and open water areas).

Temporal variations - GEOPROBE results

GEOPROBE tripods were deployed in 1976 and 1977 at a site 60 km south of Nome (64°06' N latitude, 165°30' W longitude) near the northern margin of Yukon

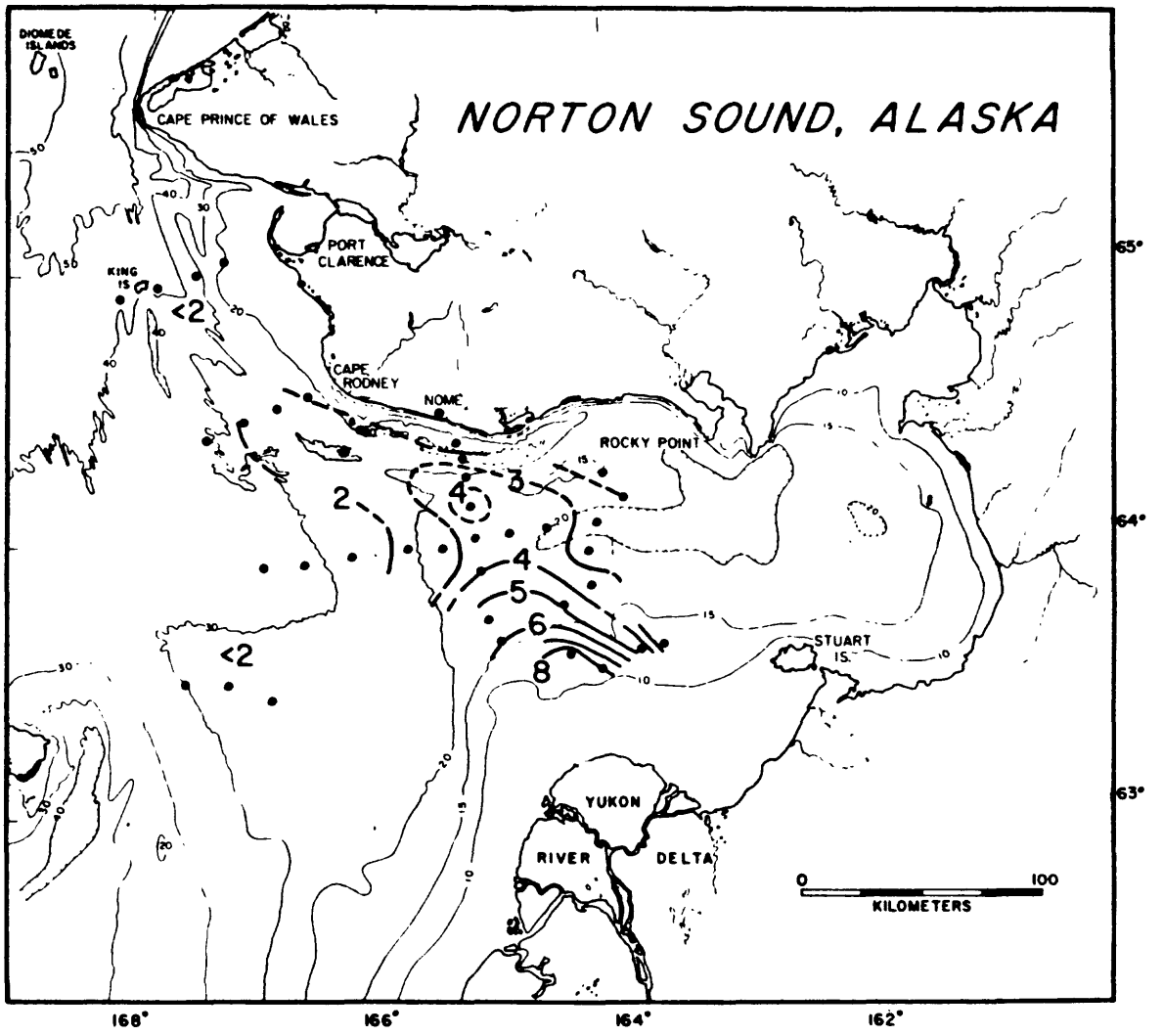

Figure 12. Total suspended matter (in mg/L) one meter above sea floor during February-March 1978. Station positions were dictated by weather and ice conditions.

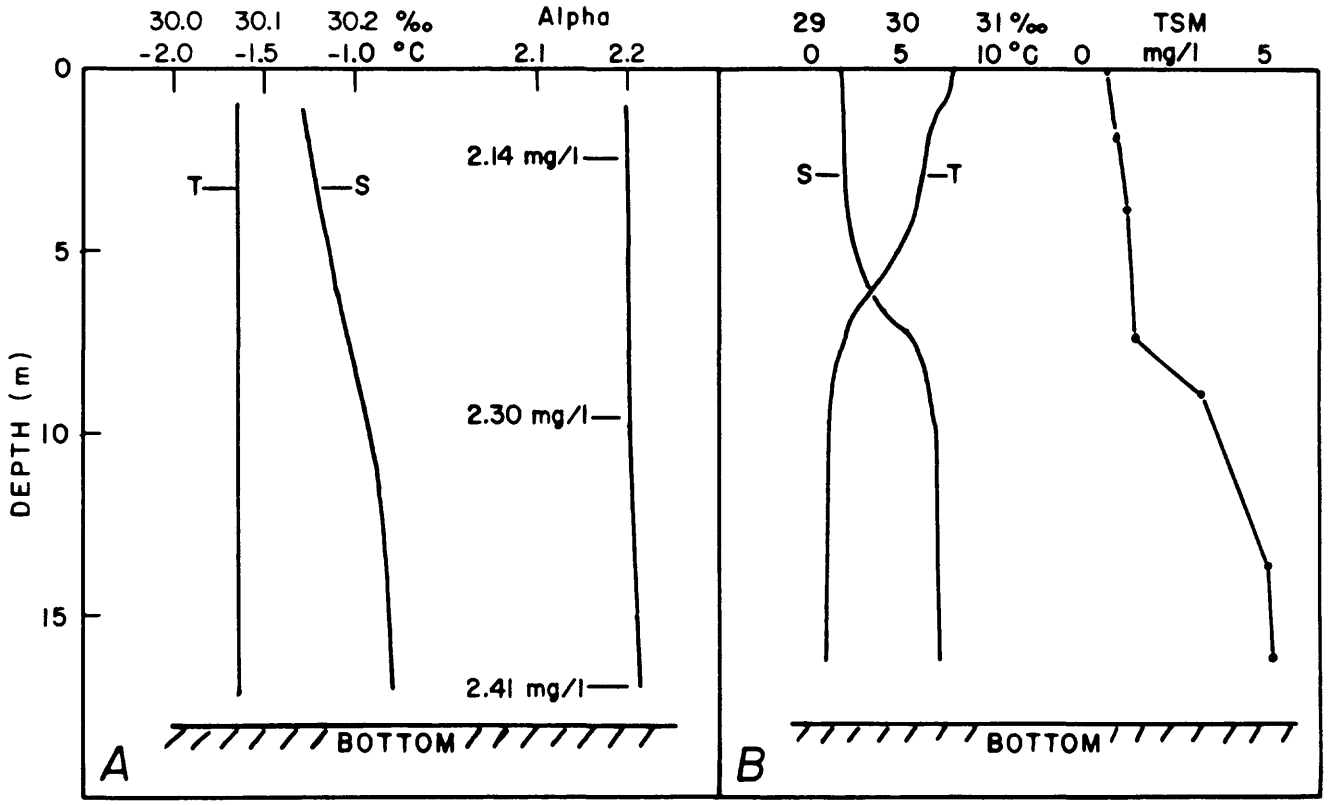

Figure 13. A. Temperature, salinity and light beam attenuation (alpha) values at the GEOPROBE site (see fig. 2) during February 1978. Three suspended matter concentrations (mg/L) are shown. B. Temperature, salinity and total suspended matter (TSM) profiles at GEOPROBE site in July 1977. Note the changes in temperature and salinity scales between panels A and B.

TABLE 1: Suspended Matter

Sample Location	Texture*	Combustible Matter**
1. Norton Sound (21 stations)	Fine to medium silt (4-32 μm with <10% clay. Sand present only at stations 34 and 34 (Fig. 1).	78 to 94% with a mean of 87% Surface water: 78-84% Bottom water: 82-94%
2. Sphanberg Strait (3 stations)	Fine to medium silt. Minor clay and no inorganic sand.	Surface water: 67-79% Bottom water: 74-83%
3. Cape Rodney Transect (4 stations)	Fine to medium silt. Minor clay and biogenic detritus.	Surface water: 76-83% Bottom water: 64-88%

*Based on microscopic examination of all samples and microscopic size analysis of selected samples.

**Samples were combusted for 6 hours at 550°C in tared platinum foil crucibles.

prodelta deposits (Fig. 2). Both deployments resulted in successful measurements of bottom currents, pressure, temperature and the optical parameters, transmission and scattering. The 1977 record covered an 80-day period, July 8-September 26, and this data set provides an excellent comparison between fair weather and storm conditions.

Currents are measured at 5 positions on each GEOPROBE tripod as shown in Figure 3. The rotor/vane values represent average currents for each 1 hour interval; each e-m current sensor produces "burst" measurements taken one per second for 60 seconds during each 1 hour interval. The hourly averages for each current sensor over the entire 80 day period are shown in Appendix I. Also shown for each sensor are the statistics and histograms of speed and direction for the entire record.

Several significant results are obvious in the current data and are pointed out here. Refer to Appendix I for the figures.

(1) The speed and direction records are dominated by a tidal periodicity for the first 57 days (to about September 5). The tidal current has a mixed periodicity with a dominant diurnal component prevalent in the more intense E-W motion. A distinct spring-neap fortnightly cycle is evident, with relatively low currents with confused direction occuring during the neap stage. For example, CM 4 has weak, neap tidal current-speeds during the period around July 10 and again 2 weeks later on July 24, August 8, etc. The strongest tidal currents occur during peak springs: achieving speeds of about 25 cm/sec at CM 1 to about 35 cm/sec at CM 4. The E-W tidal currents are very energetic; these records compare favorably with the current meter record taken by PMEL near site G1 (not shown).

(2) The current records show events that are longer in duration than the daily tidal cycle. For example, on July 24-25, September 4-7, and especially during September 13-16 and subsequently the current speed records show prolonged

periods (>1 day) of increased, non-tidal flows. As will be discussed below, these events are correlated with increased wind speeds and wind direction shifts.

(3) The dominant low frequency non-tidal flow (daily-averaged) is generally northward, with added eastward component at CM 1 and CM 4 (Appendix I - "stick" diagrams). The small magnitudes of the daily averages, denoted by the short "sticks" in the daily vector records are statistically insignificant. However, the large northward daily component during September is significant and occurs during strong southerly winds. The progressive vectors plots essentially estimate the daily drift over the 80-day record at each sensor, and show the north-northeastward motion (about 2.5 km/day or 3 cm/sec at CM 4).

(4) The storm-intensified bottom flow during September 13-15 has hourly average values (i.e. burst averaged) of nearly 25 cm/sec at 20 cm above the bed (CM 1) and greater than 40 cm/sec at 100 cm above the bed (CM 4).

(5) Strong non-tidal flows subsequent to the September 13-15 storm event are quite evident. The N-S component has a marked northward component of about 10 cm/sec at CM 4 throughout the period September 21-22 and the diurnal overtones. The other sensors show a similar northward polarization during the post-storm period.

Graphs of the power spectra for each time-series record of burst-averaged currents are also given in Appendix I. The kinetic energy spectrum for each sensor shows that the diurnal and semi-diurnal components dominate the motion field; however, a lower frequency peak (not significant at 95% confidence interval) is present at a period of about 140 (5.8 days). The spectral plots for E-W and N-S components generally show largest power at the diurnal period.

The e-m current sensors were sampled each second over a single 60 second burst to obtain measurements of the surface wave-induced currents. The data are too numerous to present as time series plots for the entire 1,900 burst sequences. The total number of burst data points for each e-m current sensor is about 1.2×10^5.

The most significant finding is that the large surface waves and swell (1-2 m) during September 13-14 occurred during strong southwesterly winds (~20 knots) that persisted for over 24 hours. Additionally, this was a period of high spring tides. The combined wind-driven, wave-induced, and tidal currents produced near-bottom currents of 60-70 cm/sec at the times of measurements.

The maximum periods of the wave motion derived from the pressure data were 5 sec., 7 sec., and 11 sec. The relatively long periods during the strong winds in September 13-14 are particularly significant because of the shallow water depth of 20 m at site G1. These waves probably were swell that had propagated into the area from the SW.

Figure 14 contains GEOPROBE sensor data for the first 30 days (July 8-August 7) of the 1977 experiment. The uppermost graph shows hourly averages of current speed obtained with the rotor/vane sensors. Semi-diurnal tidal motion and two fortnightly tidal cycles are quite obvious in this record. Spring tidal current speeds have daily maxima of 25-32 cm/sec; neap tidal current maxima are 10-15 cm/sec.

The plots of light transmission (TRANS) and light scattering (NEPHEL) in Figure 14 are presented as relative units of measurement taken once each hour (basic interval). The relatively persistent, low levels of scattering, about 0.24 relative, corresponds to about 3-5 mg/L as derived from calibration data (not shown here). These levels are representative of the quiescent conditions in the region of measurement as determined by independent shipboard sampling (about 4.4 mg/L).

Light transmission is more sensitive to turbidity fluctuations than scattering at relatively low levels of suspended concentrations. Therefore, the diurnal fluctuations in light transmission, not apparent in the scattering record (July 8-July 21), correspond to real changes in the turbidity levels

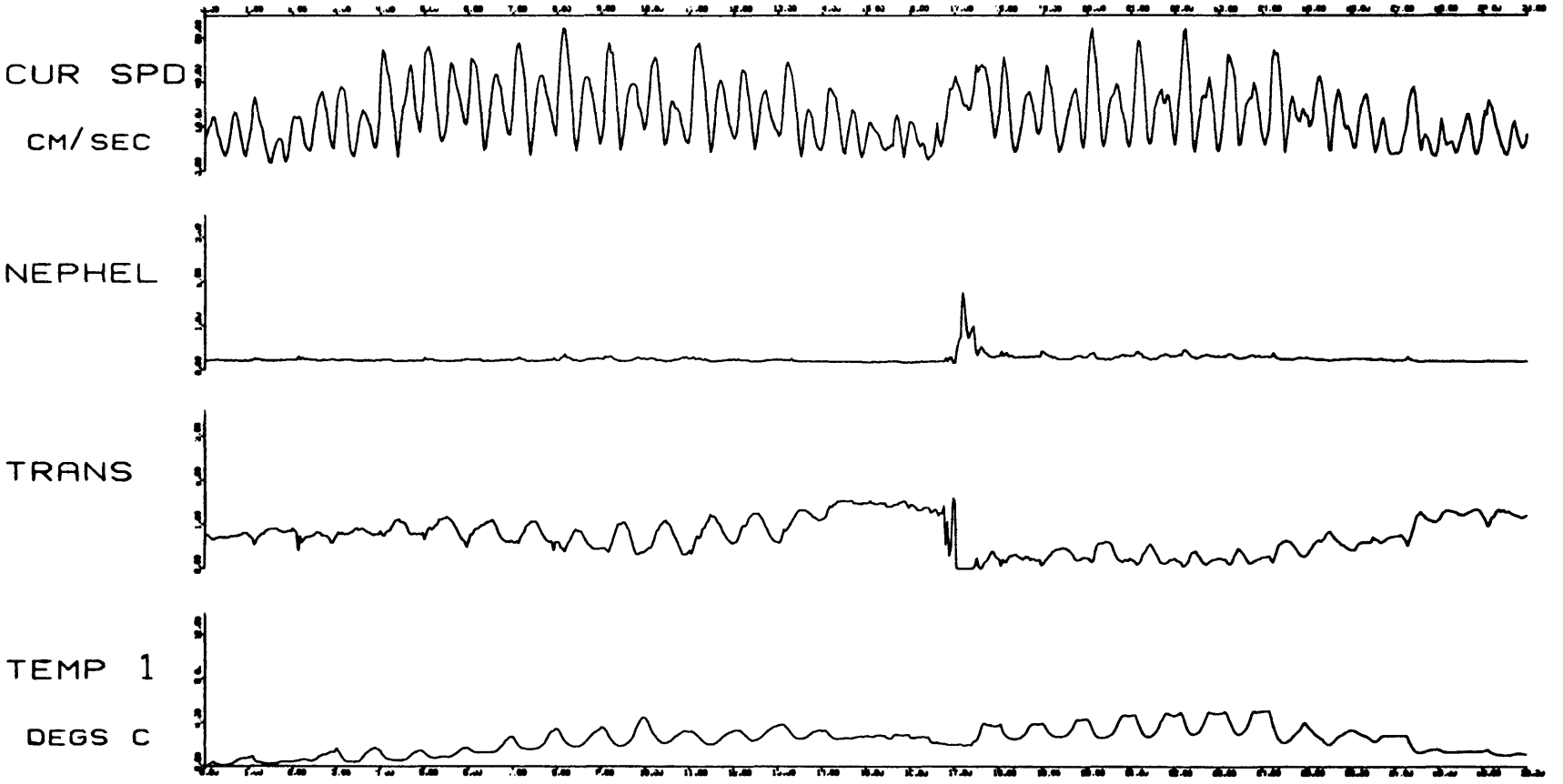

Figure 14. Hourly GEOPROBE data taken over the period, 0000, July 8 - 0000, August 7, 1977. Current speed (CUR SPD) at top are hourly averages obtained with the Savonius rotor (1.4 m above bottom). Light scattering (NEPHEL) and light transmission (TRANS) are in relative units; values for these and for temperature (TEMP 1) were taken once each hour. The horizontal axis is in days and the maximum current speeds were about 32 cm/s.

(about 1-2 mg/L peak-to-peak). These tidal fluctuations in turbidity are correlated with similar diurnal oscillations in the temperature data. A more detailed examination of these results shows several significant features:

(a) The oscillations are distinctly diurnal, not semi-diurnal.

(b) Periods of low temperatures ("cold") are correlated with values of low turbidity ("clear").

(c) During times of neap tide (July 8, July 23, August 6) both turbidity and temperature are relatively steady.

The above features suggest that tidal advection, specifically the E-W diurnal motion evident in the current speed (E-W) values transports water into and out of Norton Sound, sweeping past site G1. This mechanism is a more plausible explanation for the observed values than vertical advection or mixing caused by the internal tide because of the correlation of "cold" with "clear" water. Since the bottom water is colder and more turbid than the surface layer, a vertical mixing or advection process would presumably cause a correlation of "cold" with "turbid" values. The horizontal tidal advection implies then that with a rms diurnal tidal speed of about 10 cm/sec, reversing lateral E-W transport of about 4.5 km will occur every 12 hours.

Even more noteworthy in Figure 14 is the unusual "event" that occurs on July 25, characterized by a sudden increase in scattering, decrease in transmission (i.e. sharp increase in turbidity), and a significant speed increase due to a non-tidal current. The peak NEPHEL value of 2.0 relative corresponds to about 50 mg/L in sediment concentrations, an order of magnitude increase over the "normal" levels.

Figure 15 shows the weather data recorded at the National Weather Service station at Nome (about 30 miles to the north) during the period of this unusual event. Hourly values of wind speed, wind direction and air pressure are plotted

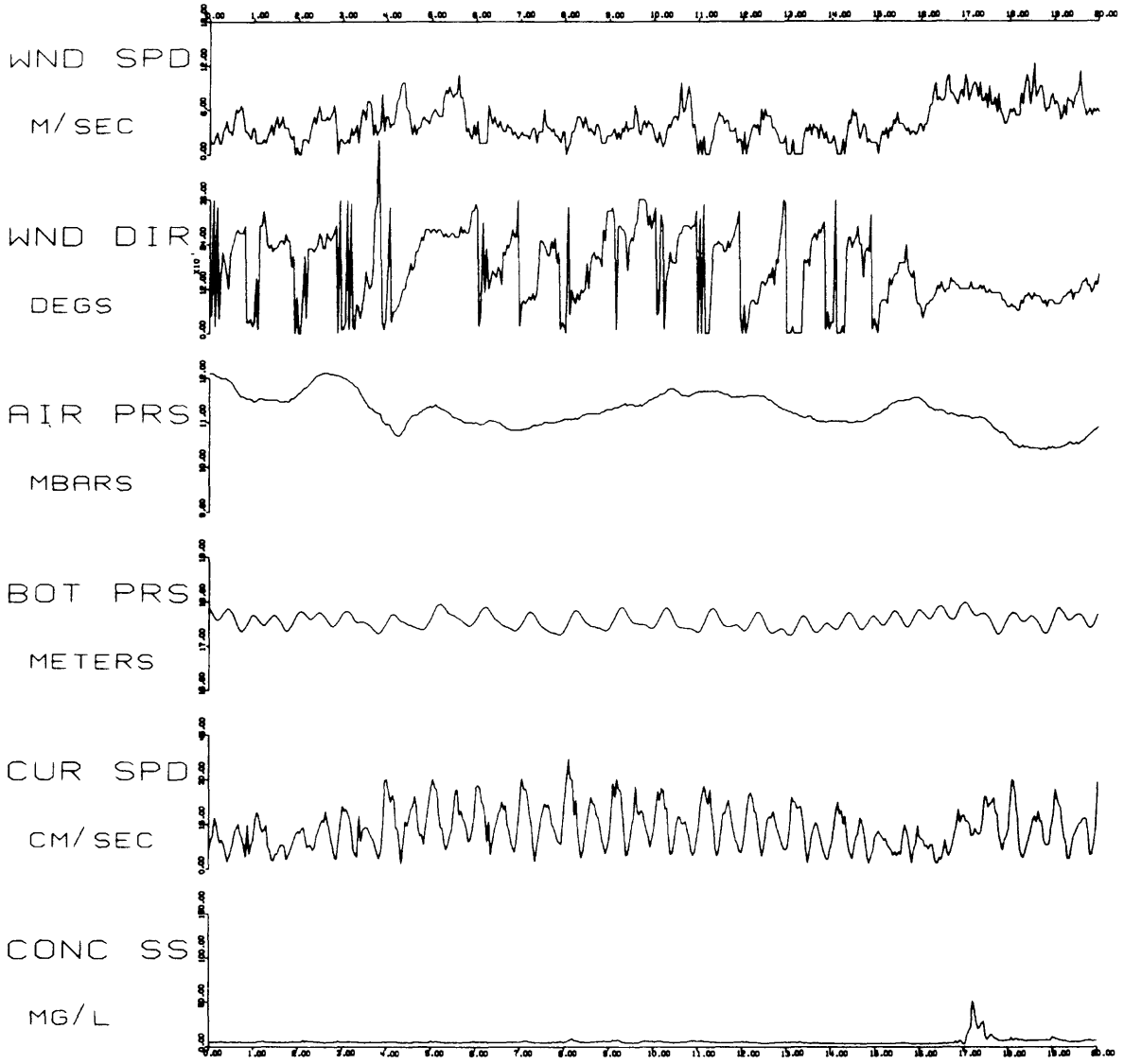

Figure 15. Meteorological data recorded at Nome, Alaska (National Weather Service) and GEOPROBE data obtained during July 8 - July 28, 1977. The data show an increase in wind speed on July 24 which was followed by a sudden increase in suspended matter at the GEOPROBE site. The current speed data are hourly averages obtained with the Savonius rotor. See figure 16 for wave-generated currents on July 24-25.

in this figure. The wind data show a regular diurnal cycle, with wind speeds generally lower during the late evening-early morning hours. During July 24 wind speeds increase to 9-10 m/sec (about 20 knots) and become persistent, above 12 knots, over the next several days. Wind direction also becomes steadier from the SE during this period. Air pressure drops off, suggesting the passage of a low pressure center through the region. The larger surface waves caused by the increased wind stress produced maximum oscillatory bottom currents as high as 35 cm/sec (Fig. 16). The increased, sustained wind stress, occurring at the end of a neap stage in the tidal regime, apparently also caused an increase in magnitude and duration of the mean bottom current speed. The combined effect of higher wave-induced and wind-driven currents produced a bottom stress competent enough to cause the relatively large increase in concentrations of suspended materials (~50 mg/L). The sudden onset and equally sudden decrease in the concentration values are probably a result of initial resuspension of fine-materials that had settled out locally during the immediately preceding time of neap tide, and to increased upward turbulent mixing of the higher near-bottom suspended load by vigorous wave activity.

National Weather Service atmospheric records show that only one intense, prolonged storm traversed the eastern portion of the Northern Bering Sea during the 80 day period of GEOPROBE measurements. A surface pressure analysis of this storm for September 13, 1977 is shown in Figure 17. The storm track was east-northeastward; its center passed well to the north of the GEOPROBE site. Wind observations at Nome show that sustained southerly to southwesterly winds commenced in the morning of September 12 and continued for about 3 days. Wind speeds of up to 30 knots (15 m/sec) with gusts to 45 knots were recorded at Nome during this period.

Hourly averaged bottom currents during the storm increased to 45 cm/sec

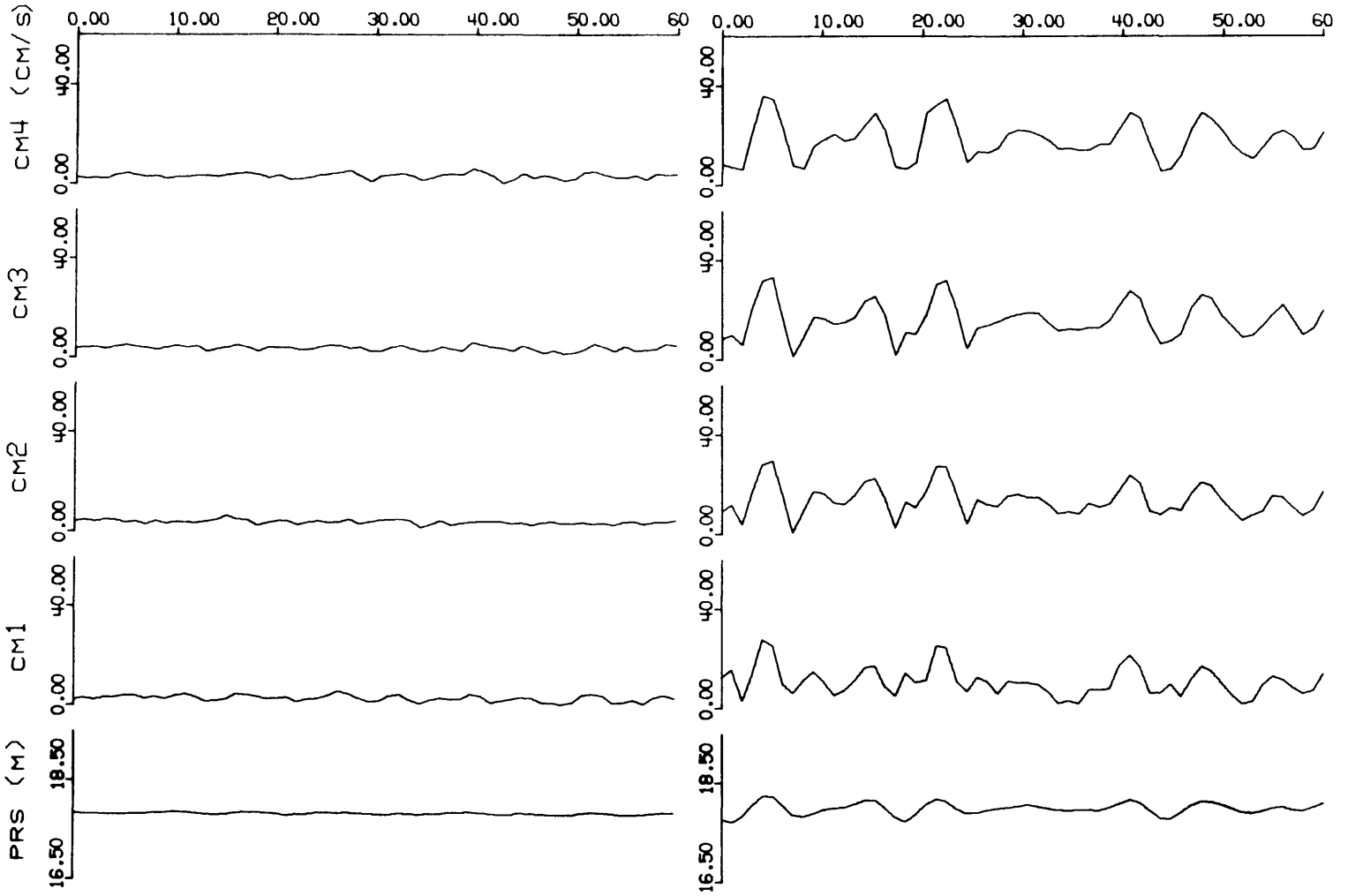

Figure 16. Burst mode data (1 per second) of the electromagnetic current meters and the pressure sensor at 2100 hours on July 24, 1977 (left panel) and 0900 hours on July 25, 1977 (right panel). The current sensors, 1 through 4, were positioned 20, 50, 70 and 100 cm respectively above the sea floor.

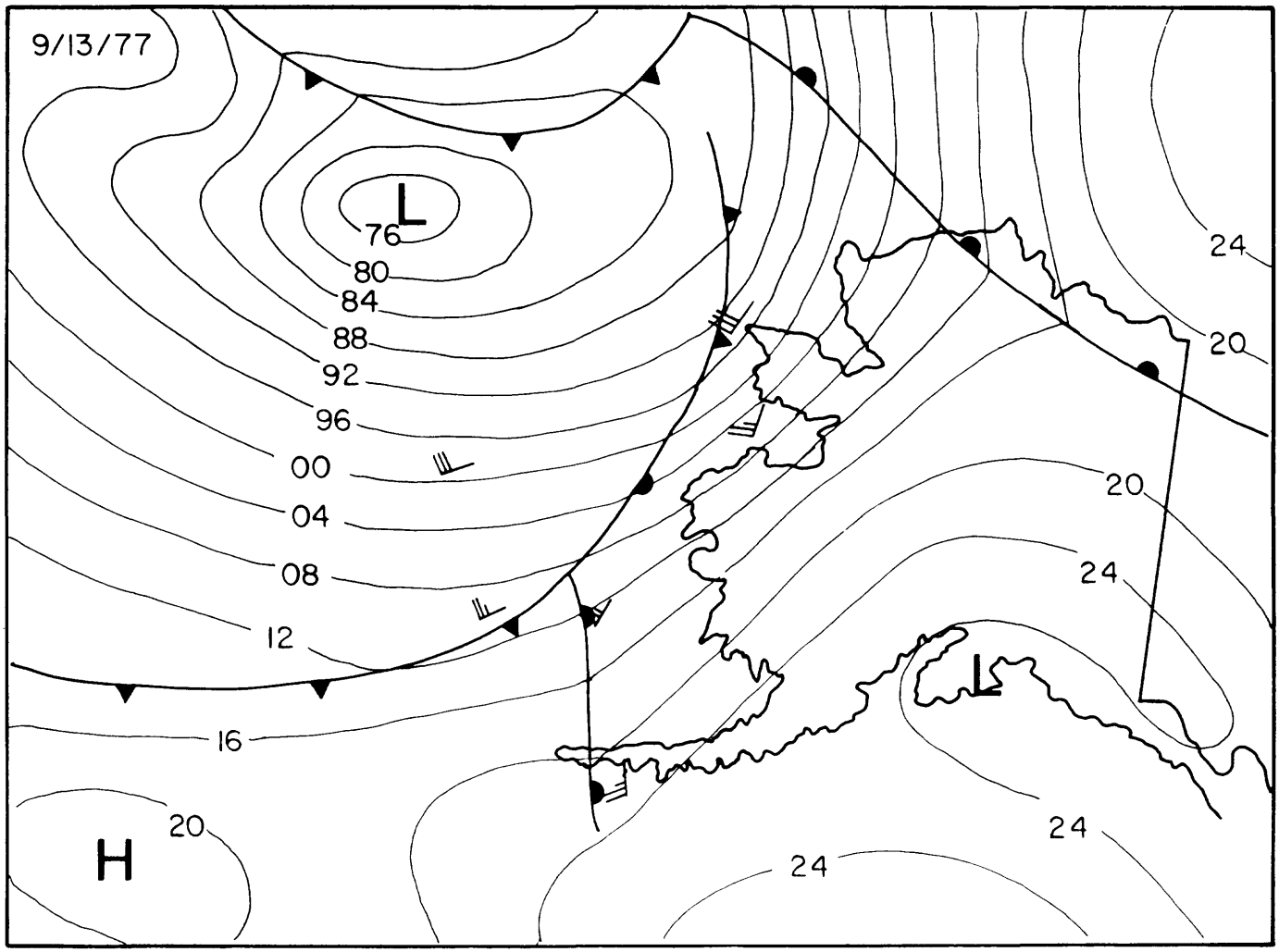

Figure 17. Surface pressure map for September 13, 1977. Steady winds at Nome, Alaska were 25 knots from the S-SW. Movement of the low pressure cell was from west to east during September 13-September 15, 1977.

(at 1 m above the bottom) early on September 14 (Fig. 18). Current directions during this period became northerly and more persistent. The strong tidal signal in the pre-storm pressure and current records was masked by the wind-driven effects. A low-frequency increase in bottom pressure during September 12-16 is caused by the combined effects of sea surface set-up along the northern shore of Norton Sound driven by strong southerly winds, and the "inverted barometer" effect of the passing low pressure system. The offshore pressure gradient associated with set-up along the Nome coast might have induced signficant along-shore geostrophic flow similar to that described by Beardsley et al. (1977) in the Middle Atlantic Bight. Future analysis of tidal station data collected at Nome and at the eastern margin of Norton Sound should provide an estimate of this flow.

TSM values increased abruptly to 115 mg/L on September 13 shortly after the increase in bottom currents (Fig. 18). Except for an abrupt decrease in TSM late on September 13, corresponding to a slight decrease in bottom current speed, TSM levels remain high throughout and even after the storm period. A peak TSM value of 150 mg/L was measured at 0600 on September 14.

Burst pressure and current data show that near bottom wave-induced currents were insignificant during the pre-storm period (Fig. 19). However, during the storm the wave-induced bottom pressures had maximum values equivalent to wave heights of about 2 m (Fig. 19). Peak wave-induced current speeds were 30 cm/sec at 1 m (cm 4) and nearly 20 cm/sec at 20 cm (cm 1) above the sea floor. Instantaneous bottom currents during the storm reached speeds of 70 cm/sec at 20 cm above the sea floor (Fig. 19).

DISCUSSION

Transport pathways of suspended sediment

Three transport pathways are important in the dispersal of terrigenous silt

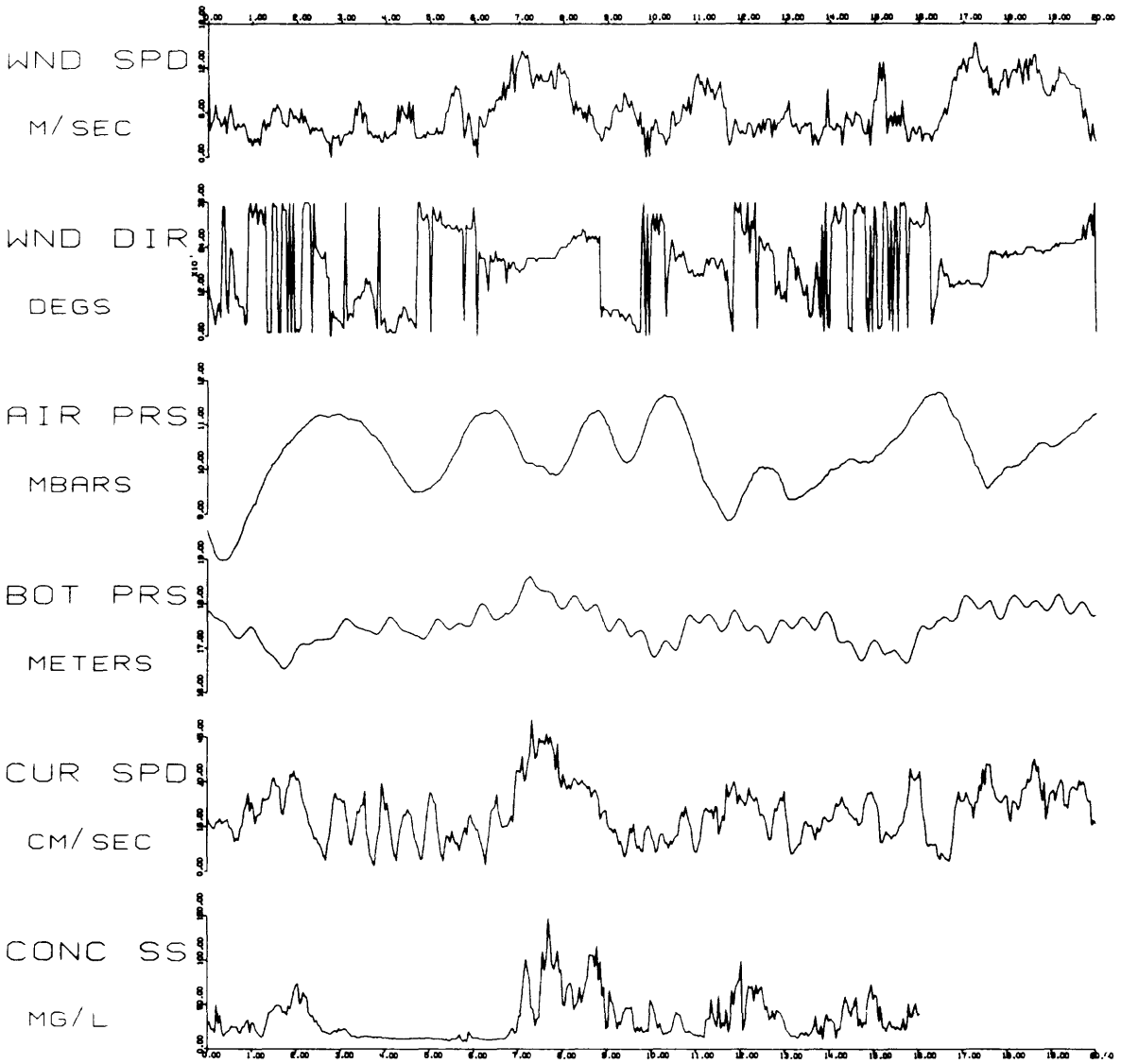

Figure 18. Meteorological data recorded at Nome, Alaska and GEOPROBE data for the 20-day period 0000, September 7 - 0000, September 27, 1977. The bottom pressure (BOT PRS) and current speed (CUR SPD) data are hourly averages. The suspended matter concentrations (CONC SS) are derived from the light scattering values using calibration data. The peak CONC SS value was 150 mg/L on September 14, 1977.

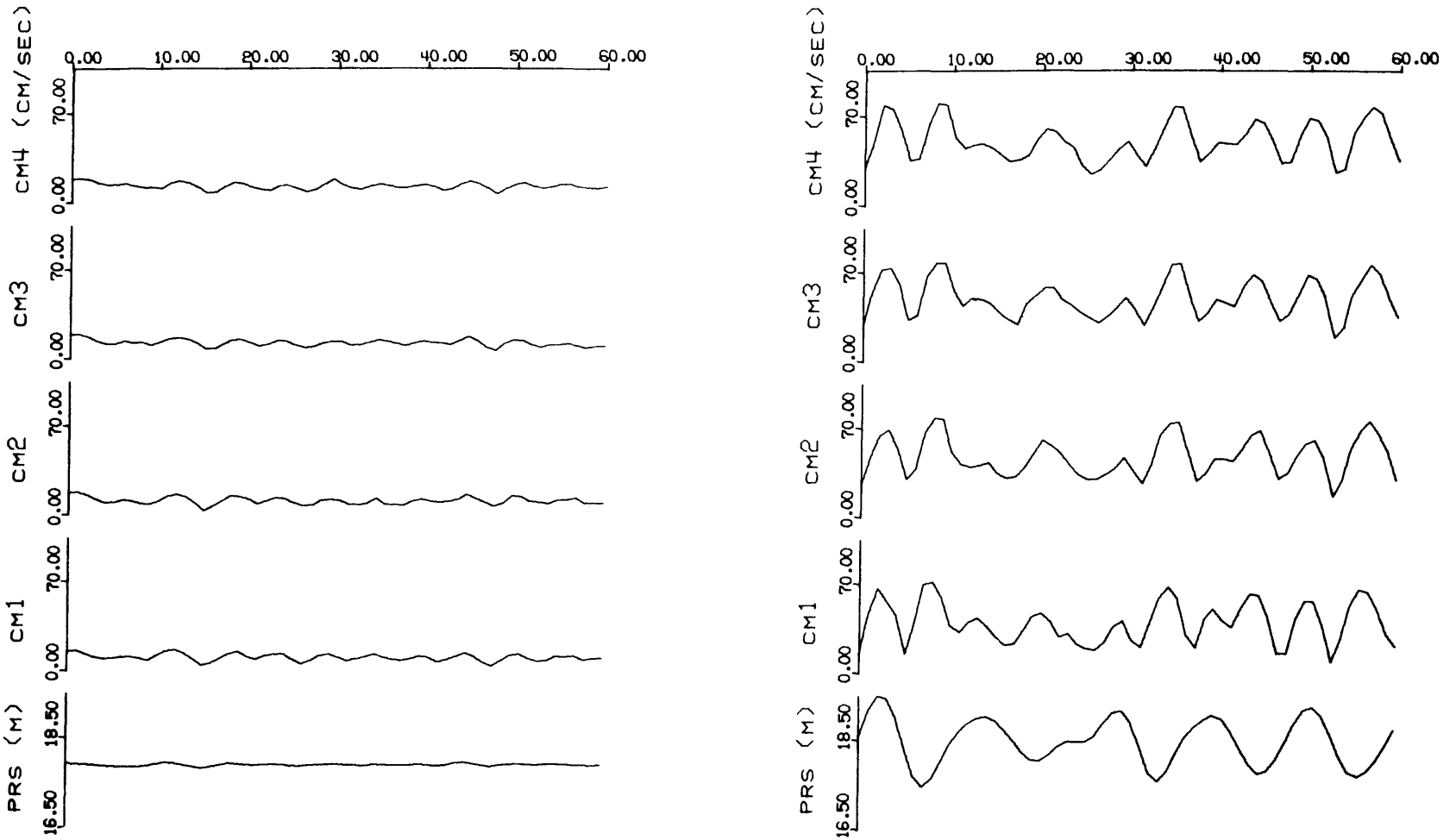

Figure 19. Bottom current speed and pressure data obtained prior to (left panel) and during (right panel) the September 14-15 storm in Norton Sound. Current speeds were recorded each second for 60s at 20, 50, 70 and 100 cm above the bottom (CM1 - CM4, respectively). The pressure data reveal an approximate wave period of 10s.

and clay delivered by the Yukon River:

1. Initial transport is characterized by westerly and southerly flow within 20 km of the Yukon Delta. Turbid water commonly extends south to Cape Romanzof and on 29 June 1977, a NOAA satellite image suggests transport as far south as Hazen Bay. This transport pattern, evident on satellite images, is rather surprising because one would expect that the density distribution would generate currents to the north and east around the delta front (owing to Coriolis effect). W. Dupré (RU 208) has found that embayments to the south of the major Yukon River distributaries contain large amounts of modern Yukon silt. This finding provides independent evidence to support the importance of southward nearshore flow.

2. Our studies, the studies of Muench et al. (1977), and a large body of data collected over the years by L. Coachman and his associates (University of Washington) demonstrate a nearly "unidirectional" flow of shelf water northward between the mainland and St. Lawrence Island. This flow is driven by the difference in sea level between the Bering Sea and the Arctic Ocean and the need to replace water lost from the Arctic Ocean to the Atlantic Ocean. The suspended matter that is moved southward along the west shore of the delta either accumulates in "low energy" lagoons and bays or returns with the Alaskan Coastal water.

As this current flows past Norton Sound it tends to mix with turbid Yukon water in the vicinity of the delta. This mixed water then extends across the mouth of the Sound toward the Nome coast. There is no question that the currents immediately N and NW of the delta are complex. Nevertheless, the distributions of both surface and near bottom suspended matter demonstrate the existence of this important northward transport pathway. Muench et al. (1977) have postulated a mean circulation system that includes a cyclonic gyre centered in the outer portion of the Sound north of the delta. In order to obtain agreement between

our results and this circulation pattern, it is necessary to postulate a split in the northward flow near the Yukon delta with part of the water moving directly across the Sound and another part moving into the Sound to feed the cyclonic gyre. More long-term current measurements are needed to fully describe the flow field over the Yukon prodelta.

3. Bottom sediments in the inner part of the Norton Sound are derived from the modern Yukon River (Nelson and Creager, 1977). In fact, accumulation rates of mud in this area (east of Cape Darby - Stuart Island) are among the highest on the northern Bering Sea shelf. Suspended matter distributions in 1977 and also in 1976 (Cacchione and Drake, 1977) suggest transport of Yukon silt and clay eastward past Stuart Island. However, the available data do not support a strong interchange of water between the inner and outer parts of Norton Sound (Muench et al., 1977; Drake et al., 1977). Satellite images tend to show a steep gradient decrease in TSM at the surface near Stuart Island such that the bulk of the suspended matter is confined to Pastol Bay (west of Stuart Island).

The effects of wind stress on the circulation in the Sound are not well understood but it seems likely that periods of westerly winds would drive surface water eastward along the southern coast and into the inner Sound. West and southwest winds exceeding 15 knots occur on about 3-4 days during each of the summer months (based on weather records at Nome); winds come from the southwest quadrant approximately 40% of the time. It is possible that flow into the inner Sound occurs whenever the wind stress is sufficient to overcome the effects of other forcing mechanisms. The transport of suspended matter eastward from the delta is not as important as other transport pathways. However, the sediment that is carried into the inner part of Norton Sound tends to remain there. We believe that key factors in this sediment retention are the low energy of bottom currents in this area and the limited exchange of bottom water with the

outer Sound (as shown by the presence of remnant, winter bottom water well into the ice-free season). Of these two factors we suspect that the latter is the more significant because TSM concentrations in the remnant water are relatively high indicating that this water, although isolated, is not motionless. Current data collected by R. Muench within the postulated remnant water body southwest of Cape Darby (Fig. 1) show tidal currents of up to 30-40 cm/sec but essentially no net motion. It seems likely that a similar but less vigorous current regime also would characterize the bottom water within the inner Sound. Additional data are needed.

Comparison of 1976 and 1977 Results: summer season

Suspended sediment distributions on many continental shelves exhibit a large degree of spatial and temporal variability. Much of the variability is caused by wind-driven transport combined with variable rates of fine sediment resuspension by wave action.

The data for Norton Sound in late summer of 1976 and early summer of 1977 reveal strikingly similar suspended sediment patterns. In both cases the distributions at the surface and near the bottom are dominated by a broad tongue of turbid water that originates along the western side of the Yukon Delta and extends across the mouth of Norton Sound. Temperature and salinity values show that this water is a mixture of Alaska Coastal water and Yukon River water.

These results along with the GEOPROBE measurements indicate that current patterns and speeds in the outer part of the Sound are caused principally by the tides and the regional transport of Bering Sea shelf water toward the Chukchi Sea. In particular, it appears that the regional flow establishes, to a large degree, the mean circulation pattern in the Sound whereas the tidal currents (primarily constrained to flow E-W) serve to maintain particles in suspension and also resuspend materials at times of spring tides. Tidal excursions are

approximately 4 to 5 km with only a small net motion. Consequently, they act as a diffusing element. The "clarity" of the observed suspended matter distributions (i.e. the sharpness of boundaries between clear and turbid waters) suggest the importance and consistence of the advective flow regime in the western part of Norton Sound.

The situation is different in the inner part of Norton Sound (east of Cape Darby and Stuart Island). There the suspended matter distribution tends toward greater uniformity, particularly in September 1976. This suggests that tidal and wind-driven currents are more significant compared to advection. As discussed above, the inner part of Norton Sound is strongly two-layered and the lower layer is water formed during the winter months. Substantial advective motion must be restricted to the low density surface layer and mixing across the pycnocline must be minimal (Muench et al., 1977).

Comparison of summer and winter suspended sediment transport

Ice begins to form in Norton Sound in late October, first along the shore and within protected shallow bays and later in the central area (Muench and Ahlnas, 1976). By December the sound and most of the northern Bering Sea is covered with seasonal pack ice and shorefast ice. Surface water cooling, from values of 6-8°C in October to <0°C in February (R. Tripp, personal communication, 1978) along with salt enrichment during ice formation leads to convective mixing of the shallow water column. Furthermore, local river flow is significantly lower in the winter and the pack ice restricts surface layer mixing by wind and waves. Consequently, the two-layer density system present in summer (Drake et al., in press) is replaced in winter by one layer which is nearly homogenous vertically. Profiles of temperature and salinity collected by Knut Aagaard (University of Washington) during February and March 1978 show that there is a slight density increase with depth in Norton Sound (density gradient = 7.5×10^{-5} g/cm^3 /m).

During the summer months the two-layer density system (Fig. 13) is associated with a well-developed vertical stratification of suspended matter with most of the sediment in the lower layer (Drake et al., in press). For example, in July 1977, TSM concentrations in the lower layer (~10 m thick) at the GEOPROBE site averaged about 4.4 mg/L, whereas concentrations above the pyncnocline ranged from 0.7 to 1.5 mg/L. In addition, the surface layer contained 10-15% organic matter while the bottom layer contained <5% combustible components. Muench et al. (1979) and Drake et al. (in press) present temperature, salinity, TSM and current meter data which show that the two layers tend to follow the same flow pattern over the Yukon prodelta. This circulation pattern is characterized by a general northward water drift highlighted by a tongue of turbid water extending toward the Nome-Cape Rodney coast (Fig. 6).

Although there have been no current meter observations during the winter months on the prodelta, the distribution of TSM in winter 1978 (Fig. 12) is essentially the same as that found during the summer months. This suggests that northward advection continues to dominate the circulation on the prodelta in the winter and the hydrographic data of K. Aagaard (in preparation) are in agreement with this conclusion.

A fair comparison between the summer and winter suspended matter concentrations can be made by calculating average TSM values for the water column at each station. The results of this analysis conclusively demonstrate that the amount of sediment in suspension over the prodelta during our winter sampling was essentially the same as during July 1977 (Fig. 20). Furthermore, microscope inspection of the particulate matter from the two periods reveals no significant differences in texture; inorganic fine and medium silt with subordinate amounts of clay are characteristic of both sample sets.

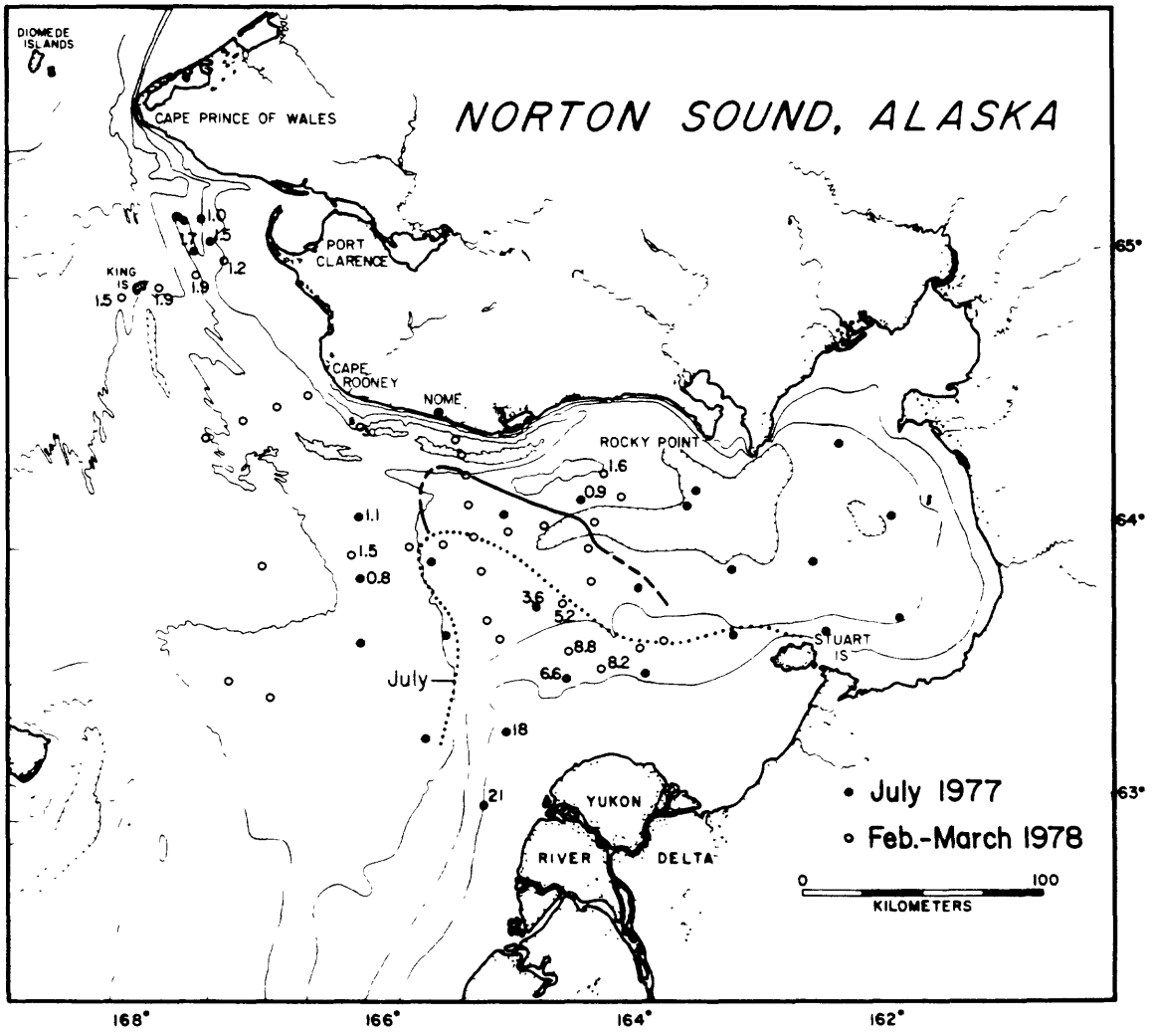

Figure 20. Depth-averaged concentrations (in mg/L) of suspended matter during July 1977 and February-March 1978. The dotted line is the approximate position of the 3 mg/L isopleth for July 1977 and the solid line is the 3 mg/L isopleth during the winter period.

The unexpectedly large amounts of TSM in the winter cannot be attributed to storms. In fact, both the summer and winter sampling programs were completed during the early stages of a neap tide cycle, and National Weather Service records for Nome, Alaska show no unusual wind or air pressure events before or during the sampling periods. In the absence of significant wind effects (waves and wind-driven flow), the concentrations and distribution of suspended matter over the Yukon prodelta must be maintained by reworking of existing sediments by the tidal currents coupled with advection by the northward mean flow. This interpretation suggests that much of the silt and very fine sand introduced early in the summer by the Yukon River must be deposited on the shallow inner part of the prodelta and on the shallow bank (called the sub-ice platform by Dupré, 1978) which rims the delta. Thereafter, this reservoir of sediment is resuspended and transported northward toward the Nome-Cape Rodney coast. Thus, at some distance from the delta, perhaps on the order of 30-50 kilometers, the effect of seasonal variations in river discharge on TSM concentrations becomes small relative to variations caused by the characteristics of the flow field in Norton Sound. In essence, the peak discharge of the Yukon River in early summer exceeds the capacity of the currents to disperse the sediment. The result is initial deposition of silt near the delta followed by resuspension through the rest of the year.

Similar sediment transport systems have been observed after major floods on the southern California shelf (Drake et al., 1972) and on the Rio de la Plata shelf, Puerto Rico (Pilkey et al., 1978). The latter authors have called the shelf sediment bypassing process "mud hopping." The term "mud hopping" may be somewhat misleading in that there is probably a continuous, albeit relatively small, amount of suspended sediment moving in the shelf bottom boundary layer at all times (Drake, 1976). Nevertheless, the term does focus attention on the large variability in the strength of shelf currents and, consequently, a similar variability in rates of sediment transport.

The tidal amplitude in the northern Bering Sea averages only 30 cm and on the open shelf west of Norton Sound the peak tidal currents are on the order of 5-10 cm/s (Muench et al., 1978). In contrast, tide-generated currents in the sound are strongly polarized to flow east-west and maximum bottom current velocities range from about 10 cm/s to 30 cm/s during neap and spring cycles, respectively (Cacchione and Drake, 1979). Surface waves during fairweather summer periods generate bottom currents of 5-7 cm/sec at the GEOPROBE site. The bottom shear velocities ($u_* = \tau/\rho$) associated with these currents are typically about 1 cm/s or less during neap tides and 1.4 to 1.5 cm/s during spring tides (Cacchione and Drake, in press). Sediment at the GEOPROBE tripod site (18 m) is moderately well sorted silty, very fine sand with a mean diameter of ~70 μm; initial motion of these materials should occur at u_* values of approximately 1.3 - 1.4 cm/s (Komar, 1976). Although cohesive effects might be expected to significantly increase the critical u_* above 1.4 cm/sec (Drake, 1976), the 1977 GEOPROBE results show that the sediment responds as a noncohesive material (Cacchione and Drake, in press). High water content (>75% by volume) of the surficial sediment and a near absence of clay (<5%) may substantially reduce cohesive forces (E. Clukey, unpublished data). Accordingly, during "non-storm" periods in both the summer and winter seasons the neap tidal currents maintain clay and fine silt in suspension but are too weak to resuspend prodelta sediments at the GEOPROBE site. At shallower sites closer to the Yukon Delta resuspension probably continues even during the neap cycle. Currents associated with spring tidal cycles are likely to exceed the threshold velocities of the bottom sediments over the entire prodelta. Thus, "mud hopping" events would be most pronounced during spring tide periods on the Yukon prodelta in the winter months.

The principal oceanographic difference between the ice-covered and ice-free regimes in Norton Sound is the reduction of storm effects (primarily wave action)

during the former period. However, sudden large changes in atmospheric pressure might generate significant "surge" currents during any season. We have no data on possible storm-generated currents in the winter.

The assumption that sediment transport on arctic and subarctic continental shelves is of little consequence during the winter season is questionable. Admittedly, the transfer of energy at the air-sea interface is significantly lower in the winter and new contributions of sediment are negligible. Yet, in some areas the tide-generated and mean advective currents apparently are sufficient to erode and transport important quantities of sediment which entered the system during the previous summer.

Indeed, there is evidence from the Beaufort Sea shelf that indicates a substantial acceleration of nearshore currents where they are constrained to flow beneath a 1-to-2-m-thick layer of floating shorefast ice (Reimnitz et al., 1977). Recent studies by W. R. Dupré (University of Houston) suggest that currents below the floating fast ice, which rims the Yukon Delta to a distance of 30-40 km offshore in the winter, may be resuspending silt and producing a band of relatively well sorted sand concentric to the delta shore at a distance of some 10-20 km. Furthermore, Nelson (1978) finds an abundance of ice-keel gouge marks at depths of 10-15 m on the Yukon delta front and prodelta in Norton Sound. He believes that many of these gouges are produced by seasonal (first year) ice within the pressure ridge-shear zone which forms along the seaward edge of the floating fast ice. It is possible that ice keels, by locally obstructing the flow, intensify the tidal currents around the front of the delta. These effects may partially offset the absence of wave-generated currents in shallow areas during the winter season. The presence of small amounts of very fine sand in suspension at two stations at a depth of 11 m on the delta front in February lends some support to this interpretation.

Temporal variability of sediment transport

The GEOPROBE tripod data provide a valuable time history of near-bottom measurements of fluid and sediment parameters for the 80 day deployment period. One of the most significant results is the contrast in the local dynamic conditions that occurs during "normal" and stormy periods. The "normal" near-bottom flow field is characterized by the data shown in Figures 14 and 15 for the period July 8 - July 24. During this time tidal forcing dominates the hourly mean values of pressure, bottom current, temperature and turbidity. Small perturbations in the tidally-dominated "normal" regime occur, principally due to short periods of increased wind-driven currents and waves.

The tidal bottom currents are most intense during spring tides, commonly achieving values of greater than 30 cm/sec at 1 m above the sea floor. During neap, the daily maximum currents at 1 m are much reduced, typically less than 15 cm/sec during the smallest tides. As Figure 15 shows, the bottom pressure has a definite change in pattern during the fortnightly cycle. The spring tides are strongly mixed with two unequal highs during each daily cycle; the neaps are more nearly a diurnal type.

Figures 18 and 19 point out the extreme importance of storm conditions in affecting the sediment transport pattern in this area. The relatively high, sustained values of hourly-averaged bottom current speed and the persistent northward directions are indicative of active, large transport of materials. These wind-generated events appear to overwhelm the rhythmic pattern that is the "normal" condition.

Threshold and established conditions of sediment transport can be computed from the Geoprobe results. Bottom shear velocity, u_*, is estimated from the e-m current meter velocity data using the Karman-Prandl logarithmic expression for the velocity, u, at a level z, above an hydraulically rough bottom:

$$u = \frac{u_*}{k} \ln z/z_o \qquad (1)$$

where u_* is the shear velocity, k ($\tilde{}$0.4) is von Karman's constant, and z_o is the roughness scale.

By definition, $u_* = (\tau_{b/\rho})^{\frac{1}{2}}$ where τ_b is bottom shear stress, and ρ is fluid density. It should be noted that approximately 80% of the hourly velocity profiles (burst-averaged) taken with the four e-m current meters over the entire 80 day experiment fit a logarithmic curve with regression coefficients of 0.95 or higher.

Wind-generated waves caused by storms over continental shelf regions can create significant bottom stresses. As Smith (1977) points out, the addition of an oscillatory stress component by wind waves augments the downward transfer of momentum in the logarithmic region of the quasi steady boundary layer, causing an effective increase in the total eddy viscosity (K), or alternatively, an apparent increase in k. If we assume that maximum stress occurs when wave and quasi-steady components act instantaneously in the same direction, then

$$\tau_b = \rho \left[(u_*^s)^2 + (u_*^w)^2\right] \qquad (2)$$

u_*^s and u_*^w are the quasi-steady and maximum wave-induced components of shear velocity, respectively.

It should be noted here that the wave-induced and quasi-steady stress components are coupled non-linearly (Grant and Madsen, 1979), and that values of u_*^s and u_*^w taken from the e-m current data will each contain the effects of the non-linear wave-current interaction.

The e-m velocity measurements were taken well above the wave-driven turbulent boundary layer whose thickness, δ_w, is 0 (1 cm). Therefore, to estimate u_*^w we use the technique of Smith (1977):

$$u_*^w = \frac{U_o K}{z} \; f\,(\omega, z_o, K) \qquad (3)$$

U_o is the maximum oscillatory speed above δ_w. ω is wave frequency, and f (w, z_o, K) is a combination of Bessel functions that can be evaluated graphically.

Table II summarizes computed values of u_*^s, u_*^w, and z_o during the period 9 - 15 September 1977. Averages of hourly "bursts" of e-m current speed data were calculated for each of the four current meters, and used to compute u_*^s and z_o from equation (1). The maximum hourly values of u_* (column 2) and the 24-hour average values of u_*^s (column 3) and z_o (column 5) are shown in Table II. Daily maxima of u_*^w, computed from equation (3), are listed in column 4. Values of U_o were obtained at z = 20 cm; estimates of ω were taken from the burst pressure data.

The average values of u_*^s increase dramatically during the period of intensified wind-driven bottom currents of 13-14 September. On September 13, $\bar{u}_*^s$ = 3.1 cm/sec equivalent to a mean bottom stress of 10 dynes/cm^2. Maximum hourly stresses also are highest during the storm period. The ratio u_*^w/u_*^s (max.) (column 6, Table II indicates the relative importance of waves in the total bottom stress (equation 2); maximum wave stress occurred on September 14; u_*^w/u_*^s(max) = 1.9. The largest value of roughness reported in Table II is $\bar{z}_o$ = 1 cm, also on September 14. The equivalent physical roughness for z_o = 1 cm is about 30 cm (Schlichting, 1968) suggesting that either large bed forms developed during the storm, or the z_o value is anomalously large. Since the post-storm bottom photographs showed no development of sediment bed forms with relief exceeding 3 centimeters, the large computed

Table II. Shear velocity and roughness during September 9-15, 1977, in Norton Sound, Alaska

Date (Sept.)	u_*^s, max (cm/s)	$\bar{u}_*^s$ (cm/s)	u_*^w, max (cm/s)	$\bar{z}_1$ (cm)	$(u_*^w/u_*^s)_{max}$
9	2.5	1.1	<0.1	0.4	<0.1
10	2.3	1.1	<0.1	.7	<0.1
11	1.5	.8	<0.1	.1	<0.1
12	2.1	1.1	<0.2	.2	<0.2
13	5.4	3.1	3.0	.6	0.6
14	3.8	2.4	3.1	1.0	0.8
15	1.9	.9	1.8	.5	0.9

values of z_o are probably a result of the non-linear wave-current interaction which caused the wave stresses to generate an "apparent roughness" on the quasi-steady flow. This increased, "apparent" z_o agrees with the theoretical arguments of Grant and Madsen (1979) and Smith (1977).

When the local instantaneous shear stress, τ_b, exceeds a critical stress value, τ_c, needed for initiation of bottom sediment movement (i.e. $\tau_b > \tau_c$), then transport of the local bottom sediments will occur. An estimate of τ_c = 1.7 dynes/cm^2 for sediments at the Geoprobe site was obtained from the modified Sheild's diagram applicable to threshold conditions of sediment movement by waves and currents (Madsen and Grant, 1976). This critical stress determines a critical shear velocity, u_{*c}; here $u_{*c} \simeq 1.3$ cm/sec.

The results in Table II clearly show that during the storm period, bottom stresses increased markedly due to the combined action of waves and "quasi-steady" currents. On September 13-15, $\bar{u}_*^s + u_*^w >> u_{*c}$. These excessive stresses indicate that significant transport occurred during this time. During the pre-storm the period, bottom currents were predominantly tidal ("quasi-steady"), with no appreciable wave components. Subcritical mean bottom stresses were common, although daily maximum values of u_*^s did exceed the threshold level. This result suggests that the textural characteristics of the local surface sediments at the Geoprobe site are in balance with the tidal and steady stress components.

Hourly TSM values (Fig. 18) measured at 2 m above the bottom are highest during September 13-14, closely correlated with the times of maximum bottom stress. During the pre-storm period, near-bottom concentrations of 5-10 mg/L, relatively high for most open continental shelf areas (Drake, 1976) reflect the combined effects of the northwestward projecting sediment plume of the Yukon River and turbulent mixing caused by maximum tidal stresses. The tidal stresses are

large enough during spring tides to resuspend the surficial materials and to maintain a turbid, near-bottom layer. This turbid layer was also observed in the bottom photographs; its thickness appears to be about 1-2 meters, thinning during low or neap tides.

Bottom stress values in Table II can be used to estimate the volume flux of sediment transported per unit flow width, Q, past the Geoprobe site using the Yalin bed load equation (Smith, 1976). The limitations of this and other bed load equations, particularly when applied to situations where waves and currents are both significant, are discussed by Smith (1976). Using τ_b in equation (2), and the values of u_* in Table 1 and equation (2), Q = 2.1 cm^2/sec and Q = 2.2 cm^2/sec on September 13 and September 14, respectively. On September 15, after the maximum storm effects had occurred, Q = 0.1 cm^2/sec. These estimates suggest that most of the transport of bottom material northward away from the Yukon prodelta during ice-free periods is caused by subarctic storms.

CONCLUSIONS

The transport of sediment in Norton Sound can be conveniently described in terms of the distincly different quiescent and storm regimes. The quiescent or fair weather regime is characterized by generally low levels of sediment transport caused principally by the tides and mean flow augmented by surface waves during spring tide cycles. The quiescent regime is characterized by surface winds of <8-10 m/s, short period surface waves (<6 sec) and a predominance of fine silt and clay moving as "wash load." Bedload transport is small except in shallow areas where the surface waves become important (for example on the "2 m bank" which surrounds the Yukon delta). Although calm weather conditions occur for about 90% of the year in the northern Bering Sea, our GEOPROBE data suggest that less than 50% of the sediment transport occurs under these conditions. In fact, the GEOPROBE measurements show that critical shear stresses on the prodelta are

reached only briefly during spring tides during quiescent periods. This implies that much of the fine-grained suspended matter present over the prodelta is material that was resuspended at shallow dephts near the delta and moved northward with the mean current.

During about 30-40 days of each year the surface wind approaches or exceeds 10 m/s, although National Weather Service records for Nome, Alaska show that sustained winds >15 m/s recur with less than annual frequency. The 2-day storm in September 1977 appears to be representative of the more energetic late summer atmospheric events in Norton Sound. In September, October and November the polar front migrates south and tends to steer low pressure weather systems from the southwest to the northeast across the northern Bering Sea. Norton Sound is commonly exposed to strong southerly and southwesterly winds generated by the low pressure cells. Winds from this quadrant generate 1-3 m waves with periods of 8-11 seconds because of the essentially infinite fetch southwest of Norton Sound. It is waves like these which can cause severe damage along the northern coast of the sound (Fathauer, 1975).

The instantaneous shear velocity (u_*) at the GEOPROBE during the September 1977 storm reached 6 cm/s and the light scattering data demonstrate a 20-fold increase in TSM at 2 m above the bottom. The amount of sediment transported during this brief event was approximately equal to the transport that would occur during 4 months of quiescent conditions. Although the amount of sediment eroded during storms does not represent a hazard at depths of 15 m or greater, the impact of storms (particularly the surface wave scour) could be highly significant at depths of <10 m. Indeed, the morphology of the Yukon delta shows that wave and current energy is concentrated on the western margin of the delta which is exposed to the open Bering Sea and the full impact of southwesterly storm winds (Dupré and Thompson, 1979).

The results of our winter study strongly suggest that (1) tidal currents are the most important sediment transport agent during non-storm periods, in the summer as well as in the winter, and (2) a substantial amount of Yukon River sediment remains in the system at the close of the ice-free season. Some of this sediment is temporarily deposited on the shallow sub-ice platform and fringing areas after early summer river flooding. As the flow of the Yukon diminishes in November this mud reservoir becomes an important source of the suspended matter present over the prodelta during the winter. Finally, the surface ice layer may actually intensify the tidal currents over the broad sub-ice platform which rims the Yukon Delta by obstructing and reducing the flow cross section (Dupré, 1978).

REFERENCES

Beardsley, R. C. and Butman, B., 1974, Circulation on the New England continental shelf: response to strong winter storms: Geophys. Res. Letters, 1(4), pp. 181-184.

Cacchione, D. A. and Drake, D. E., 1977, Sediment transport in Norton Sound, northern Bering Sea, Alaska: Annual report to NOAA/OCSEAP for year ending March 1977, Juneau, Alaska, 19 p.

Cacchione, D. A. and Drake, D. E., 1979, A new instrument system to investigate sediment dynamics on continental shelves: Marine Geology, v. 30, pp. 299-312.

Cacchione, D. A. and Drake, D. E., in press, Storm-generated sediment transport on the Bering Sea shelf: Geophys. Res. Letters,

Coachman, L. K., Aagaard, K., and Tripp, R. B., 1975, Bering Strait, the regional physical oceanography: Seattle, Univ. Washington Press, 186 p.

Drake, D. E., 1976, Suspended sediment transport and mud deposition on continental shelves; in Stanley, D. J. and Swift, D. J. P. (eds.), Marine sediment transport and environmental management: John Wiley and Sons, New York, pp. 127-158.

Drake, D. E., Kolpack, R. L., and Fischer, P. J., 1972, Sediment transport on the Santa Barbara - Oxnard shelf, Santa Barbara Channel, in Swift, D. J. P., Duane, D. B., and Pilkey, O. H. (eds.), Shelf sediment transport: Process and pattern: Dowden, Hutchinson and Ross, Inc., Stroudsburg, Pa., pp. 307-332.

Drake, D. E., Cacchione, D. A., Muench, R. D., and Nelson, C. H., in press, Sediment transport in Norton Sound, Alaska: Marine Geology,

Dupré, W. R., 1978, Yukon Delta coastal processes study: U.S. Natl. Oceanog. Atmospheric Admin. and U.S. Bureau of Land Management Principal Investigators Rept., year ending March 1978, 62 p.

Dupré, W. R. and Thompson, R., 1979, The Yukon delta: a model for deltaic sedimentation in an ice-dominated environment: Proc. Offshore Technol. Conf. Paper 3434, May 1979, Houston, Texas, pp. 657-664.

Fathauer, T. F., 1975, The great Bering Sea storms of 9-19 November 1974: Weatherwise Mag., Amer. Meteorological Soc., v. 28, pp. 76-83.

Grant, W. D. and Madsen, O. S., 1979, Combined wave and current interaction with a rough bottom: Jour. Geophys. Res., v. 84, no. C4, p. 1797-1808.

Madsen, O. S. and Grant, W. D., 1976, Sediment transport in the coastal environment: Report 209, Ralph M. Parsons Lab. for Water Resources and Hydrodynamics, Mass. Inst. of Technol., Cambridge, 105 p.

McManus, D.A., Kolla, V., Hopkins, D.M., and Nelson, C.H., 1977. Distribution of bottom sediments on the continental shelf, northern Bering Sea: U.S. Geol. Surv. Prof. Pap. 759-C, pp. C1-C31.

McManus, D.A., Venkatarathnam, Kolla, Hopkins, D.M., and Nelson, C.H., 1974. Yukon River sediment of the northernmost Bering Sea shelf: J. Sediment. Petrol., v. 44, p. 1052-1060.

Muench, R.D., Pearson, C., and Tripp, R.B., 1978. Winter currents in the northern Bering Sea and Bering Strait: EOS, Trans. Amer. Geophys. Union, v. 59, p. 304.

Muench, R.D., Charnell, R.L., Cline, J.D. and Coachman, L.K., 1979. Summer water masses and circulation in Norton Sound, Alaska: in preparation.

Nelson, C.H. and Creager, J.S., 1977. Displacement of Yukon-derived sediment from Bering Sea to Chukchi Sea during Holocene time. Geology, 5:141-146.

Nelson, C.H., Hopkins, D.M. and Scholl, D.W., 1974. Tectonic setting and Cenozoic sedimentary history of the Bering Sea. In: Y. Herman (editor), Arctic Geology and Oceanography. Springer-Verlag, New York, pp. 119-140.

Pilkey, O. H., Trumbull, J. V. A., and Bush, D. M., 1978, Equilibrium shelf sedimentation, Rio de la Plata shelf, Puerto Rico: Jour. Sed. Petrology, v. 48, pp. 389-400.

Reimnitz, E., Toimil, L. J., and Barnes, P. W., 1977, Stamukhi zone processes: implications for developing the Arctic coast: Proc. Offshore Technology Conf. Paper 2945, May 1977, pp. 513-518.

Schlichting, H., 1968, Boundary Layer Theory: 4th ed., McGraw-Hill, New York, 647 p.

Sharma, G. D., Wright, F. F., Burns, J. J., and Burbank, D. C., 1974, Sea surface circulation, sediment transport and marine mammal distribution, Alaska continental shelf: ERTS Final Rept.: Natl. Tech. Service Rept. E74-10711, 77 p.

Smith, J.D., 1977. Modeling of sediment transport on continental shelves. In: E.D. Goldberg, I.N. McCave, J.J. O'Brien and J.H. Steele (editors), The Sea, Vol. 6: Marine Modeling. J. Wiley and Sons, New York, pp. 539-577.

Smith, J.D. and Hopkins, T.S., 1972. Sediment transport on the continental shelf off of Washington and Oregon in the light of recent current measurements. In: D.J.P. Swift, D.B. Duane, and O.H. Pilkey (editors), Shelf Sediment Transport: Process and Pattern. Dowden, Hutchinson, and Ross, Stroudsburg, Pa., pp. 143-180.

Smith, J.D. and McLean, S.R., 1977. Boundary layer adjustments to bottom topography and suspended sediment. In: J.C.J. Nihoul (editor), Bottom Turbulence. Elsevier, New York, pp. 123-151.

APPENDIX I

Bottom currents on the Yukon prodelta during July 8 - September 25, 1977. The data were obtained by the electromagnetic current sensors on the GEOPROBE tripod. The raw data consist of "burst" measurements of horizontal current speeds taken once per second for 60 consecutive seconds each hour.

STATISTICS AND HISTOGRAMS OF CURRENTS AT CM1 - GEOPROBE, NS77
LOCATION = LAT 64 00N, LONG 165 00W, DEPTH = 17.5 METERS
OBSERVATION PERIOD = 0000 8 JUL 77 TO 2300 25 SEP 77 (80.0 DAYS)
N = 1920 DT = 1.00 HOURS, UNITS = (CM/SEC)

	MEAN	VARIANCE	ST-DEV	SKEW	KURT	MAX	MIN
S	8.93	25.96	5.10	0.622	2.862	28.18	0.03
U	2.14	78.95	8.89	0.279	2.281	28.01	-18.94
V	1.60	19.53	4.42	0.920	4.804	21.92	-16.12

S = SPEED
U = EAST-WEST COMPONENT OF VELOCITY, EAST =POSITIVE U
V = NORTH-SOUTH COMPONENT OF VELOCITY, NORTH = POSITIVE V

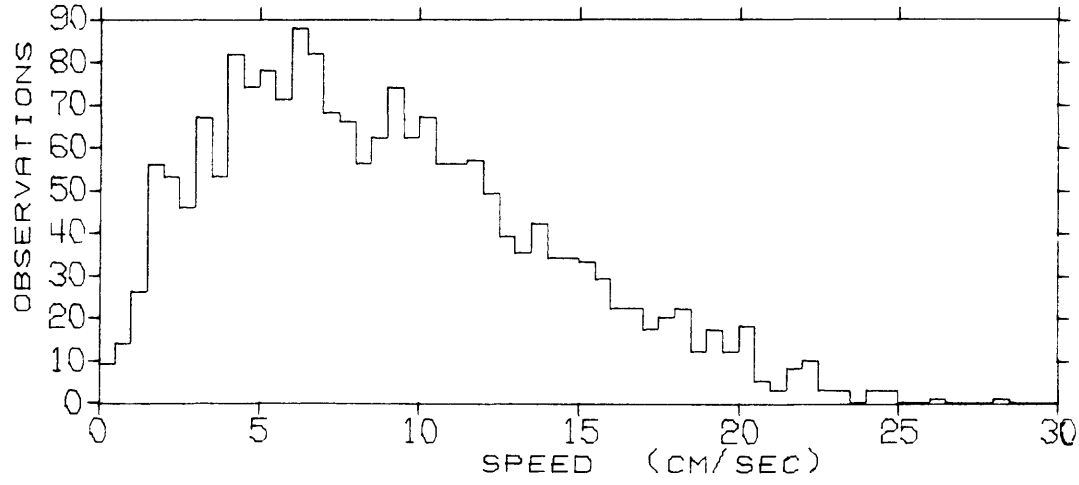

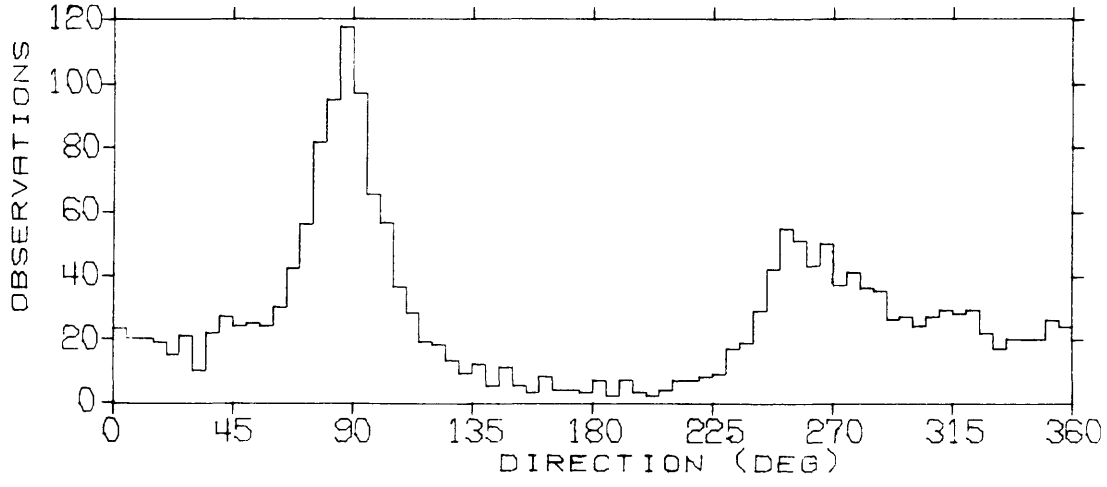

TIME SERIES OF VECTOR AVERAGED CURRENTS AT CM1 - GEOPROBE, NS77
LOCATION = LAT 64 00N, LONG 165 00W, DEPTH = 17.5 METERS
OBSERVATION PERIOD = 0000 8 JUL 77 TO 2300 27 JUL 77 (20.0 DAYS)
AVERAGING INTERVAL = 1.0 HOURS (1 POINTS)

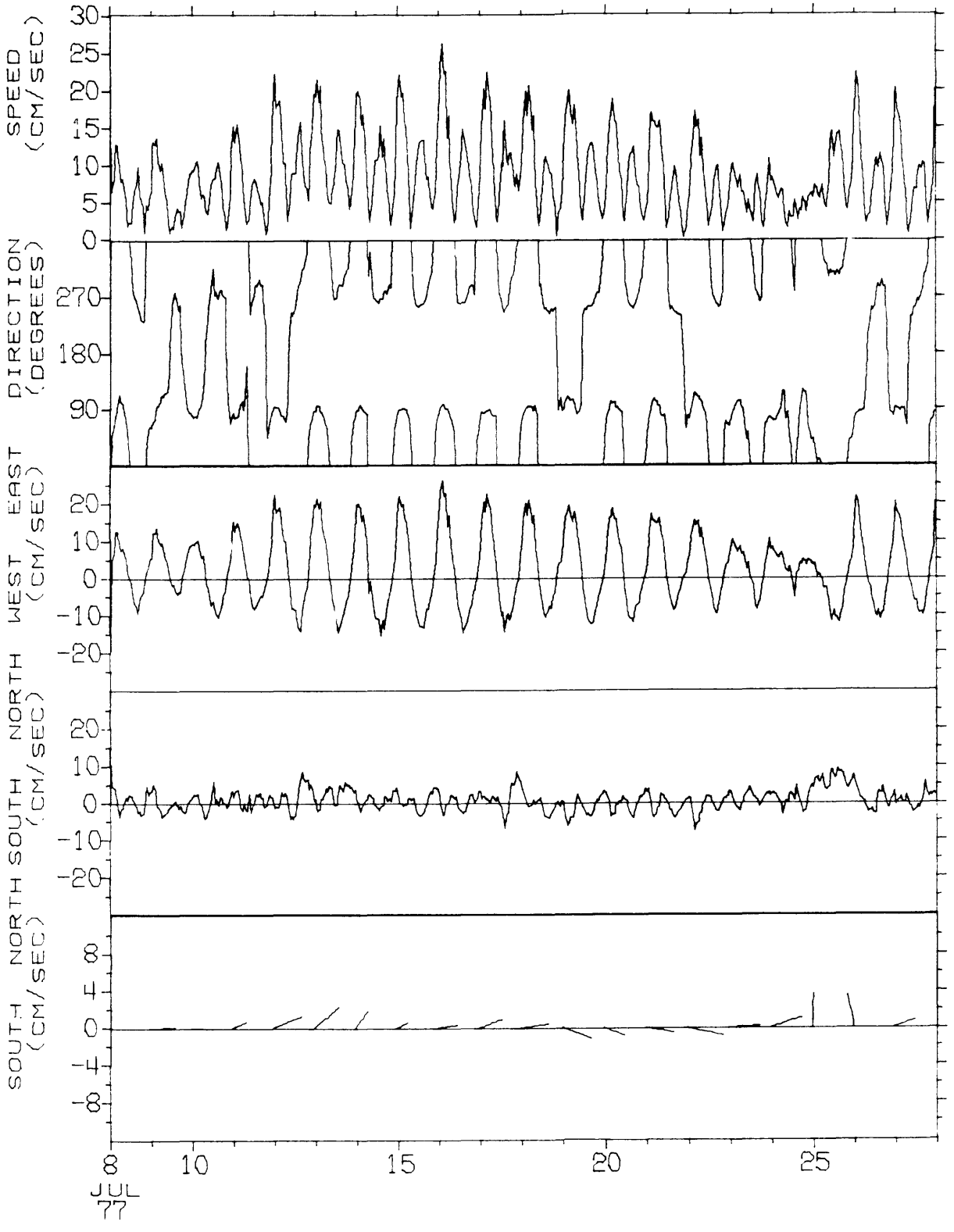

TIME SERIES OF VECTOR AVERAGED CURRENTS AT CM1 - GEOPROBE, NS77
LOCATION = LAT 64 00N, LONG 165 00W, DEPTH = 17.5 METERS
OBSERVATION PERIOD = 0000 28 JUL 77 TO 2300 16 AUG 77 (20.0 DAYS)
AVERAGING INTERVAL = 1.0 HOURS (1 POINTS)

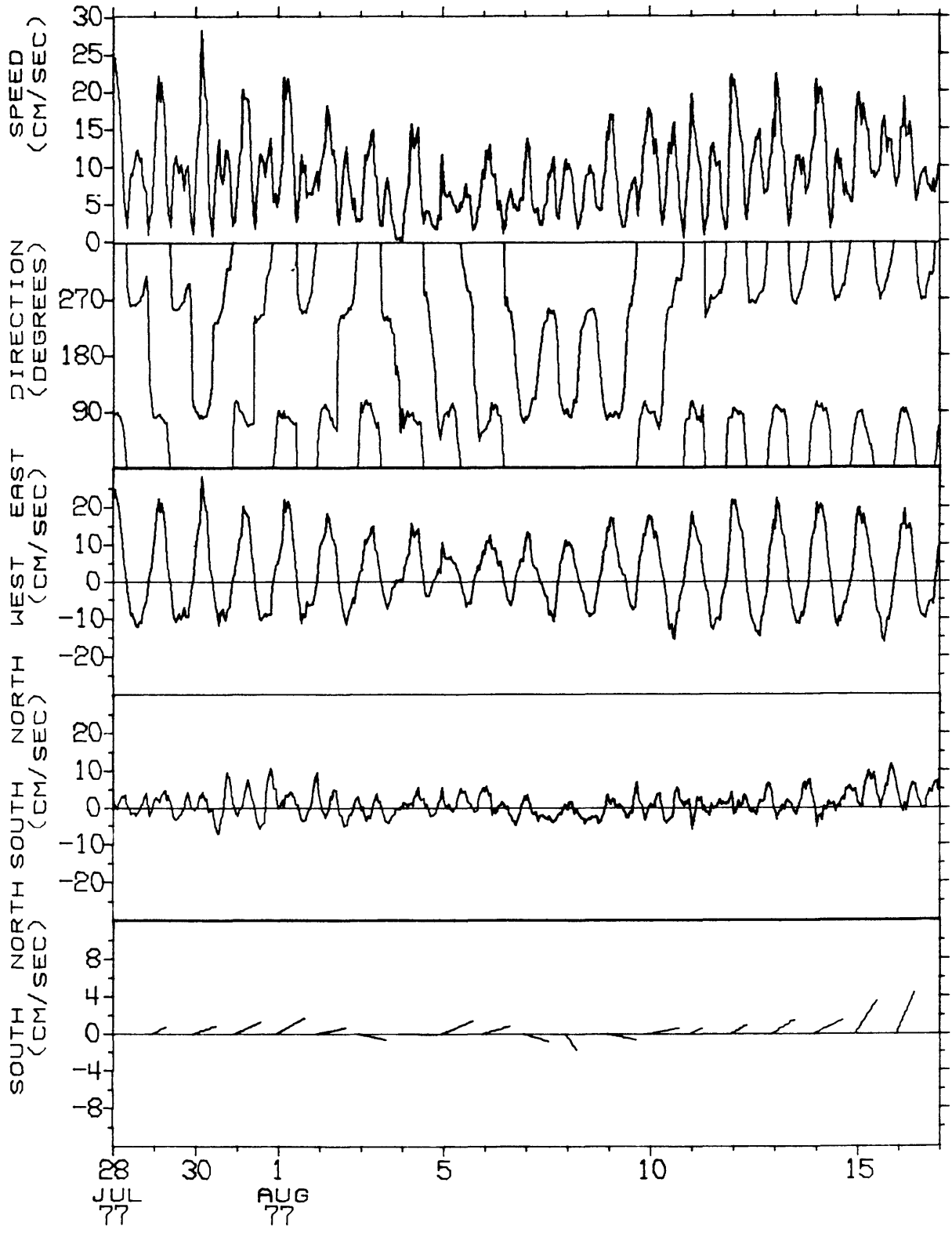

TIME SERIES OF VECTOR AVERAGED CURRENTS AT CM1 - GEOPROBE, NS77
LOCATION = LAT 64 00N, LONG 165 00W, DEPTH = 17.5 METERS
OBSERVATION PERIOD = 0000 17 AUG 77 TO 2300 5 SEP 77 (20.0 DAYS)
AVERAGING INTERVAL = 1.0 HOURS (1 POINTS)

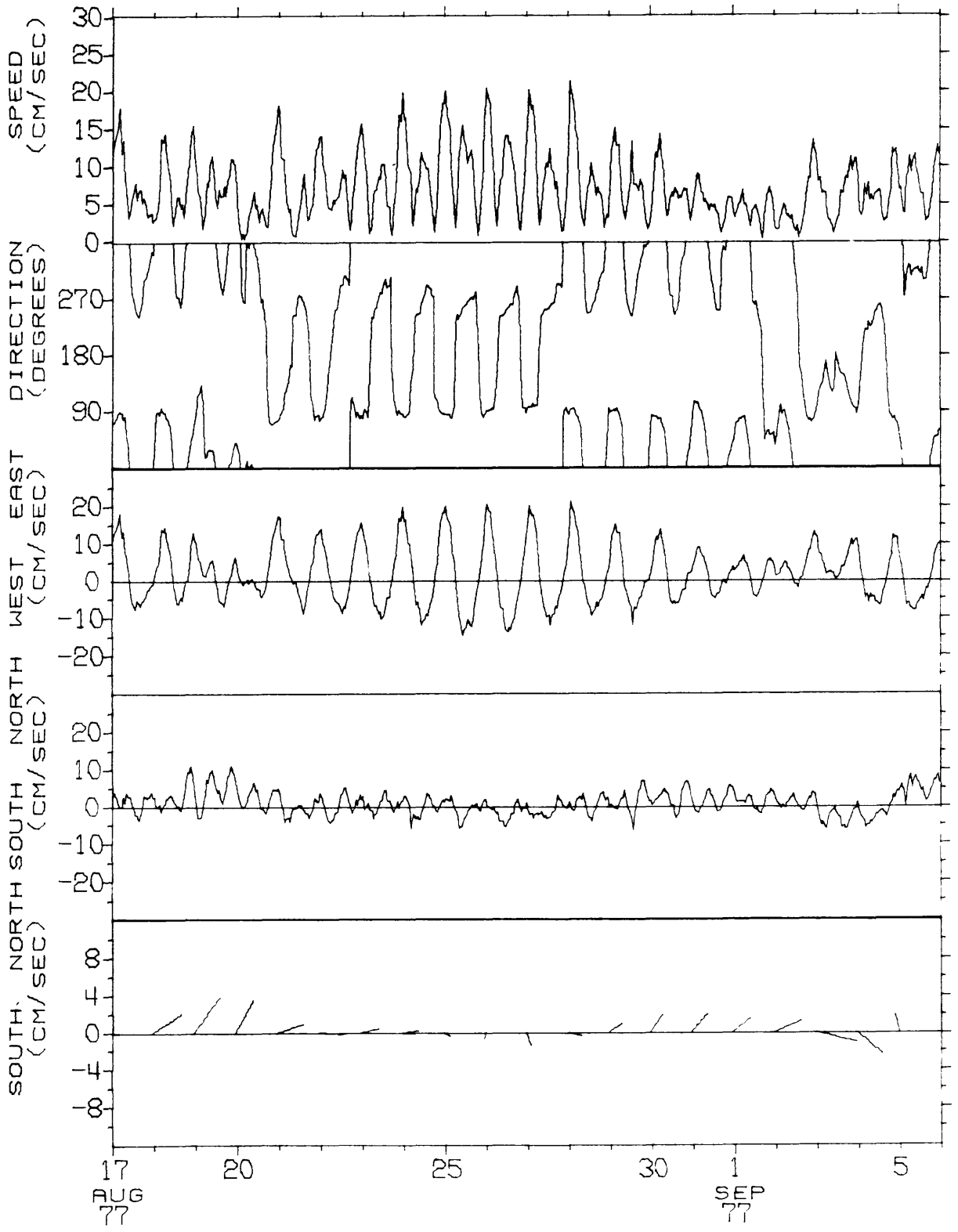

TIME SERIES OF VECTOR AVERAGED CURRENTS AT CM1 - GEOPROBE, NS77
LOCATION = LAT 64 00N, LONG 165 00W, DEPTH = 17.5 METERS
OBSERVATION PERIOD = 0000 6 SEP 77 TO 2300 25 SEP 77 (20.0 DAYS)
AVERAGING INTERVAL = 1.0 HOURS (1 POINTS)

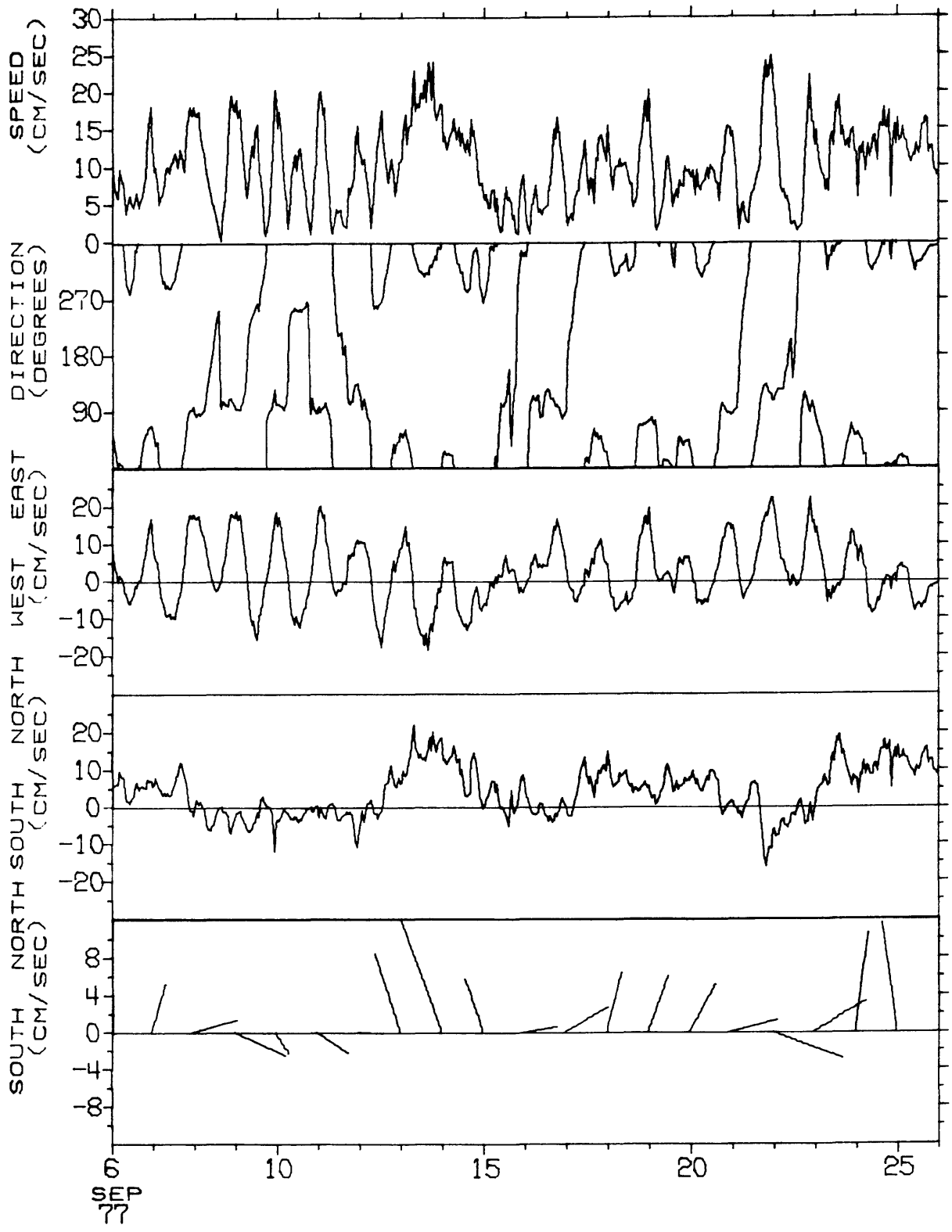

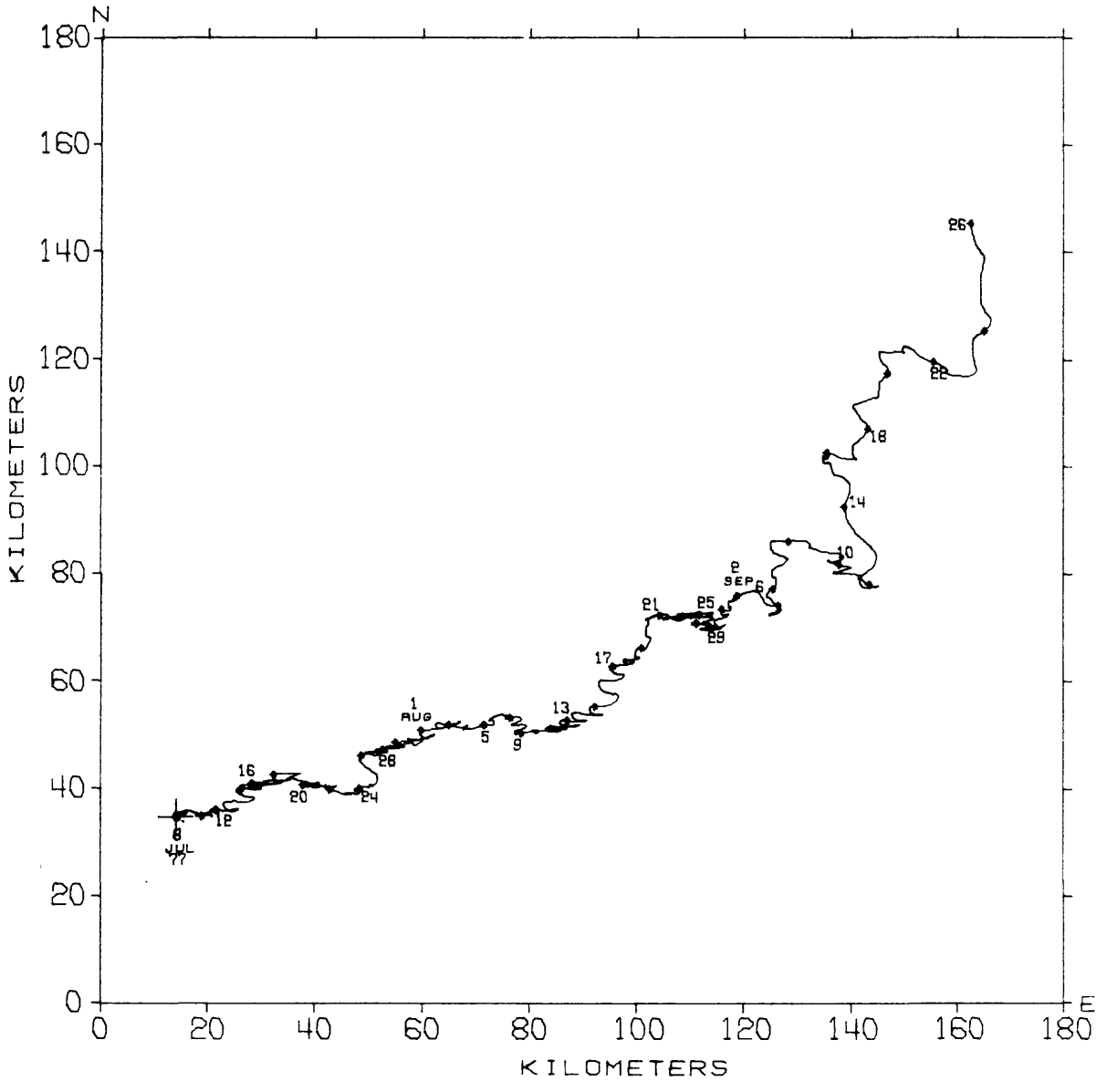

PROGRESSIVE VECTOR DIAGRAM OF CURRENTS AT CM1 - GEOPROBE, NS77
LOCATION = LAT 64 00N, LONG 165 00W, DEPTH = 17.5 METERS
OBSERVATION PERIOD = 0000 8 JUL 77 TO 2300 25 SEP 77 (80.0 DAYS)
◆ EVERY 2.0 DAYS BEGINNING AT 0000 8 JUL 77

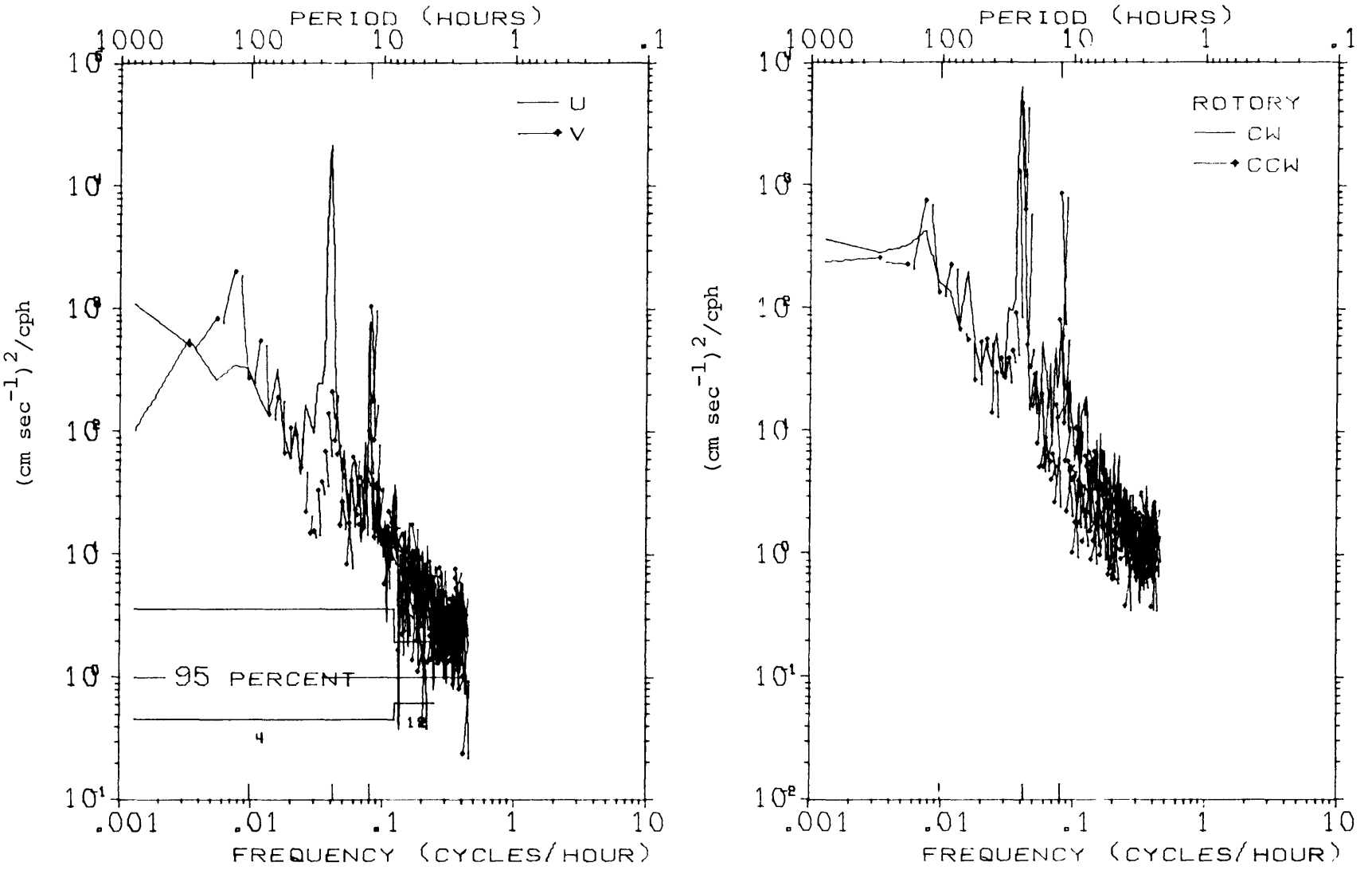

U, V AND ROTORY SPECTRA OF CURRENTS AT CM1 - GEOPROBE, NS77
LOCATION = LAT 64 00N, LONG 165 00W, DEPTH = 17.5 METERS
OBSERVATION PERIOD = 0000 8 JUL 77 TO 2300 25 SEP 77 (80.0 DAYS)
N = 1920, DT = 1.0 HOURS, SMOOTHING - DANIELL WINDOW

KINETIC ENERGY SPECTRUM OF CURRENTS AT CM1 - GEOPROBE, NS77
LOCATION = LAT 64 00N, LONG 165 00W, DEPTH = 17.5 METERS
OBSERVATION PERIOD = 0000 8 JUL 77 TO 2300 25 SEP 77 (80.0 DAYS)
N = 1920, DT = 1.0 HOURS, SMOOTHING - DANIELL WINDOW

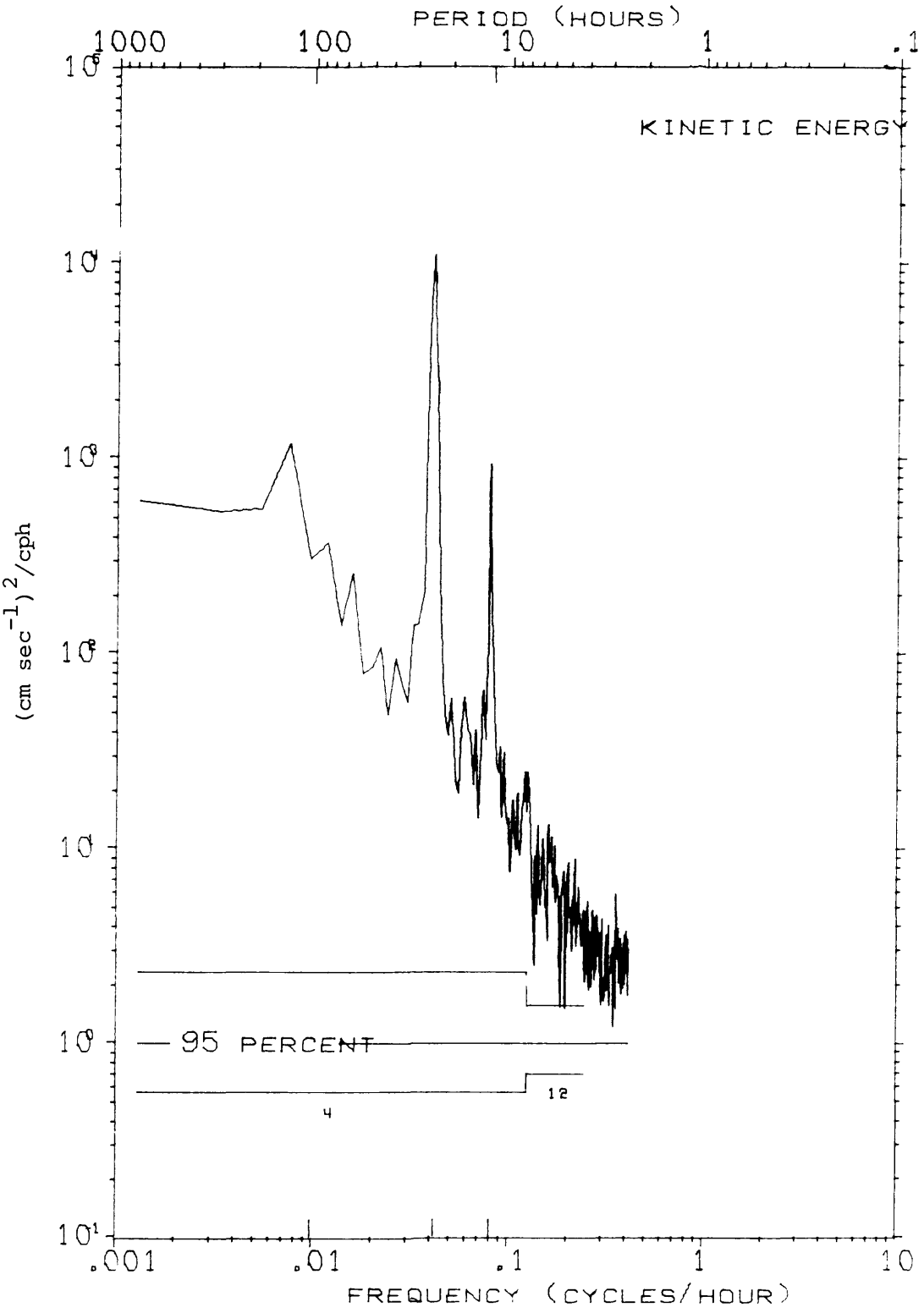

STATISTICS AND HISTOGRAMS OF CURRENTS AT CM2 - GEOPROBE, NS77
LOCATION = LAT 64 00N, LONG 165 00W, DEPTH = 17.5 METERS
OBSERVATION PERIOD = 0000 8 JUL 77 TO 2300 25 SEP 77 (80.0 DAYS)
N = 1920 DT = 1.00 HOURS, UNITS = (CM/SEC)

	MEAN	VARIANCE	ST-DEV	SKEW	KURT	MAX	MIN
S	12.11	40.29	6.35	0.465	2.896	36.99	0.23
U	0.96	122.97	11.09	0.173	2.144	32.11	-23.48
V	2.81	55.16	7.43	0.684	4.509	35.84	-27.62

S = SPEED
U = EAST-WEST COMPONENT OF VELOCITY, EAST =POSITIVE U
V = NORTH-SOUTH COMPONENT OF VELOCITY, NORTH = POSITIVE V

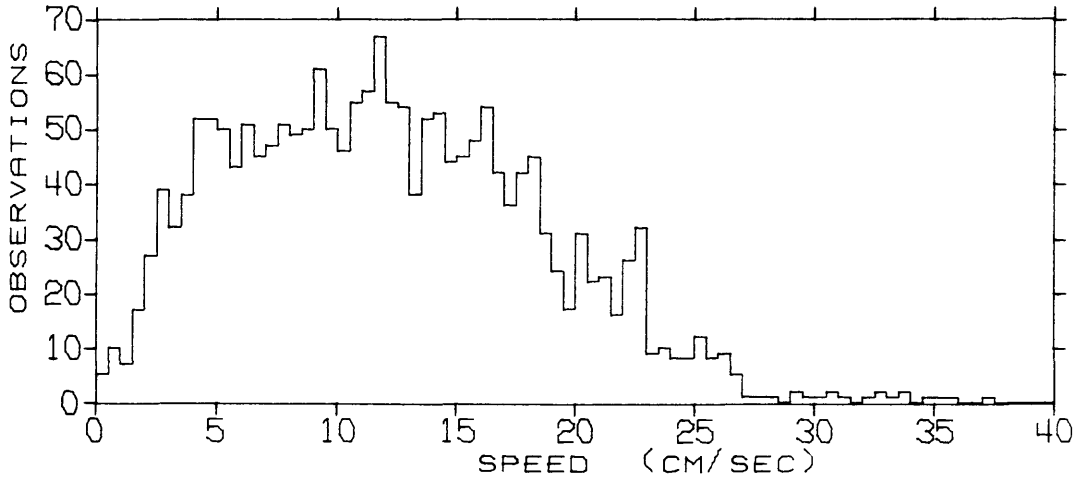

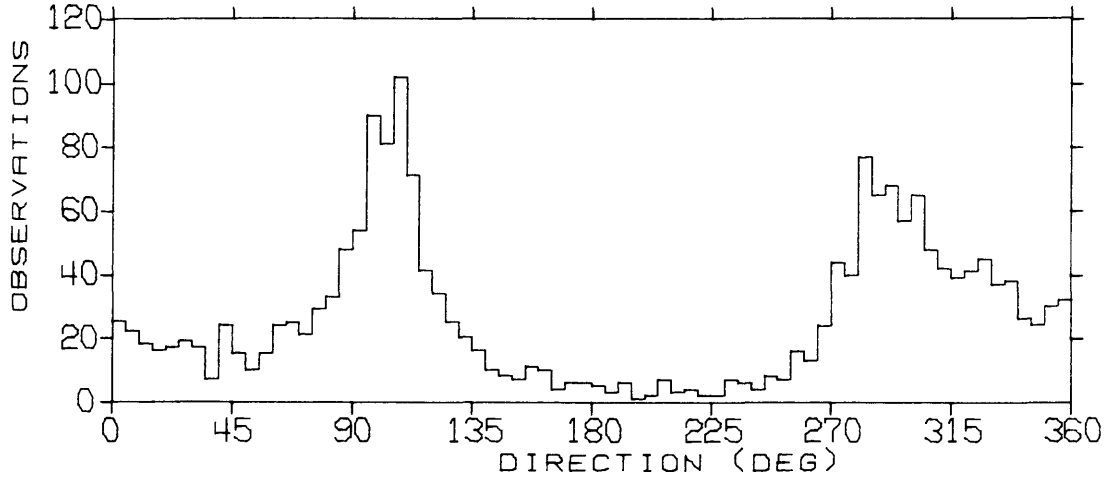

TIME SERIES OF VECTOR AVERAGED CURRENTS AT CM2 - GEOPROBE, NS77
LOCATION = LAT 64 00N, LONG 165 00W, DEPTH = 17.5 METERS
OBSERVATION PERIOD = 0000 8 JUL 77 TO 2300 27 JUL 77 (20.0 DAYS)
AVERAGING INTERVAL = 1.0 HOURS (1 POINTS)

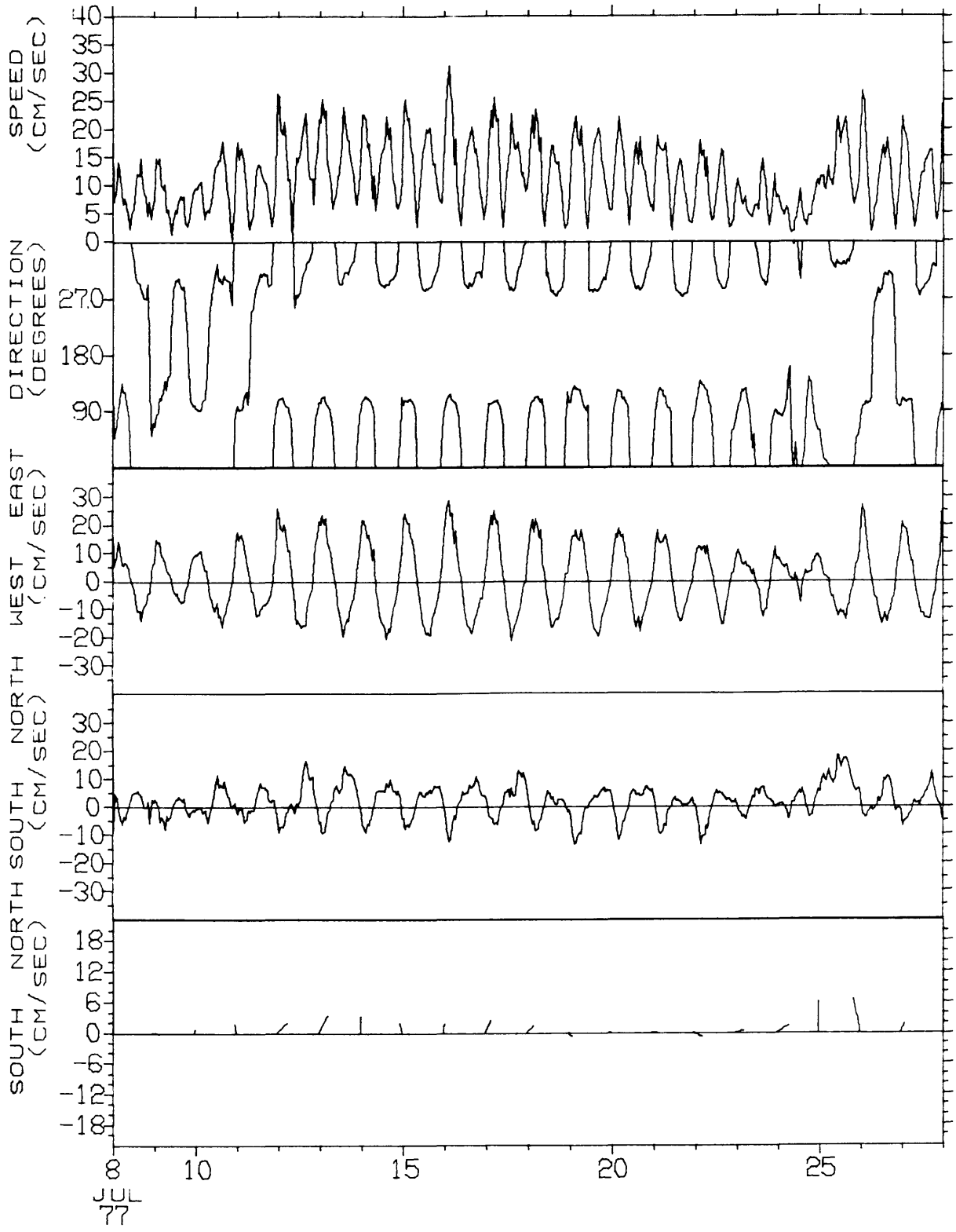

TIME SERIES OF VECTOR AVERAGED CURRENTS AT CM2 - GEOPROBE, NS77
LOCATION = LAT 64 00N, LONG 165 00W, DEPTH = 17.5 METERS
OBSERVATION PERIOD = 0000 28 JUL 77 TO 2300 16 AUG 77 (20.0 DAYS)
AVERAGING INTERVAL = 1.0 HOURS (1 POINTS)

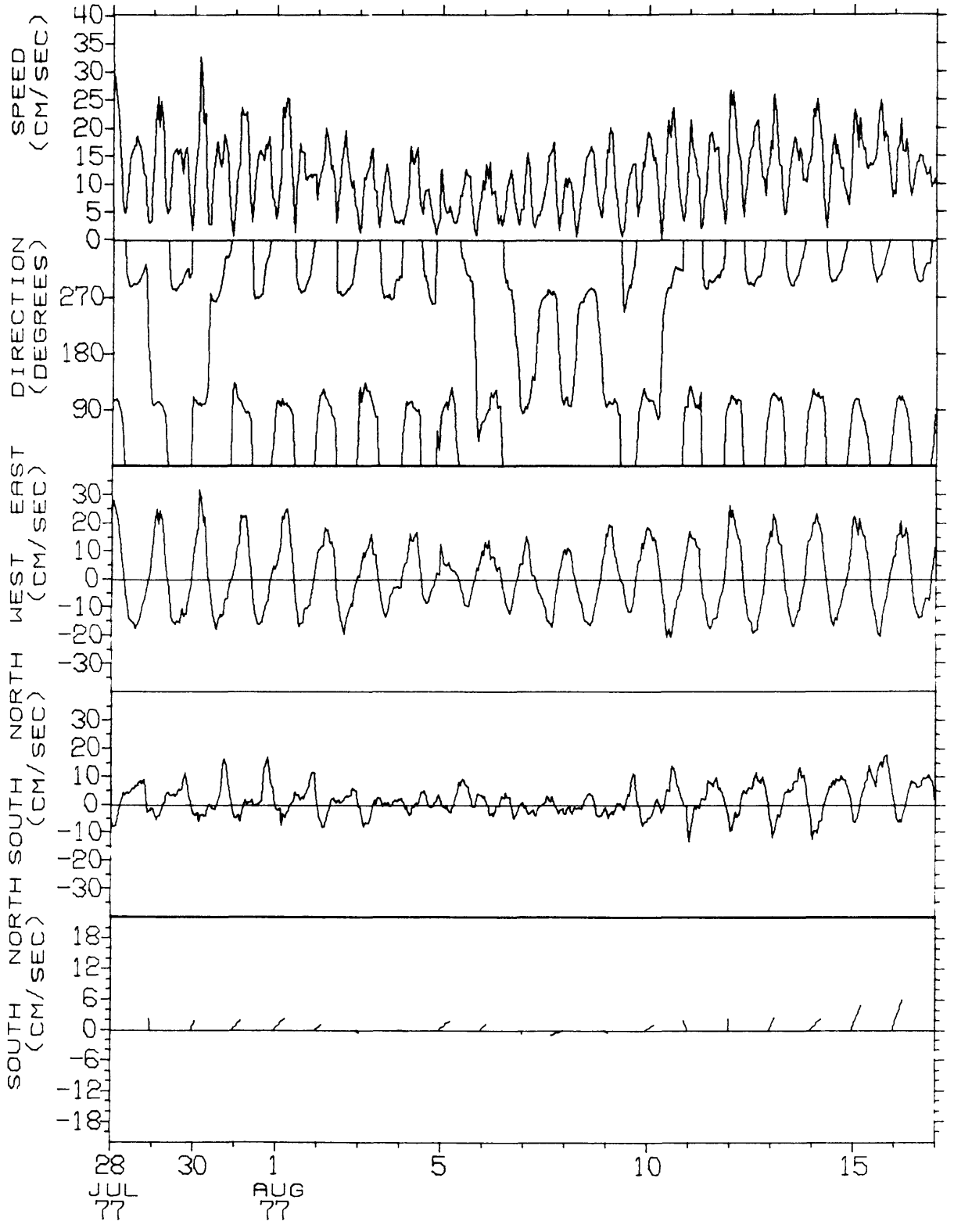

TIME SERIES OF VECTOR AVERAGED CURRENTS AT CM2 - GEOPROBE, NS77
LOCATION = LAT 64 00N, LONG 165 00W, DEPTH = 17.5 METERS
OBSERVATION PERIOD = 0000 17 AUG 77 TO 2300 5 SEP 77 (20.0 DAYS)
AVERAGING INTERVAL = 1.0 HOURS (1 POINTS)

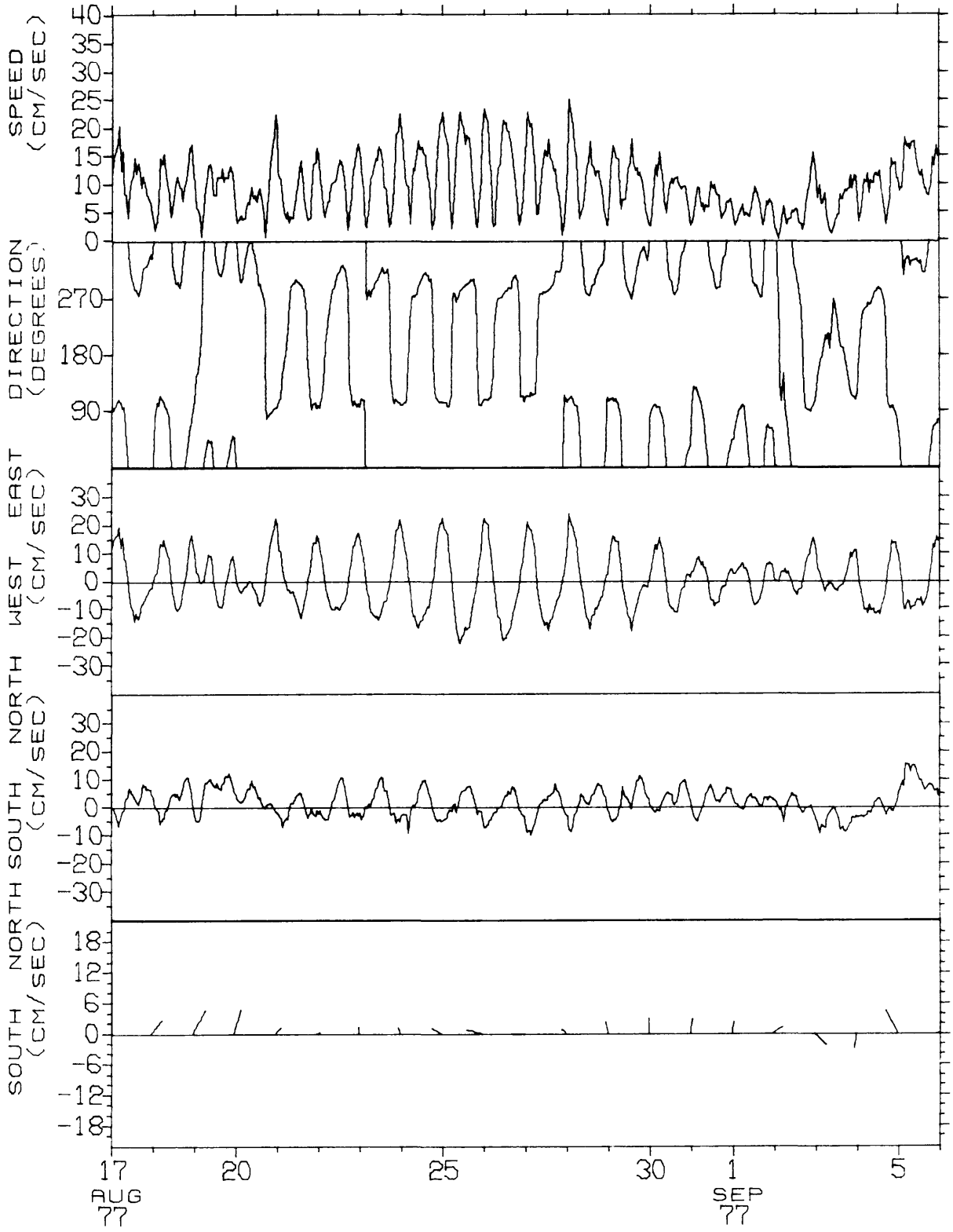

TIME SERIES OF VECTOR AVERAGED CURRENTS AT CM2 - GEOPROBE, NS77
LOCATION = LAT 64 00N, LONG 165 00W, DEPTH = 17.5 METERS
OBSERVATION PERIOD = 0000 6 SEP 77 TO 2300 25 SEP 77 (20.0 DAYS)
AVERAGING INTERVAL = 1.0 HOURS (1 POINTS)

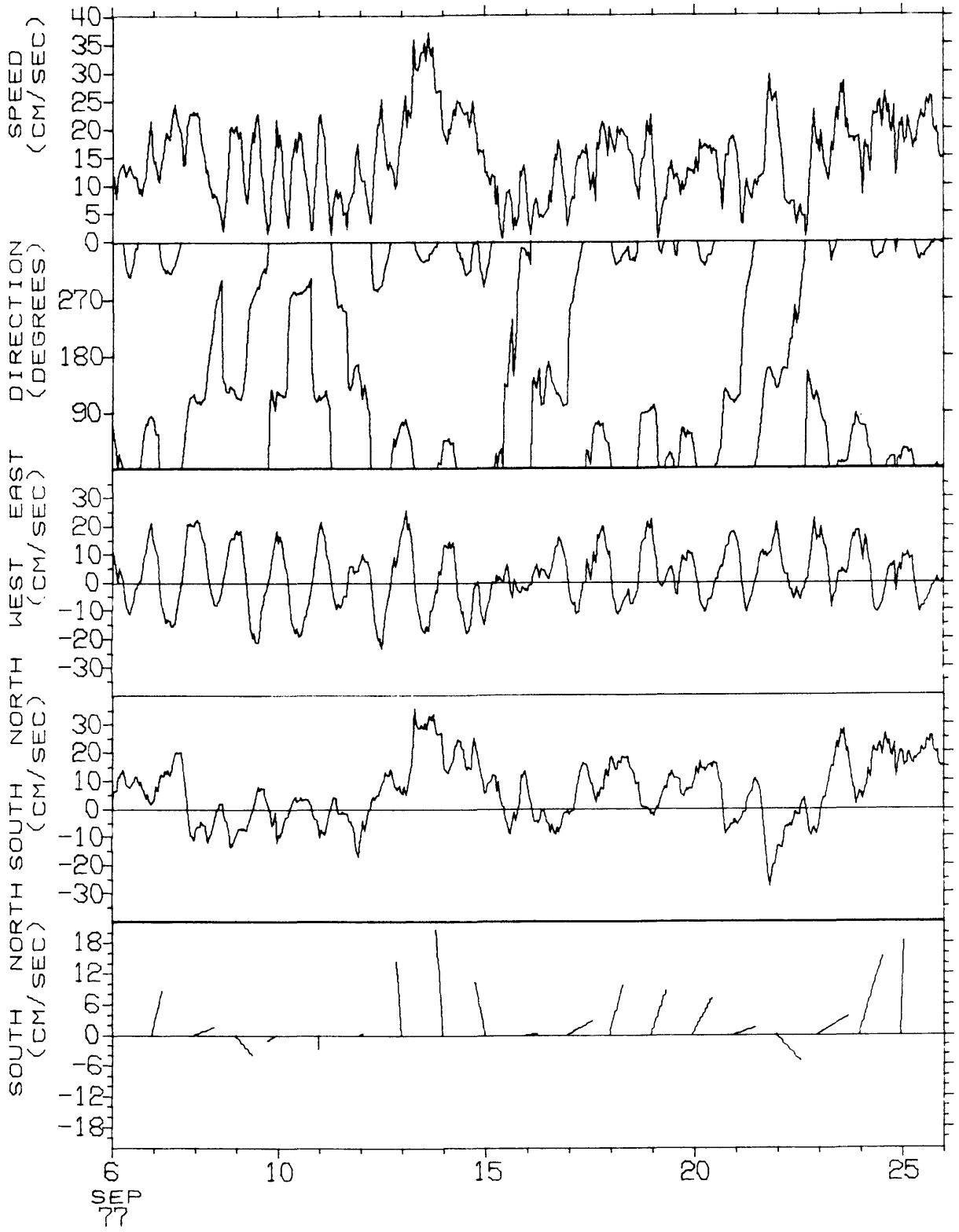

PROGRESSIVE VECTOR DIAGRAM OF CURRENTS AT CM2 - GEOPROBE, NS77
LOCATION = LAT 64 00N, LONG 165 00W, DEPTH = 17.5 METERS
OBSERVATION PERIOD = 0000 8 JUL 77 TO 2300 25 SEP 77 (80.0 DAYS)
♦ EVERY 2.0 DAYS BEGINNING AT 0000 8 JUL 77

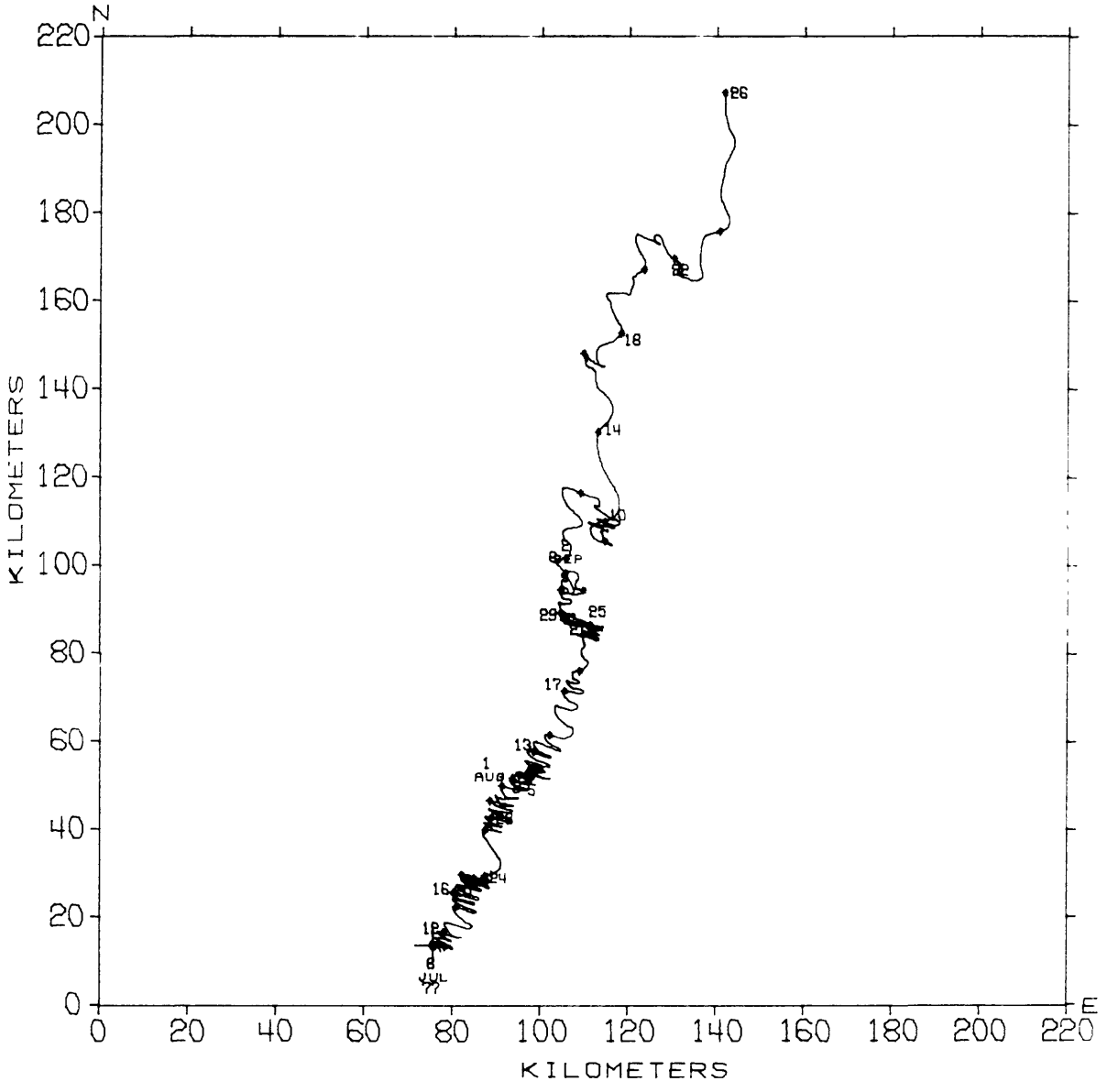

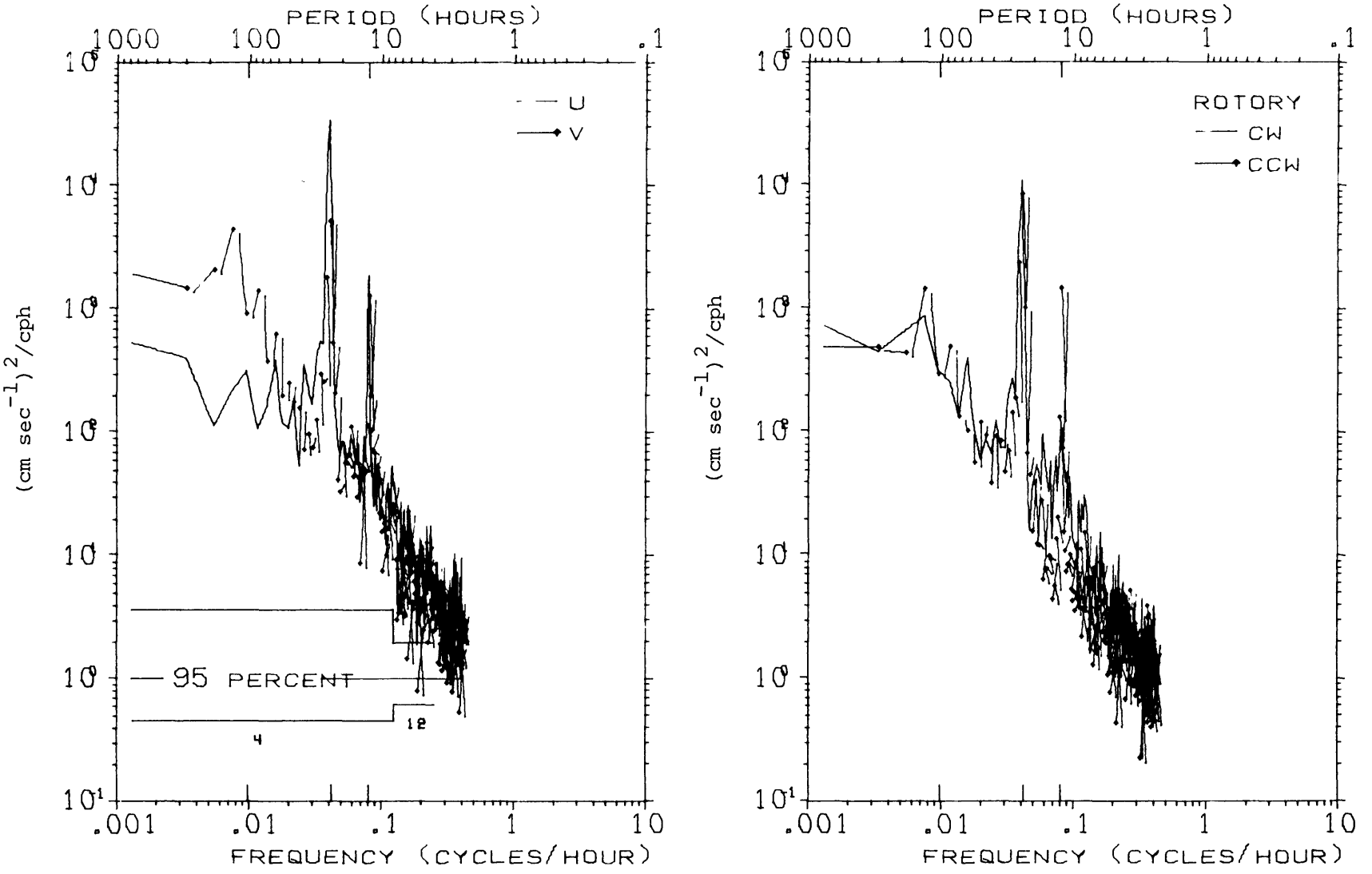

U, V AND ROTORY SPECTRA OF CURRENTS AT CM2 - GEOPROBE, NS77
LOCATION = LAT 64 00N, LONG 165 00W, DEPTH = 17.5 METERS
OBSERVATION PERIOD = 0000 8 JUL 77 TO 2300 25 SEP 77 (80.0 DAYS)
N = 1920, DT = 1.0 HOURS, SMOOTHING - DANIELL WINDOW

KINETIC ENERGY SPECTRUM OF CURRENTS AT CM2 - GEOPROBE, NS77
LOCATION = LAT 64 00N, LONG 165 00W, DEPTH = 17.5 METERS
OBSERVATION PERIOD = 0000 8 JUL 77 TO 2300 25 SEP 77 (80.0 DAYS)
N = 1920, DT = 1.0 HOURS, SMOOTHING - DANIELL WINDOW

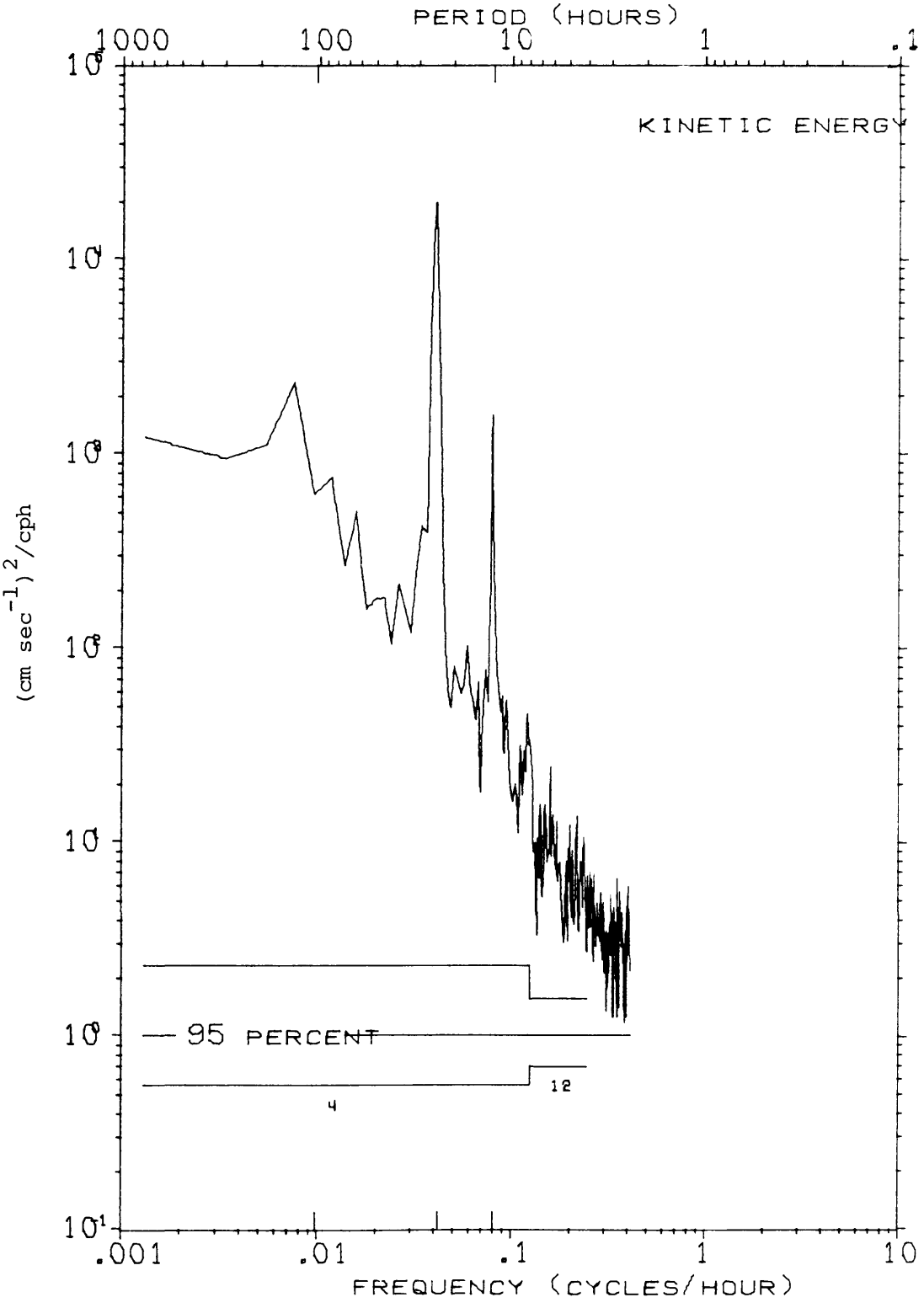

STATISTICS AND HISTOGRAMS OF CURRENTS AT CM3 - GEOPROBE, NS77
LOCATION = LAT 64 00N, LONG 165 00W, DEPTH = 17.5 METERS
OBSERVATION PERIOD = 0000 8 JUL 77 TO 2300 25 SEP 77 (80.0 DAYS)
N = 1920 DT = 1.00 HOURS, UNITS = (CM/SEC)

	MEAN	VARIANCE	ST-DEV	SKEW	KURT	MAX	MIN
S	13.00	47.84	6.92	0.558	3.020	39.68	0.66
U	1.42	155.17	12.46	0.209	2.107	34.77	-27.55
V	3.62	46.52	6.82	1.113	5.413	37.24	-23.09

S = SPEED
U = EAST-WEST COMPONENT OF VELOCITY, EAST =POSITIVE U
V = NORTH-SOUTH COMPONENT OF VELOCITY, NORTH = POSITIVE V

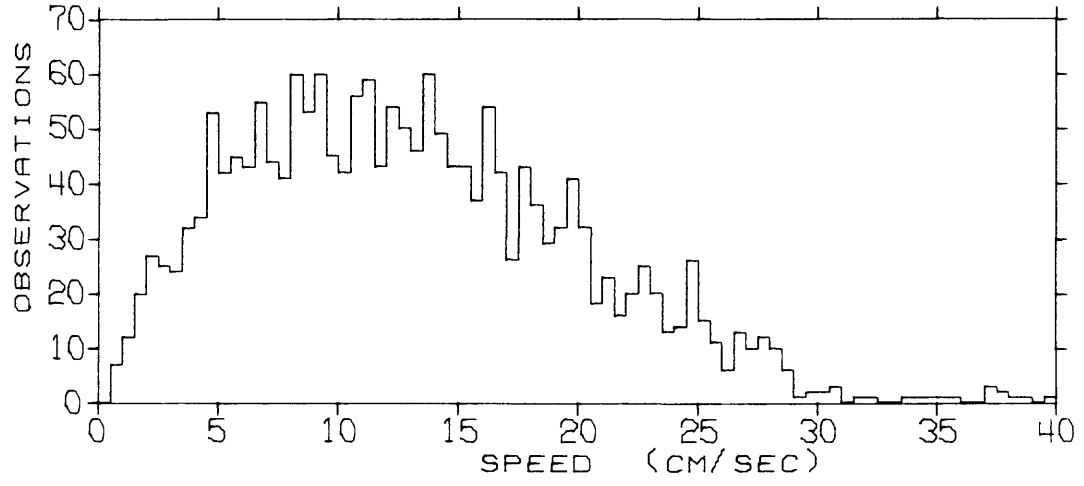

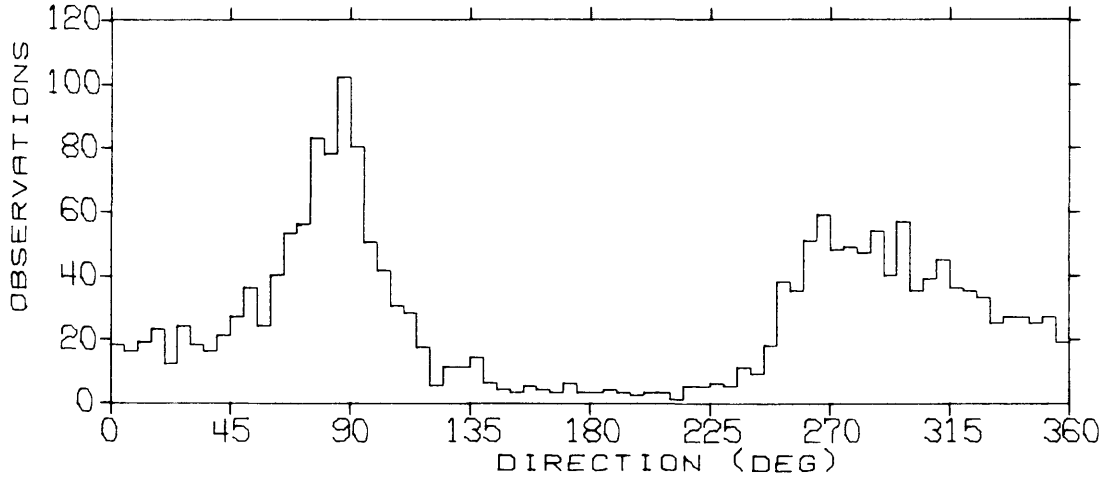

TIME SERIES OF VECTOR AVERAGED CURRENTS AT CM3 - GEOPROBE, NS77
LOCATION = LAT 64 00N, LONG 165 00W, DEPTH = 17.5 METERS
OBSERVATION PERIOD = 0000 8 JUL 77 TO 2300 27 JUL 77 (20.0 DAYS)
AVERAGING INTERVAL = 1.0 HOURS (1 POINTS)

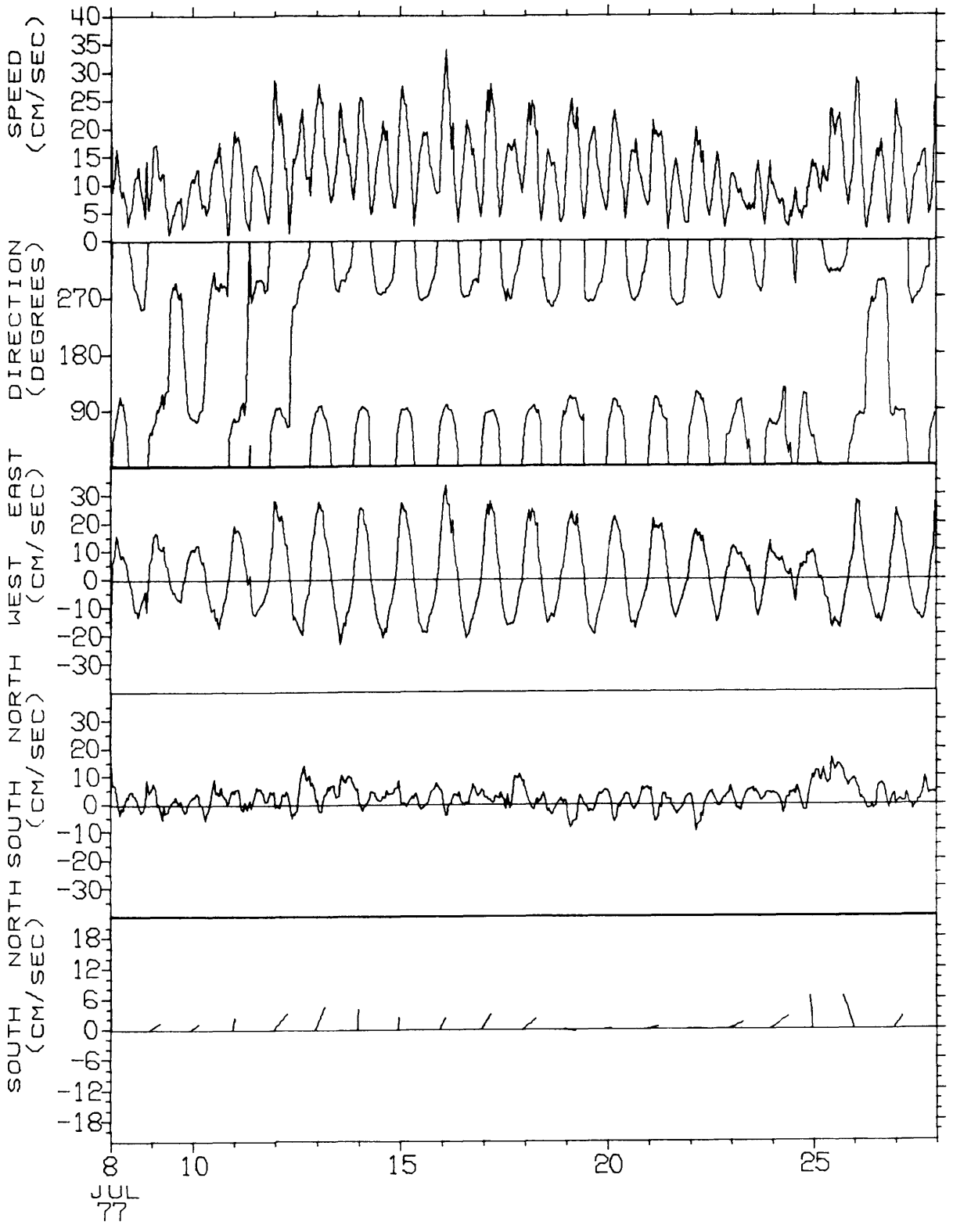

TIME SERIES OF VECTOR AVERAGED CURRENTS AT CM3 - GEOPROBE, NS77
LOCATION = LAT 64 00N, LONG 165 00W, DEPTH = 17.5 METERS
OBSERVATION PERIOD = 0000 28 JUL 77 TO 2300 16 AUG 77 (20.0 DAYS)
AVERAGING INTERVAL = 1.0 HOURS (1 POINTS)

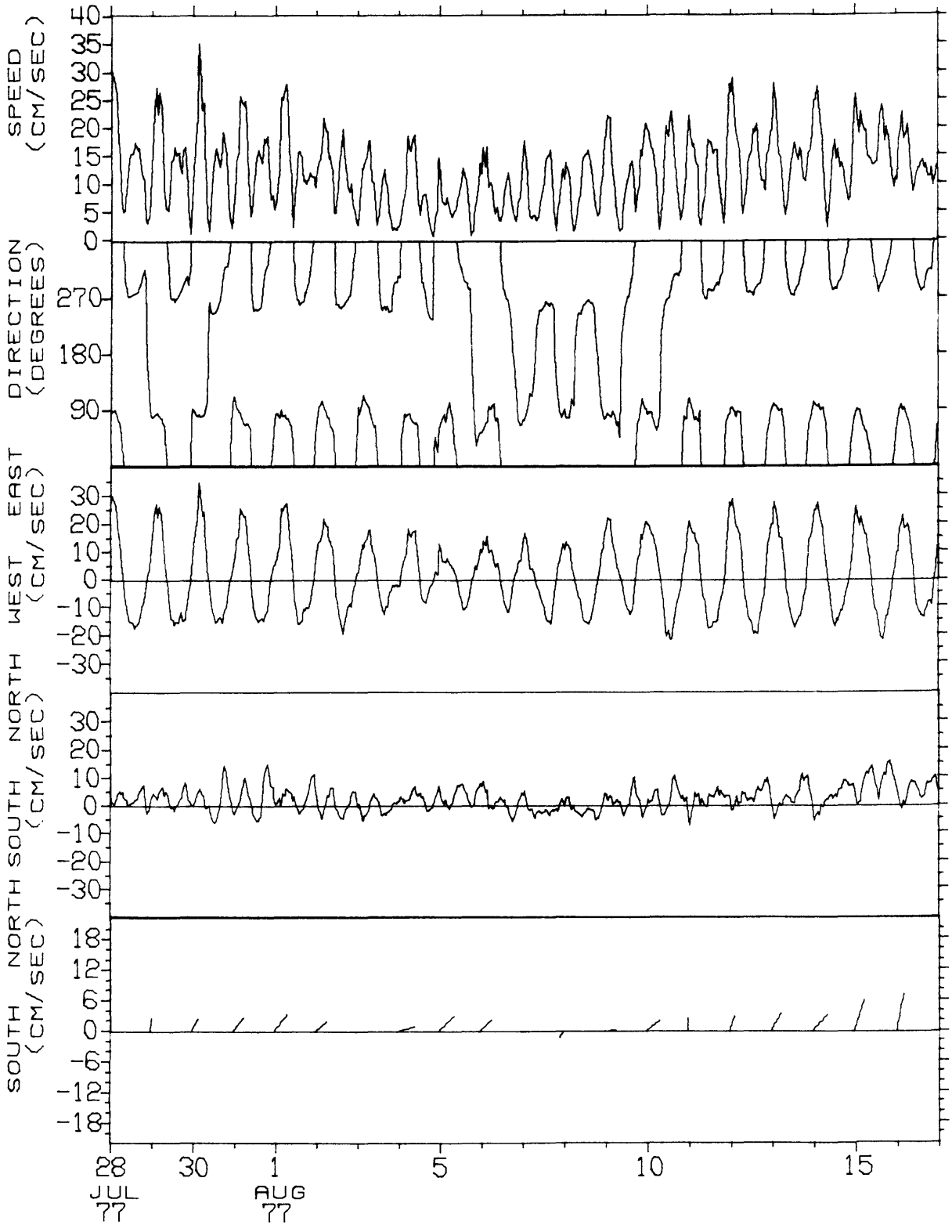

TIME SERIES OF VECTOR AVERAGED CURRENTS AT CM3 - GEOPROBE, NS77
LOCATION = LAT 64 00N, LONG 165 00W, DEPTH = 17.5 METERS
OBSERVATION PERIOD = 0000 17 AUG 77 TO 2300 5 SEP 77 (20.0 DAYS)
AVERAGING INTERVAL = 1.0 HOURS (1 POINTS)

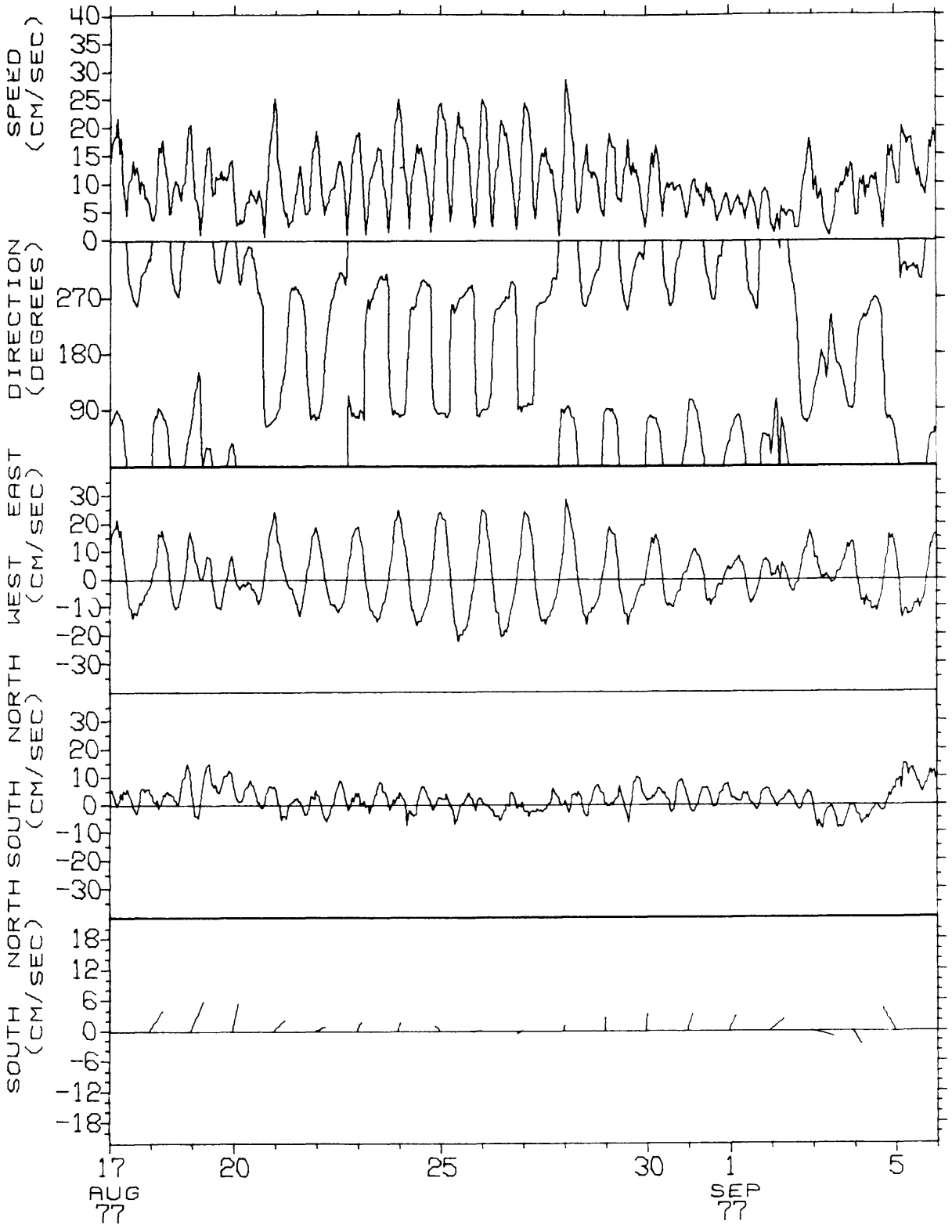

TIME SERIES OF VECTOR AVERAGED CURRENTS AT CM3 - GEOPROBE, NS77
LOCATION = LAT 64 00N, LONG 165 00W, DEPTH = 17.5 METERS
OBSERVATION PERIOD = 0000 6 SEP 77 TO 2300 25 SEP 77 (20.0 DAYS)
AVERAGING INTERVAL = 1.0 HOURS (1 POINTS)

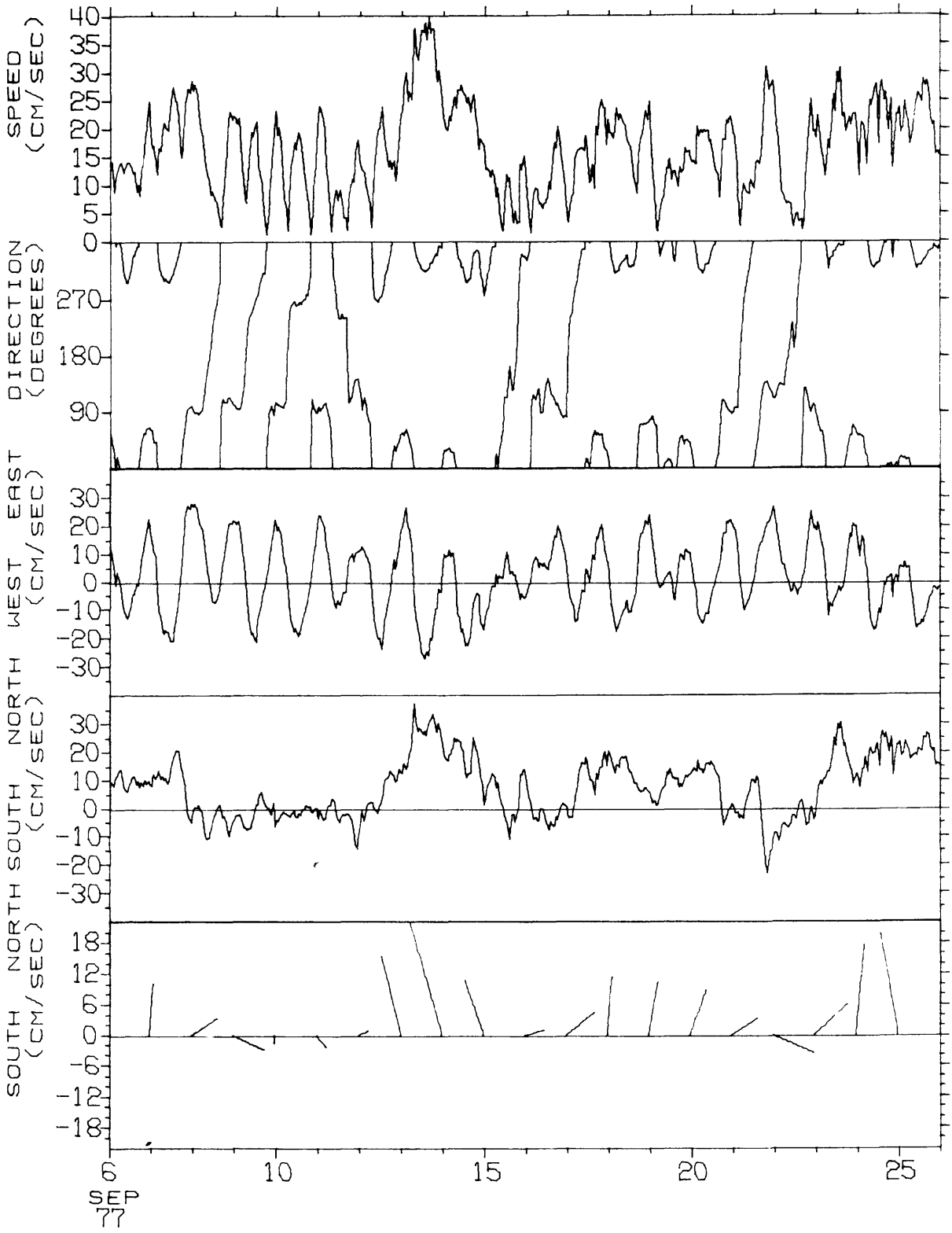

PROGRESSIVE VECTOR DIAGRAM OF CURRENTS AT CM3 - GEOPROBE, NS77
LOCATION = LAT 64 00N, LONG 165 00W, DEPTH = 17.5 METERS
OBSERVATION PERIOD = 0000 8 JUL 77 TO 2300 25 SEP 77 (80.0 DAYS)
• EVERY 2.0 DAYS BEGINNING AT 0000 8 JUL 77

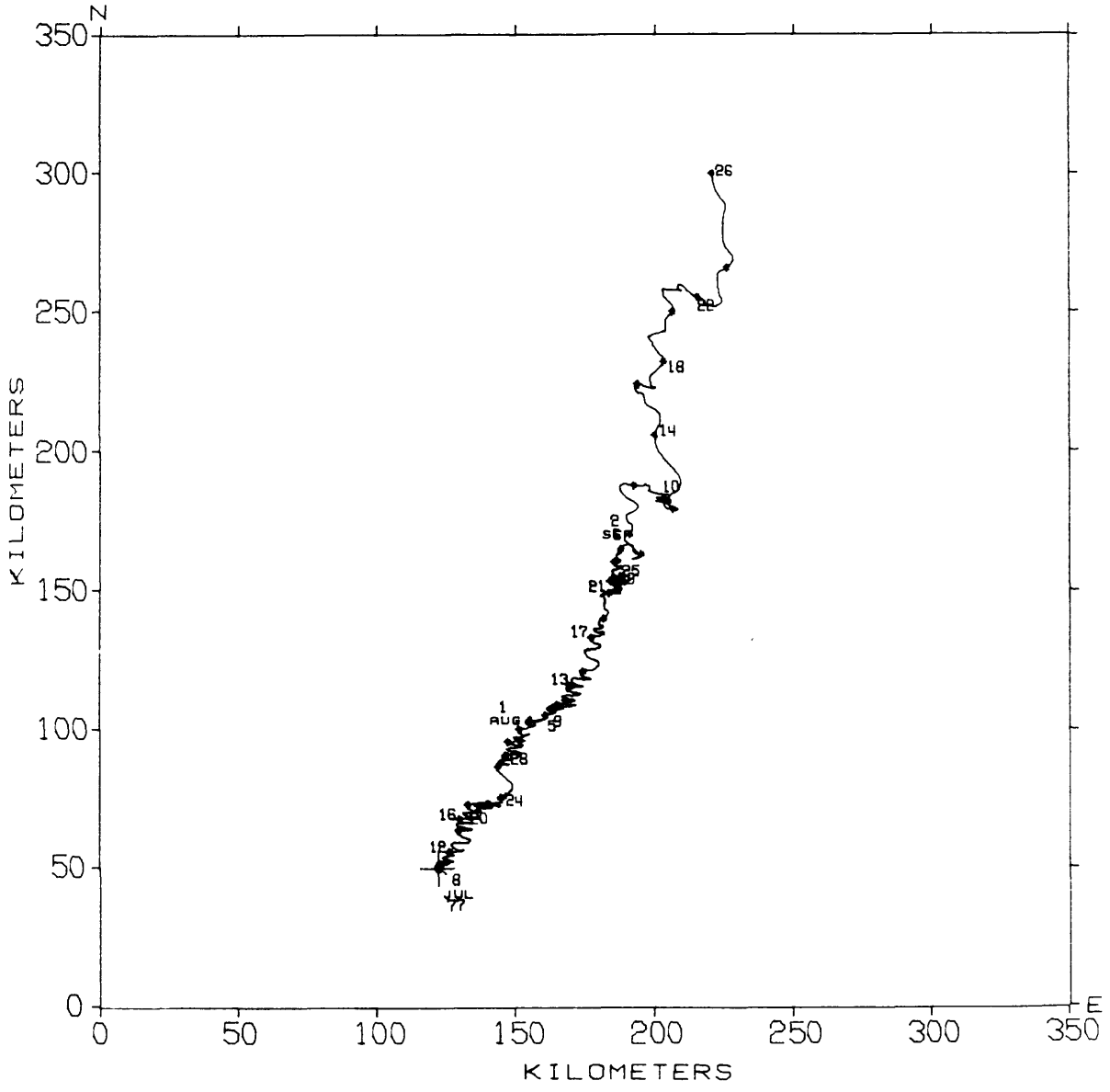

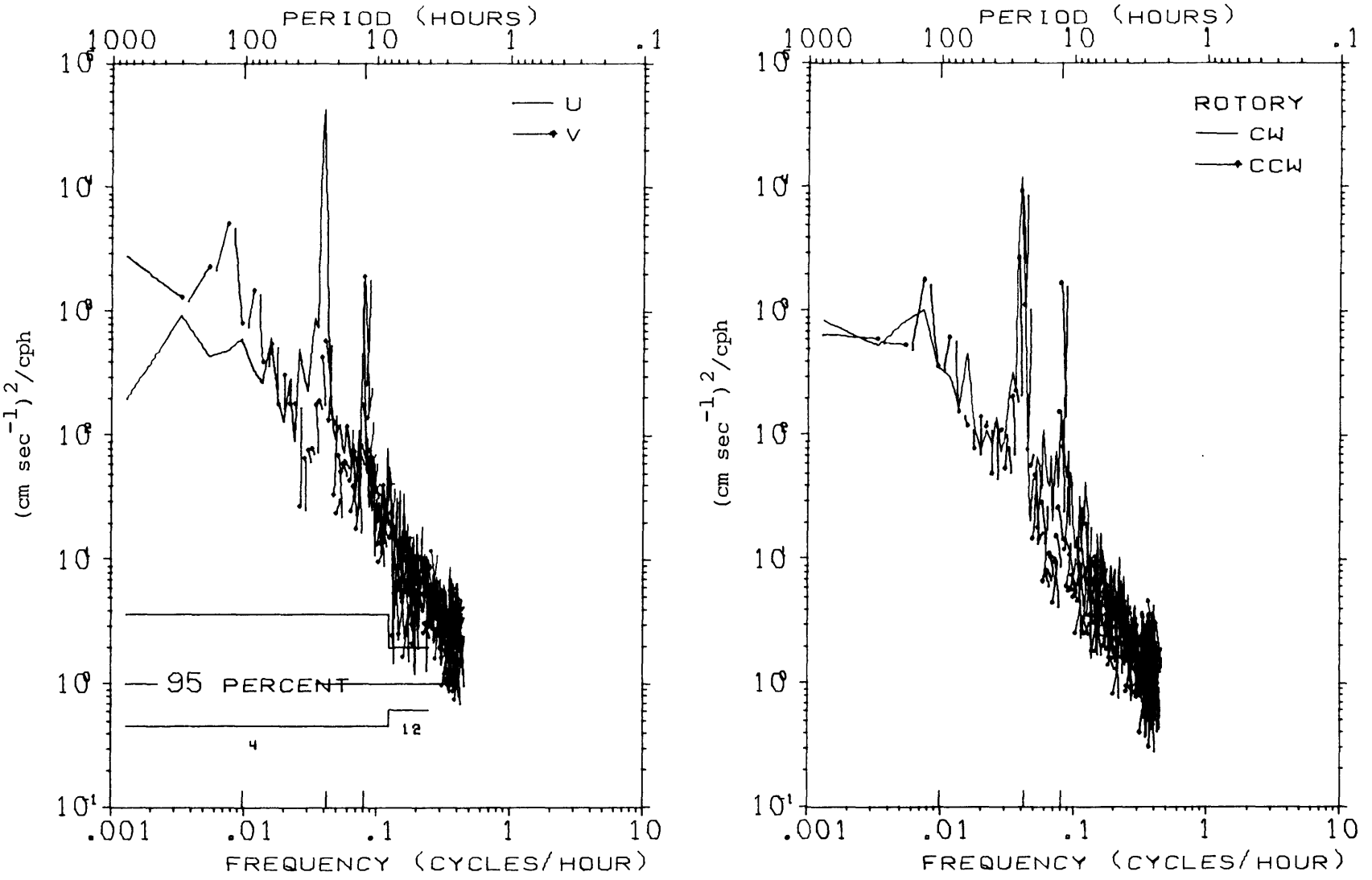

U, V AND ROTORY SPECTRA OF CURRENTS AT CM3 - GEOPROBE, NS77
LOCATION = LAT 64 00N, LONG 165 00W, DEPTH = 17.5 METERS
OBSERVATION PERIOD = 0000 8 JUL 77 TO 2300 25 SEP 77 (80.0 DAYS)
N = 1920, DT = 1.0 HOURS, SMOOTHING - DANIELL WINDOW

KINETIC ENERGY SPECTRUM OF CURRENTS AT CM3 - GEOPROBE, NS77
LOCATION = LAT 64 00N, LONG 165 00W, DEPTH = 17.5 METERS
OBSERVATION PERIOD = 0000 8 JUL 77 TO 2300 25 SEP 77 (80.0 DAYS)
N = 1920, DT = 1.0 HOURS, SMOOTHING - DANIELL WINDOW

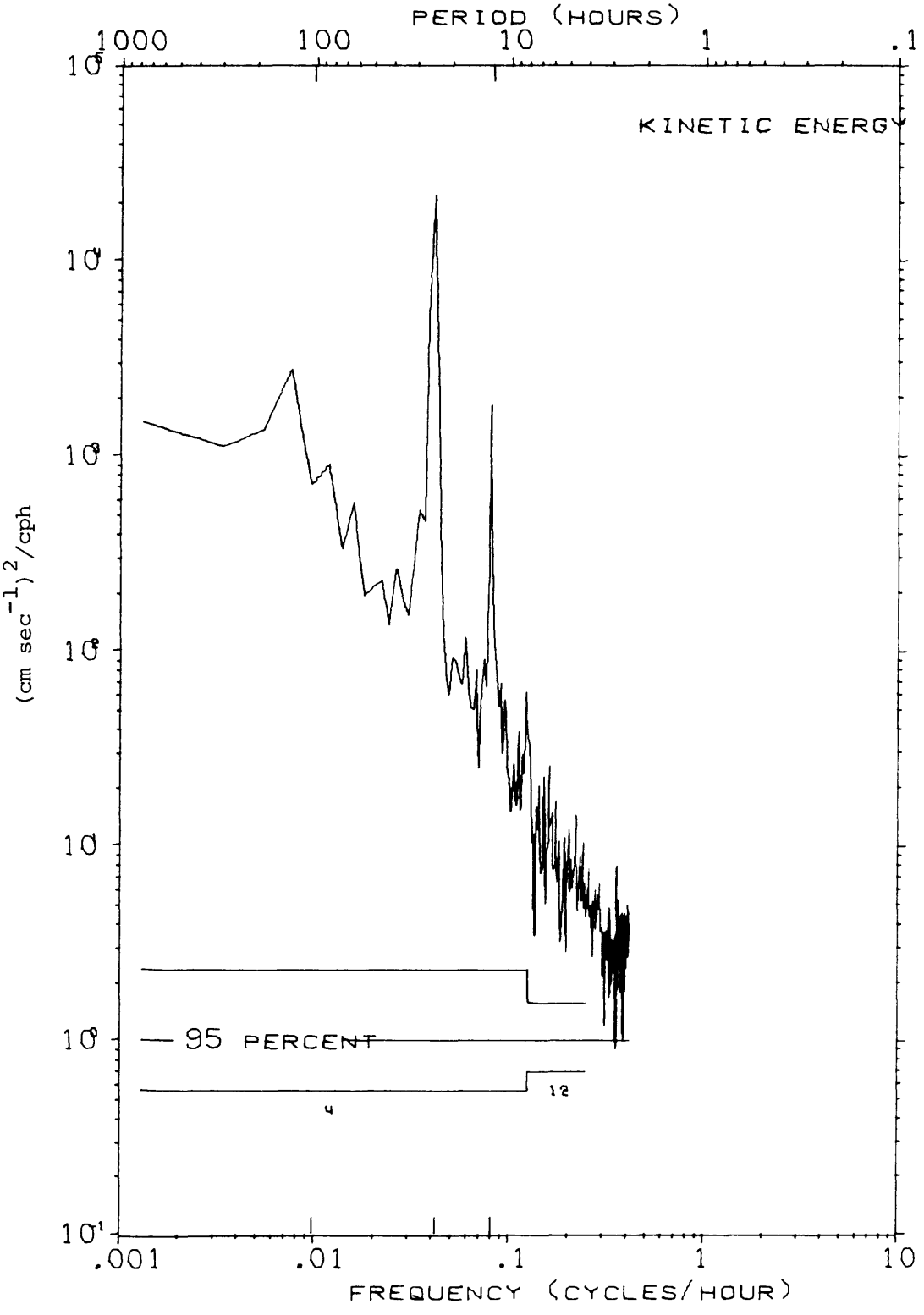

STATISTICS AND HISTOGRAMS OF CURRENTS AT CM4 - GEOPROBE, NS77
LOCATION = LAT 64 00N, LONG 165 00W, DEPTH = 17.5 METERS
OBSERVATION PERIOD = 0000 8 JUL 77 TO 2300 25 SEP 77 (80.0 DAYS)
N = 1920 DT = 1.00 HOURS, UNITS = (CM/SEC)

	MEAN	VARIANCE	ST-DEV	SKEW	KURT	MAX	MIN
S	14.05	56.05	7.49	0.543	2.966	43.10	0.16
U	2.43	159.37	12.62	0.135	2.099	36.86	-24.59
V	2.03	84.10	9.17	0.678	4.407	42.22	-32.04

S = SPEED
U = EAST-WEST COMPONENT OF VELOCITY, EAST =POSITIVE U
V = NORTH-SOUTH COMPONENT OF VELOCITY, NORTH = POSITIVE V

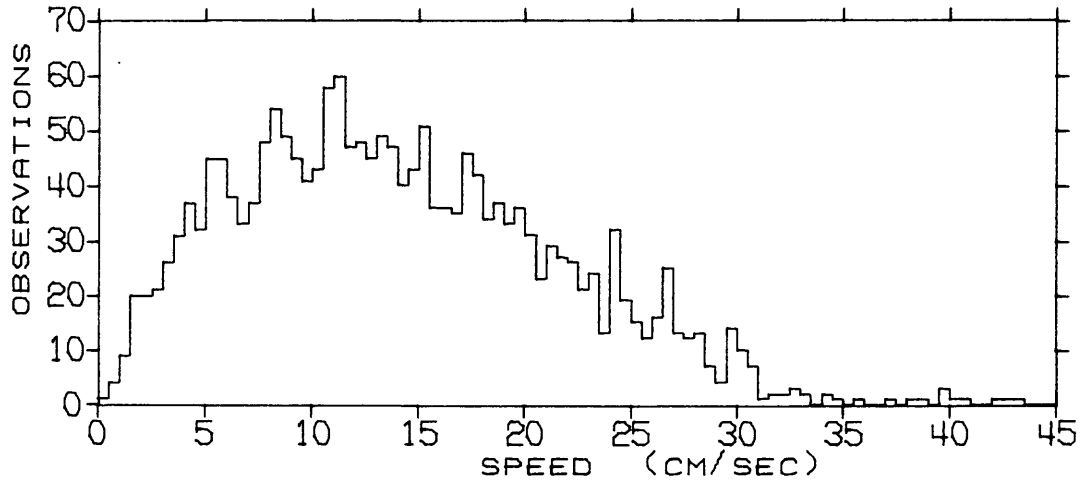

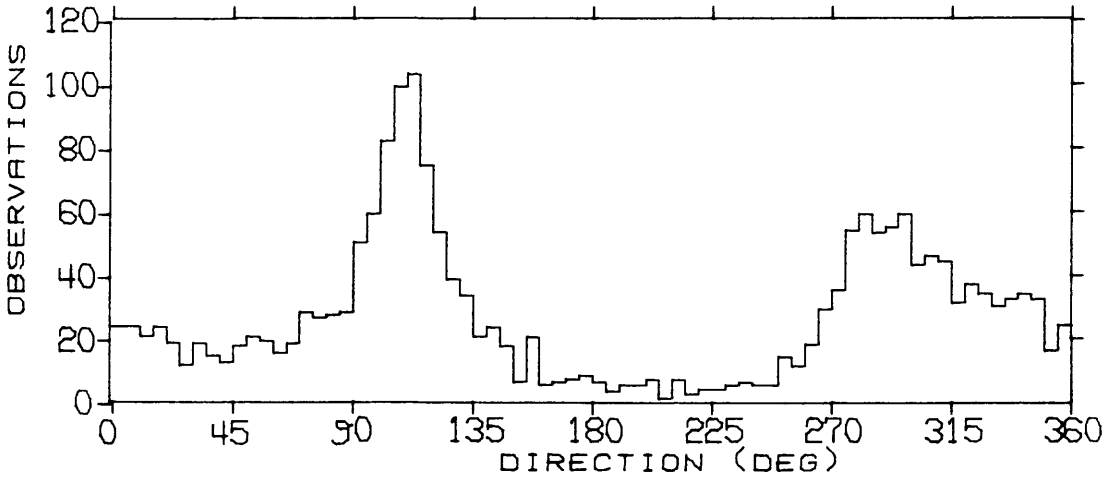

TIME SERIES OF VECTOR AVERAGED CURRENTS AT CM4 - GEOPROBE, NS77
LOCATION = LAT 64 00N, LONG 165 00W, DEPTH = 17.5 METERS
OBSERVATION PERIOD = 0000 8 JUL 77 TO 2300 27 JUL 77 (20.0 DAYS)
AVERAGING INTERVAL = 1.0 HOURS (1 POINTS)

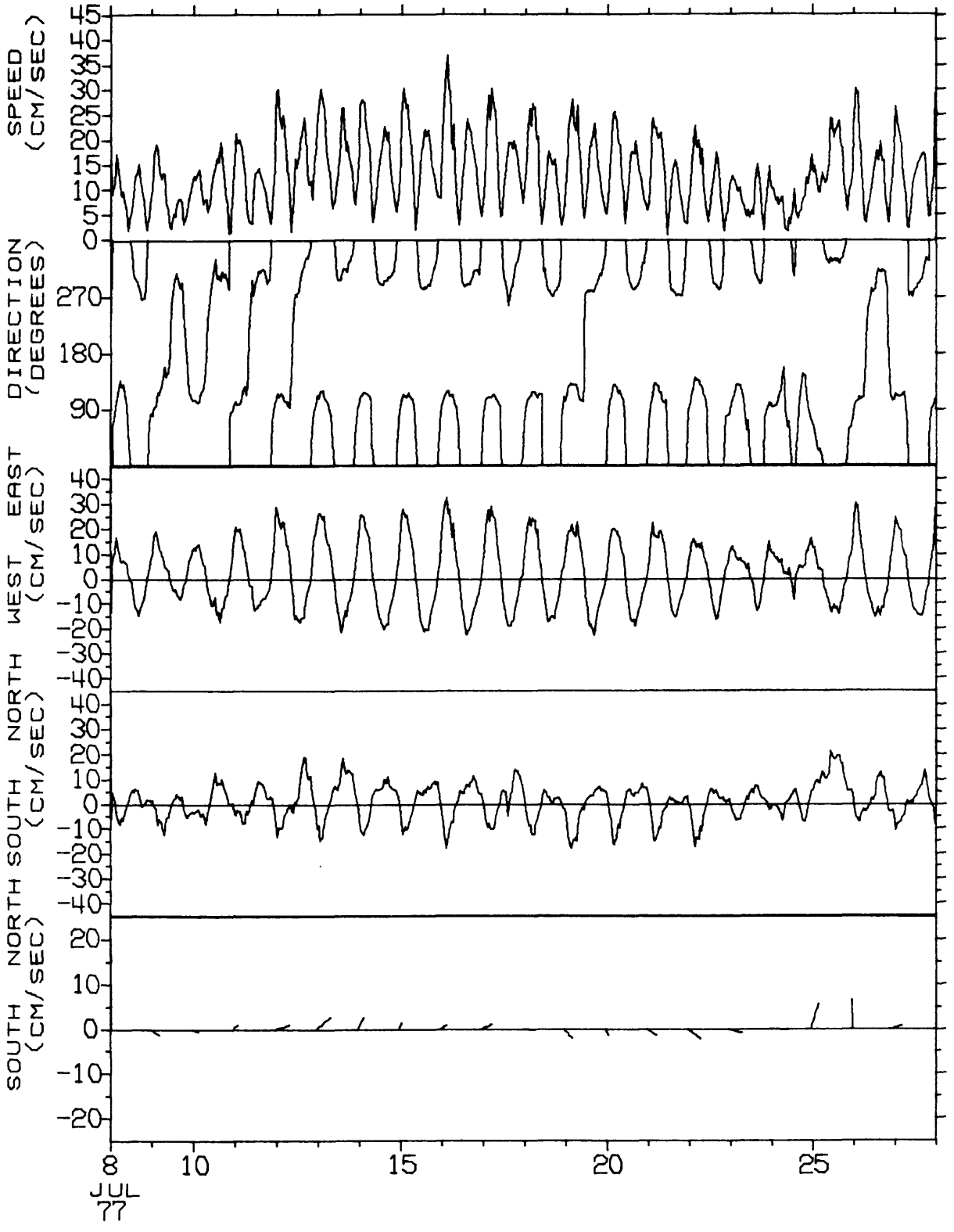

TIME SERIES OF VECTOR AVERAGED CURRENTS AT CM4 - GEOPROBE, NS77
LOCATION = LAT 64 00N, LONG 165 00W, DEPTH = 17.5 METERS
OBSERVATION PERIOD = 0000 28 JUL 77 TO 2300 16 AUG 77 (20.0 DAYS)
AVERAGING INTERVAL = 1.0 HOURS (1 POINTS)

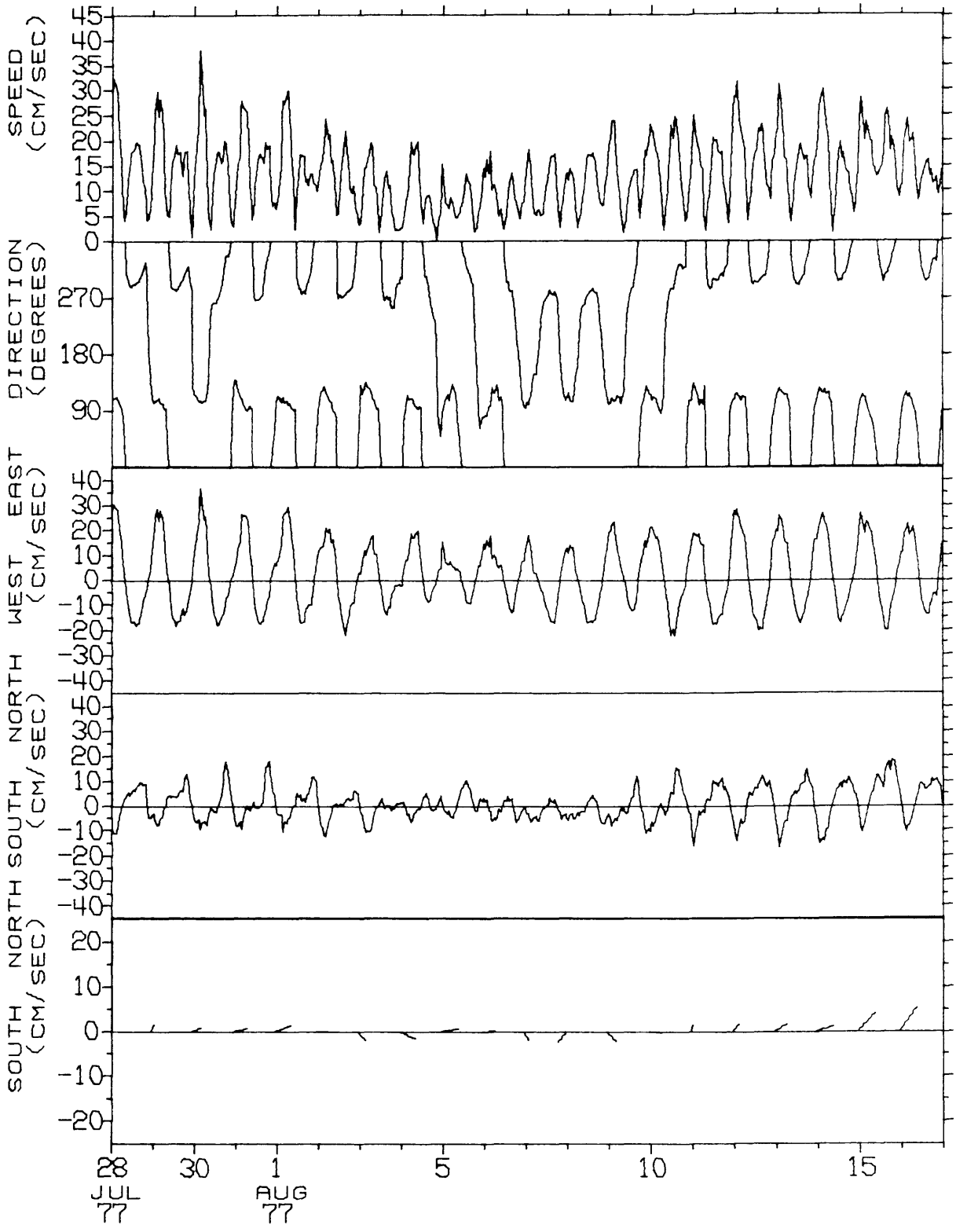

TIME SERIES OF VECTOR AVERAGED CURRENTS AT CM4 - GEOPROBE, NS77
LOCATION = LAT 64 00N, LONG 165 00W, DEPTH = 17.5 METERS
OBSERVATION PERIOD = 0000 17 AUG 77 TO 2300 5 SEP 77 (20.0 DAYS)
AVERAGING INTERVAL = 1.0 HOURS (1 POINTS)

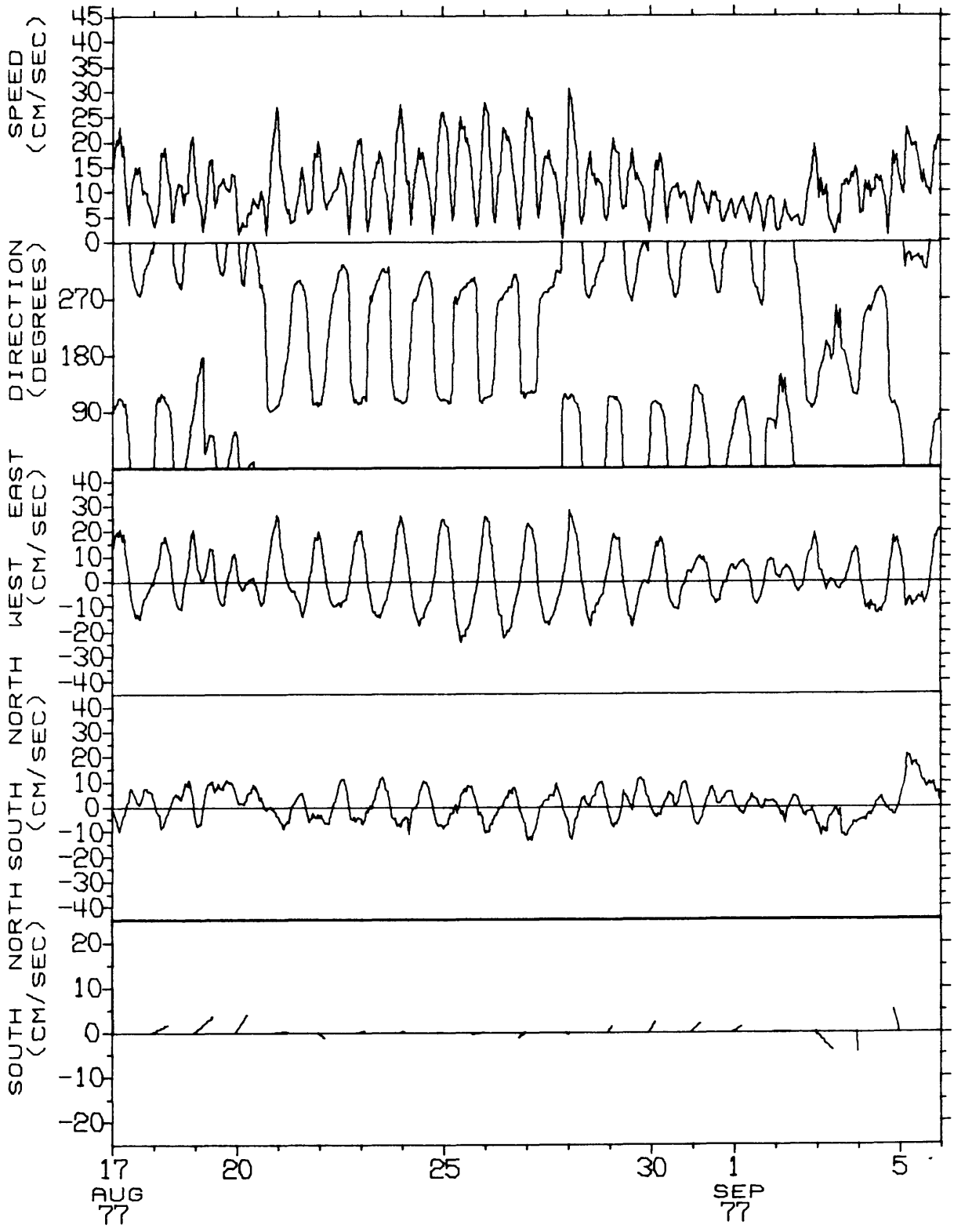

TIME SERIES OF VECTOR AVERAGED CURRENTS AT CM4 - GEOPROBE, NS77
LOCATION = LAT 64 00N, LONG 165 00W, DEPTH = 17.5 METERS
OBSERVATION PERIOD = 0000 6 SEP 77 TO 2300 25 SEP 77 (20.0 DAYS)
AVERAGING INTERVAL = 1.0 HOURS (1 POINTS)

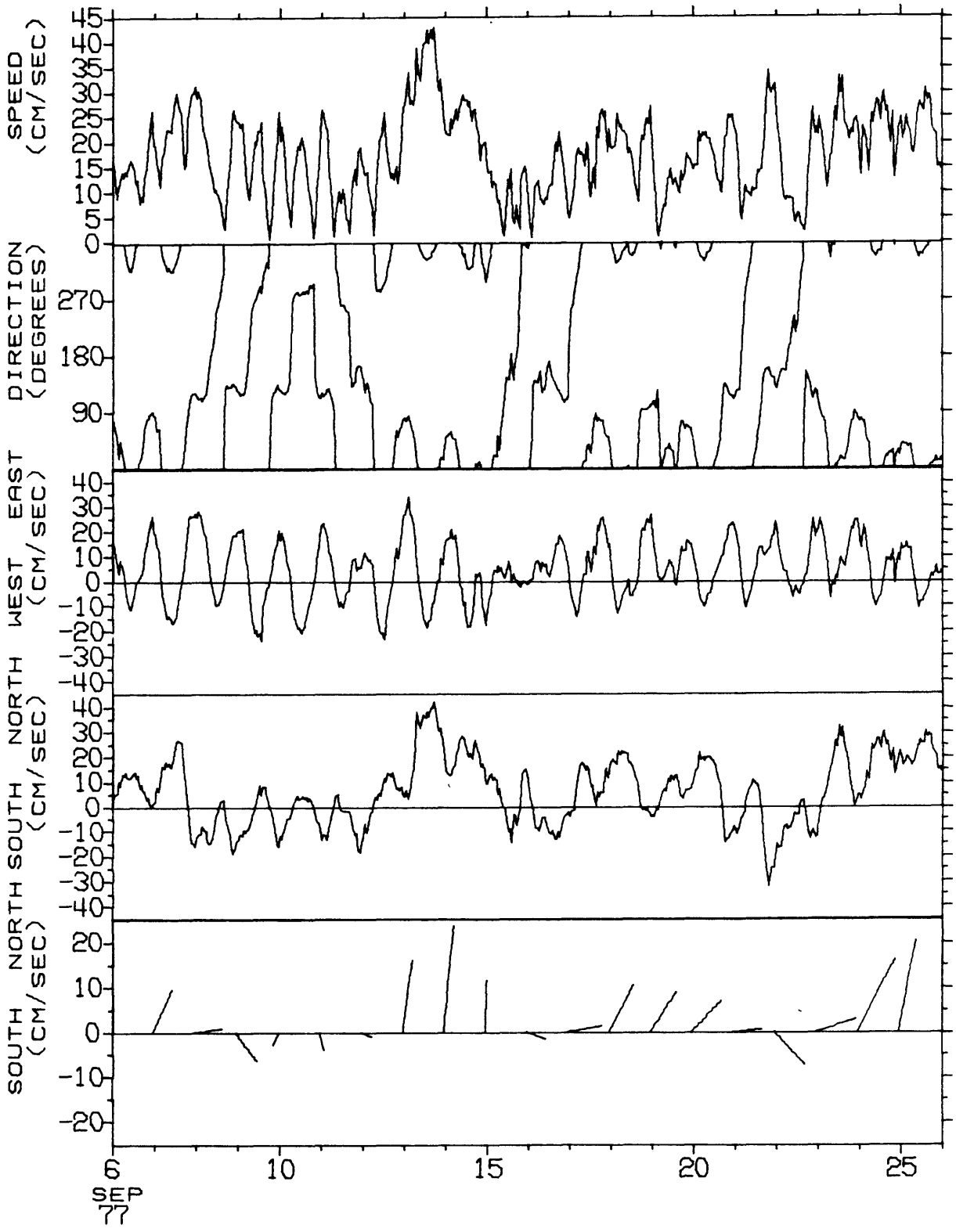

PROGRESSIVE VECTOR DIAGRAM OF CURRENTS AT CM4 - GEOPROBE, NS77
LOCATION = LAT 64 00N, LONG 165 00W, DEPTH = 17.5 METERS
OBSERVATION PERIOD = 0000 8 JUL 77 TO 2300 25 SEP 77 (80.0 DAYS)
♦ EVERY 2.0 DAYS BEGINNING AT 0000 8 JUL 77

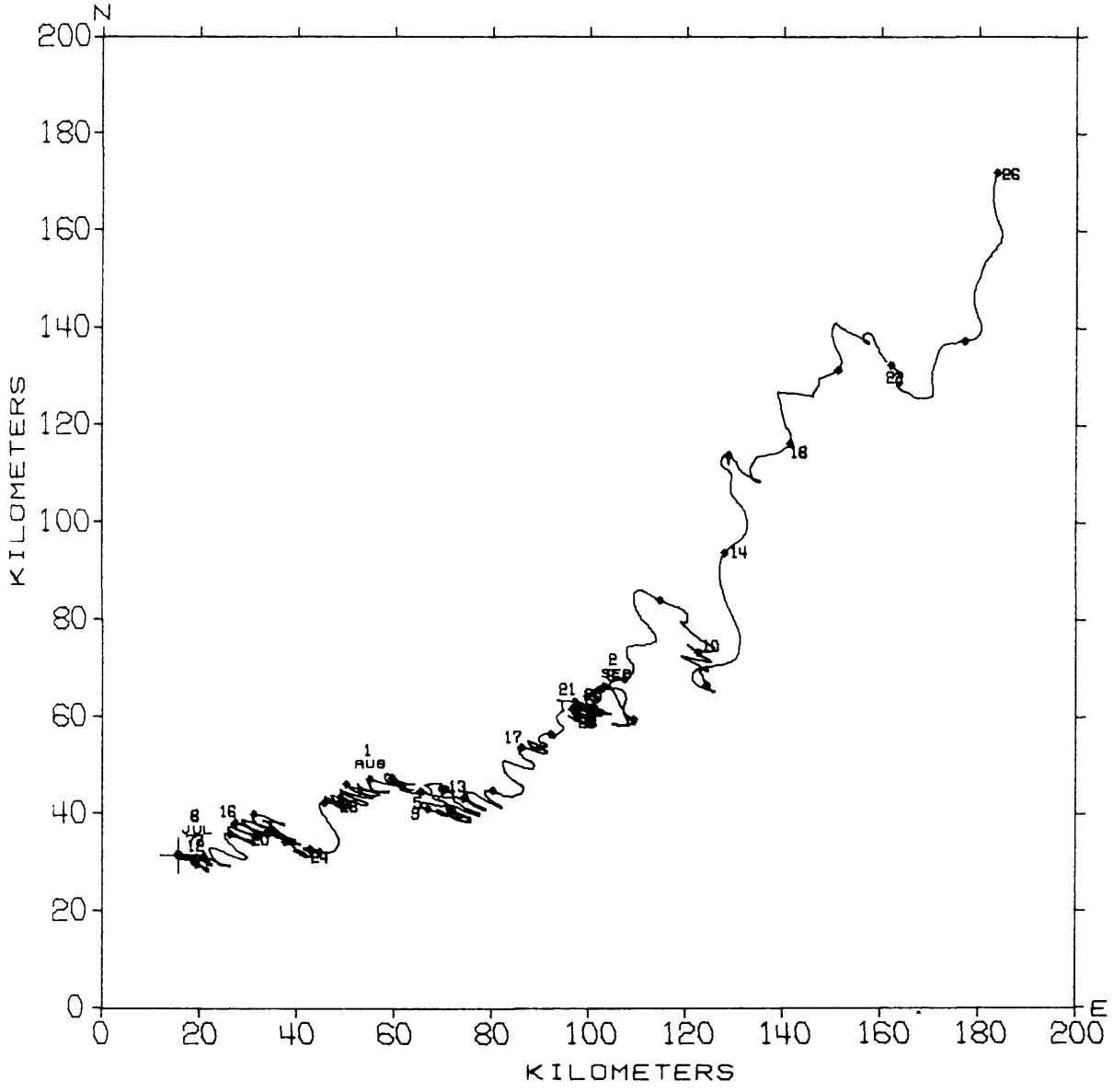

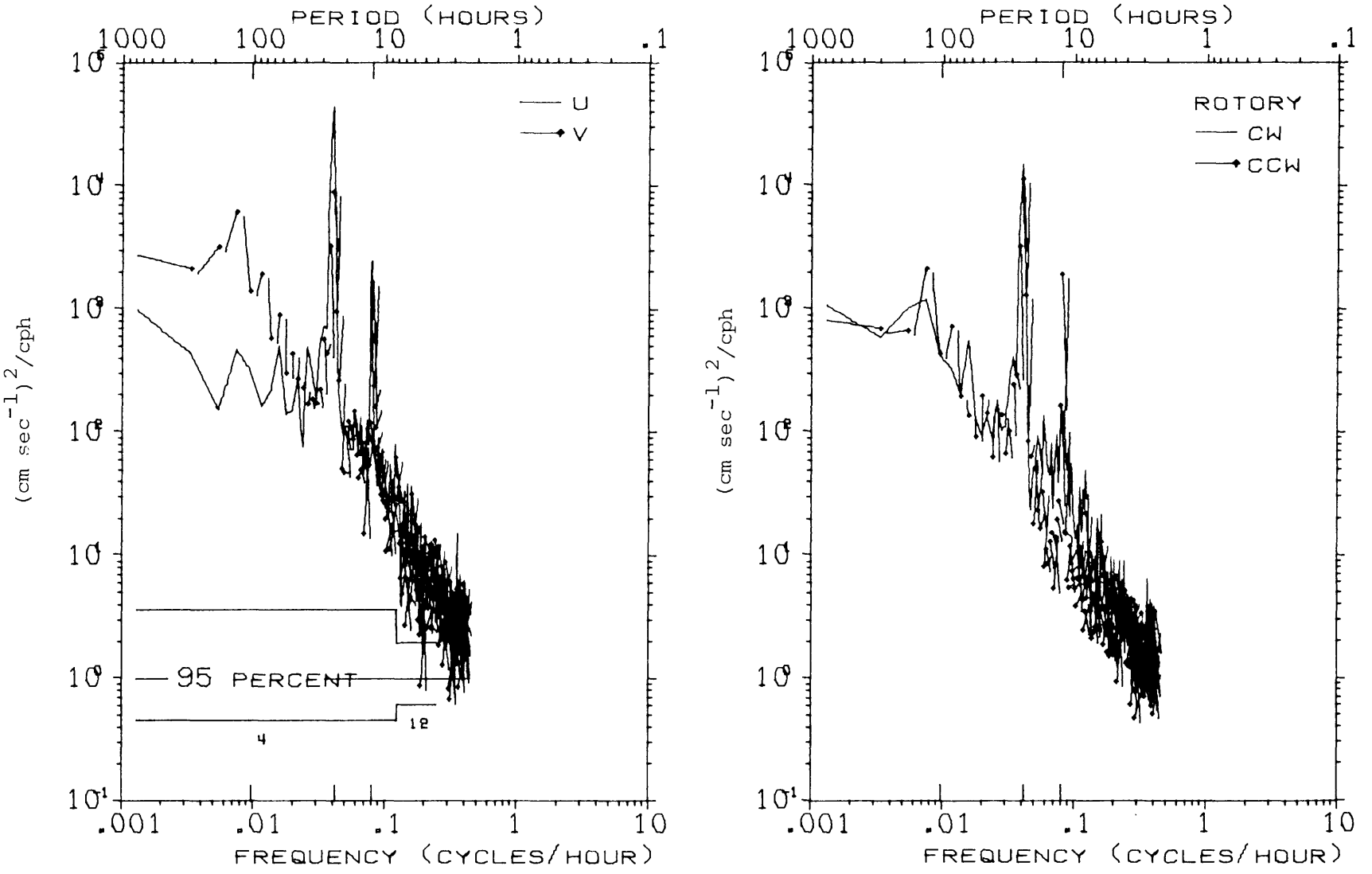

U, V AND ROTORY SPECTRA OF CURRENTS AT CM4 - GEOPROBE, NS77
LOCATION = LAT 64 00N, LONG 165 00W, DEPTH = 17.5 METERS
OBSERVATION PERIOD = 0000 8 JUL 77 TO 2300 25 SEP 77 (80.0 DAYS)
N = 1920, DT = 1.0 HOURS, SMOOTHING - DANIELL WINDOW

KINETIC ENERGY SPECTRUM OF CURRENTS AT CM4 - GEOPROBE, NS77
LOCATION = LAT 64 00N, LONG 165 00W, DEPTH = 17.5 METERS
OBSERVATION PERIOD = 0000 8 JUL 77 TO 2300 25 SEP 77 (80.0 DAYS)
N = 1920, DT = 1.0 HOURS, SMOOTHING - DANIELL WINDOW

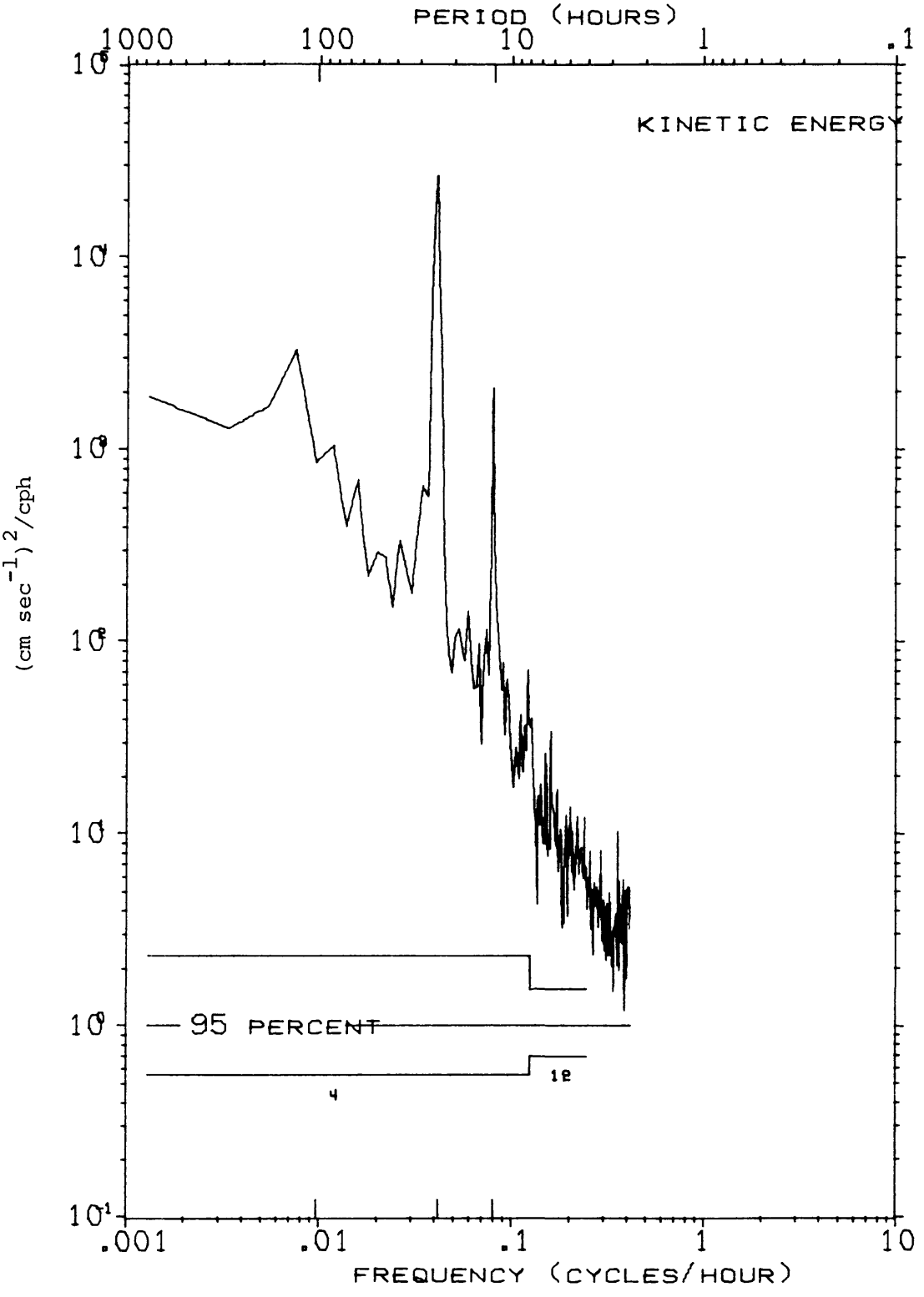

GPO 689-143